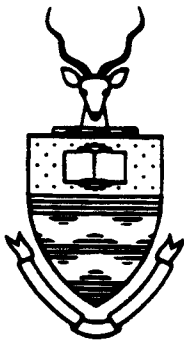


**UNIVERSITY OF THE WITWATERSRAND, JOHANNESBURG  
SCHOOL OF MECHANICAL ENGINEERING**



**MECN 446 - RESEARCH PROJECT**

**TITLE** : MODEL OF THE TORQUE-TENSION  
ROTATION BEHAVIOUR OF A  
48 mm TRIANGULAR STRAND  
STEEL WIRE ROPE OPERATING ON  
A DRUM WINDER.

**AUTHOR** : GERHARD REBEL (9005840X)

**SUPERVISOR** : MR. C. CONSTANCON

**DATE** : 1 NOVEMBER 1993

## ABSTRACT

Due to the helical nature of steel wire ropes they generate a torque when subjected to a tensile force. Langs lay, triangular strand ropes are particularly prone to this phenomena which is known as the torque-tension rotation characteristics of the rope. The objective of this project is to derive an experimental model which can accurately predict the torque-tension rotation behaviour of 48 mm diameter triangular strand rope operating in vertical shafts of different depths. Such a model already exists but it does not correlate with the rope torque-tension behaviour in the shaft. Torque-tension rotation tests were conducted on a set of triangular strand Langs lay ropes at the CSIR Mine Hoisting Technology laboratories. Twists of up to  $267^{\circ}/\text{m}$  and down to  $-267^{\circ}/\text{m}$  were applied to the specimens during testing. Using the test results and in shaft lay length measurements three methods of predicting rope rotation are presented. The models do not predict the rotation of the rope accurately. However, the processes required to obtain an accurate rotation model have been understood and identified. Considerable recommendations have therefore been made as to the nature of further work required in this field.

## ACKNOWLEDGEMENTS

I would like to thank the Mr. M. Borello for proposing this project and for his advice and assistance throughout the duration of the project.

I would like to thank Mr. M. Van Zyl for his explanations on the project topic and for making available certain relevant literature.

Thank you to Messrs C. McDuling and N. Pilay for their assistance in setting up the test equipment.

I would also like to express my appreciation to the CSIR for making available the test facilities and necessary equipment and for the access to their literature and expertise. The CSIR also supplied the used rope test specimens required for the completion of this project.

## CONTENTS

	<b>Page</b>
DECLARATION	i
ABSTRACT	ii
ACKNOWLEDGEMENTS	iii
CONTENTS	iv
LIST OF FIGURES	vii
LIST OF TABLES	ix
LIST OF SYMBOLS	ix
1. INTRODUCTION	1
1.1 Definitions	1
1.2 Background	4
1.3 General shaft and winder layout	5
1.4 Literature review	7
2. OBJECTIVE AND PURPOSE OF PROJECT	10
3. OVERVIEW OF EXISTING THEORY	13
3.1 Torque-tension rotation	13
3.1.1 Direct Data fit method	14
3.1.2 C and T factor method	23
3.2 Validity of theory	25
4. EXPERIMENTATION	27
4.1 Experimental equipment	27
4.1.1 Mechanical system	27
4.1.2 Electrical data acquisition and control system	36

4.1.3	Control software	40
4.2	Experimental procedure	42
4.2.1	Preparation	42
4.2.2	Testing	43
4.2.3	Rope specimen end rotations	45
4.2.4	Test limitations	46
5.	TORQUE-TENSION TEST RESULTS AND ANALYSIS	50
5.1	General test information and calibration data	50
5.2	Lay length measurements	50
5.3	Test data manipulation	52
5.4	Torque-tension rotation curves	54
5.4.1	Back underlay	54
5.4.2	Middle underlay	55
5.4.3	Front underlay	56
5.5	Elongation and diameter changes	60
5.5.1	Back underlay	60
5.5.2	Middle underlay	61
5.5.3	Front underlay	62
5.6	Torque factor - C	70
5.6.1	Back underlay	70
5.6.2	Middle underlay	71
5.6.3	Front underlay	71
5.7	Torsional stiffness - T	75
5.7.1	Back underlay	75
5.7.2	Middle underlay	75
5.7.3	Front underlay	76
6.	COMPUTER MODELS OF ROPE ROTATION BEHAVIOUR	80
6.1	Rope rotation in terms of length, an approximation	81
6.2	Direct Data Fit method	89
6.3	C and T factor method	97
6.3.1	Additional note	106

7.	CONCLUSIONS	107
8.	RECOMMENDATIONS FOR FUTURE WORK	111
9.	REFERENCES	114
10.	APPENDICES	
	A - Test machine hydraulic circuits	116
	B - Description of control program "T_T_TEST"	121
	C - General test information, calibration data and CSIR rope test certificate	128
	D - Description of test data manipulation program "T_T_PLOT"	134
	E - File conversion program "FSMALL"	138
	F - MATLAB program to determine rotation as a function of rope length	141
	G - MATLAB programs for the Direct Data Fit method	144
	H - MATLAB programs for the C and T factor method	156
	I - Rotation computer model "T_T_CURVE"	164

## LIST OF FIGURES

Figure		Page
1.1	- Langs lay triangular strand rope	4
1.2	- Typical drum winding system in a vertical shaft	6
2.1	- Rope contact on the sheave wheel	11
3.1	- Torque-tension curves of a 44 mm TSR	13
3.2	- Torque tension rotation curves of a 48 mm TSR	16
3.3	- Rope twist as a function of position along the rope	20
3.4	- In-shaft rope rotation	22
3.5	- C and T factor rope and load layout	23
4.1	- General arrangement of torque-tension machine	27
4.2	- CSIR Rope torque-tension machine	28
4.3	- Test machine rotation components	29
4.4	- Rope rotation gauge	30
4.5	- Scissor mechanism and hydraulic cylinder	31
4.6	- Load-cell and loading end grips	31
4.7	- Test machine hydraulic unit	32
4.8	- Extensometer bar between loading and rotation end conical grips	33
4.9	- Diameter measuring bracket	34
4.10	- Rope vernier	35
4.11	- Test control table	36
4.12	- Strain gauge amplifiers, floppy disk drive, DVM's and Data Acquisition/Control Unit	37
4.13	- Manual control box	39
4.14	- Rope test specimen (length 4050 mm)	42
4.15	- Overheating effect on test results	48
5.1	- Torque-tension rotation curves, back underlay	57
5.2	- Torque-tension rotation curves, middle underlay	58
5.3	- Torque-tension rotation curves, front underlay	59

5.4	-	Elongation curves, back underlay	64
5.5	-	Diameter curves, back underlay	65
5.6	-	Elongation curves, middle underlay	66
5.7	-	Diameter curves, middle underlay	67
5.8	-	Elongation curves, front underlay	68
5.9	-	Diameter curves, front underlay	69
5.10	-	Torque factor curves, back underlay	72
5.11	-	Torque factor curves, middle underlay	73
5.12	-	Torque factor curves, front underlay	74
5.13	-	Torsional stiffness, back underlay	77
5.14	-	Torsional stiffness, middle underlay	78
5.15	-	Torsional stiffness, front underlay	79
6.1	-	In-shaft lay length measurements	82
6.2	-	Test rope twist and lay length	84
6.3	-	Rope twist approximation	85
6.4	-	Rope rotation approximation	86
6.5	-	Combined BCKUL and FNTUL torque-tension rotation curves	90
6.6	-	Rope twist and torque for constant force	91
6.7	-	Direct Data Fit rope twist and rope length	95
6.8	-	Direct Data Fit rope rotation and rope length	96
6.9	-	C and T rope twist and length	100
6.10	-	C and T rope rotation and length	101
6.11	-	Actual C factors along rope length	102
6.12	-	Actual T factors along rope length	103
6.13	-	Actual torque-tension rotation curves	105
A.1	-	Hydraulic circuit for tensioning cylinder	117
A.2	-	Hydraulic circuit for rotation motor	119
H.1	-	$b_c$ versus rope force	158
I.1	-	HP computer model rotation curves (100/0)	175
I.2	-	HP computer model rotation curves (50/50)	176
I.3	-	HP computer model rotation curves (33/67)	177
I.4	-	HP computer model rotation curves (0/100)	178



## LIST OF TABLES

Table		Page
3.1	- Torque-tension rotation table for a 48mm TSR	15
5.1	- Back underlay test lay lengths	50
5.2	- Middle underlay test lay lengths	51
5.3	- Front underlay test lay lengths	52
6.1	- Lay length as a function of rope length	81
6.2	- Twist as a function of lay length	83
7.1	- Rope torques and rotations for different models	109

## LIST OF SYMBOLS

Symbol	Quantity
C	- Torque factor (Nm/kN)
F	- Rope force (kN)
M	- Rope torque (Nm)
Me	- Rope torque with an empty skip (Nm)
Mf	- Rope torque with a full skip (Nm)
P	- Rope end load (kN)
$\Phi$	- Rope rotation ( $^{\circ}$ )
q	- Rope weight per unit length (kN/m)
R	- Rope twist = $d\Phi/dz$ ( $^{\circ}/m$ )
T	- Torsional stiffness (Nm/( $^{\circ}/m$ ))
z	- Distance from the skip along the rope (m)

## 1. INTRODUCTION

Triangular strand steel wire ropes are widely used by the South African mining industry. The torque-tension rotation properties of these rope are however not clearly understood. To date, there is no accurate empirical or analytic mathematical model to describe this characteristic. The torque-tension rotation behaviour is the reason why even wear is found to occur around the rope circumference. If a better understanding of rope degradation is required then it is vital to first understand the processes involved.

This project looks at the static torque-tension rotation behaviour of a 48 mm triangular strand steel wire rope. Only when the statics are fully understood and described can the dynamic aspects of this rope characteristic be considered.

### 1.1 DEFINITIONS

There are some terms that will be used in this report which may be unclear to persons not familiar with the mining industry. For this reason the terms are defined below. In some cases the definitions are specifically related to the context of the report. The terms are arranged in a logical order.

**Triangular strand steel wire rope :** A rope consisting of six strands, the cross-section of each strand approximates an equilateral triangle with rounded edges. This type of rope is highly resistant to crushing due to its compact formation, and also to abrasion due to the increased outer wearing surface as compared with round strand ropes.

**Langs lay steel wire rope :** A rope construction where the wires in a strand and the strands in a rope are wound in the

same direction.

**Double drum winder :** Shaft winding system where two rope drums are connected and rotate simultaneously winding either two conveyances or one conveyance and a counter weight up and down a vertical shaft.

**Underlay rope :** On a double drum winder this is the rope which is coiled around the one drum from the underside.

**Overlay rope :** On a double drum winder, this is the rope which is coiled around one drum from the top side. With this underlay and overlay configuration, when the two drums rotate in a direction then the underlay rope is wound in and the overlay rope is wound out or visa-versa.

**Sheave wheel :** Grooved wheel supported in the headgear over which the hoist rope passes from the winding house down the shaft.

**Skip :** A steel structure, suspended in the shaft on the end of a steel wire, in which rock is conveyed from the loading station at shaft bottom to the headgear. A skip can also be called a conveyance.

**Lay length :** The distance, measured along the axis of a rope, which a single strand takes to do one full revolution around the rope core.

**Rope torque :** The torsional moment generated by a steel wire rope when it is placed under a tensile load.

**Rope rotation :** The rotation of the rope about its own axis measured in number of turns or in degrees.

**Rope twist :** Taking the rope rotation and differentiating it with respect to rope length gives rope twist with units in degrees per meter. For the purposes of this project, a negative rope twist means that the rope is being unwound or

that the lay length is increasing. A positive rope twist means that the rope is being wound up and the lay length is decreasing.

In the test situation rope rotation and rope twist are easily related, i.e twist is ( end rotation / specimen length ). This assumes that the rate of change of rotation across the length is constant.

In the shaft the rate of change of rotation with respect to rope length is not a constant therefore twist and rotation are not simply related.

**Torque factor :** For as constant rope rotation or twist, the Torque factor is the ratio between the torque in the rope and the tensile load in the rope. The units are Nm/kN or Nm/N. Torque factor is often termed the C factor. The Torque factor is a function of rope load and rope rotation or twist.

**Torsional stiffness :** For a constant rope force, the Torsional stiffness is the ratio between the torque in the rope and the twist. The units are Nm/(deg/m) and the Torsional stiffness is often referred to as the T factor. Torsional stiffness is a function of rope load and rope rotation or twist.

## 1.2 BACKGROUND

The helical structure of triangular strand steel wire rope cause the rope to generate a torque when it is loaded in tension. Generally the torque increases with increasing tensile load.

Triangular strand ropes (TSR) generate high values of torque when used in deep shafts. According to Borello (1993) these values can be as high as 2000 Nm to 3000 Nm. Figure 1.1 below shows a typical TSR cross section and side view. In the side view it can be seen that strands and rope are wound in the same direction. This method of construction is known as Langs lay.

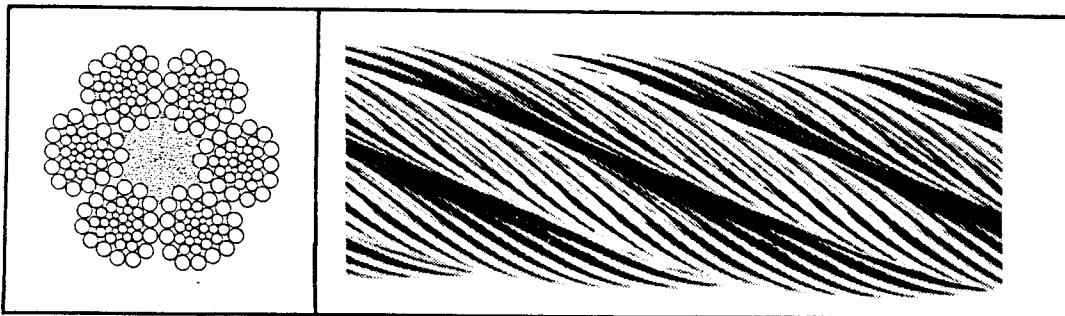


**Figure 1.1** - Langs lay triangular strand rope, (6x32(14/12/6▲)/F). From Haggie Rand (1987).

When a rope is installed on a drum winder, both ends of the rope are prevented from rotating. The front (bottom) end is fixed in the rope termination at the conveyance. The back (top) end is assumed to be fixed at the sheave wheel. Rope to sheave contact pressures of between 3 and 6 MPa result in high contact friction forces between the rope and the sheave groove, thereby preventing any rotation. Haggie Rand 1987.

If the rope hangs vertically in the shaft, the tension at the front end of the rope is lower than the tension at the

back end. The front end is at the conveyance termination and the back end is at the headgear sheave wheel. The linear change in tension in the vertical rope is due to the considerable mass per unit length of the rope. For a 48mm TSR, with which this project is concerned, the value is 9.813 kg/m. Haggie Rand (1987).

Now if the tension is higher at the back end than at the front end, then so must the torque at the back end be higher than the torque at the front end. This is not physically possible. Simple mechanics dictates that the torque must be constant throughout the rope considering that there is no external loads applied along the rope length. The rope therefore adjusts for this torque imbalance by rotating. This rotation causes an increase in lay length at the back end and a decrease in lay length at front end.

The greater the lay length of a rope section, the less helix it will have and will therefore generate less torque under the same tensile load. So, the increased lay length at the back end will result in a torque reduction to some equilibrium value. The decreased lay length at the front end will result in a torque increase to the same equilibrium value.

The extent to which the rope rotates is determined by the torque-tension characteristics of the rope construction. The details of this phenomena will be discussed in the section on EXISTING THEORY.

### **1.3 GENERAL SHAFT AND WINDER LAYOUT**

In order that there is no ambiguity as to how the various components of the shaft system are arranged a schematic diagram of such a layout has been included.

Figure 1.2 below shows a typical drum winding system and shaft layouts as used in many of the vertical mine shafts in South Africa.

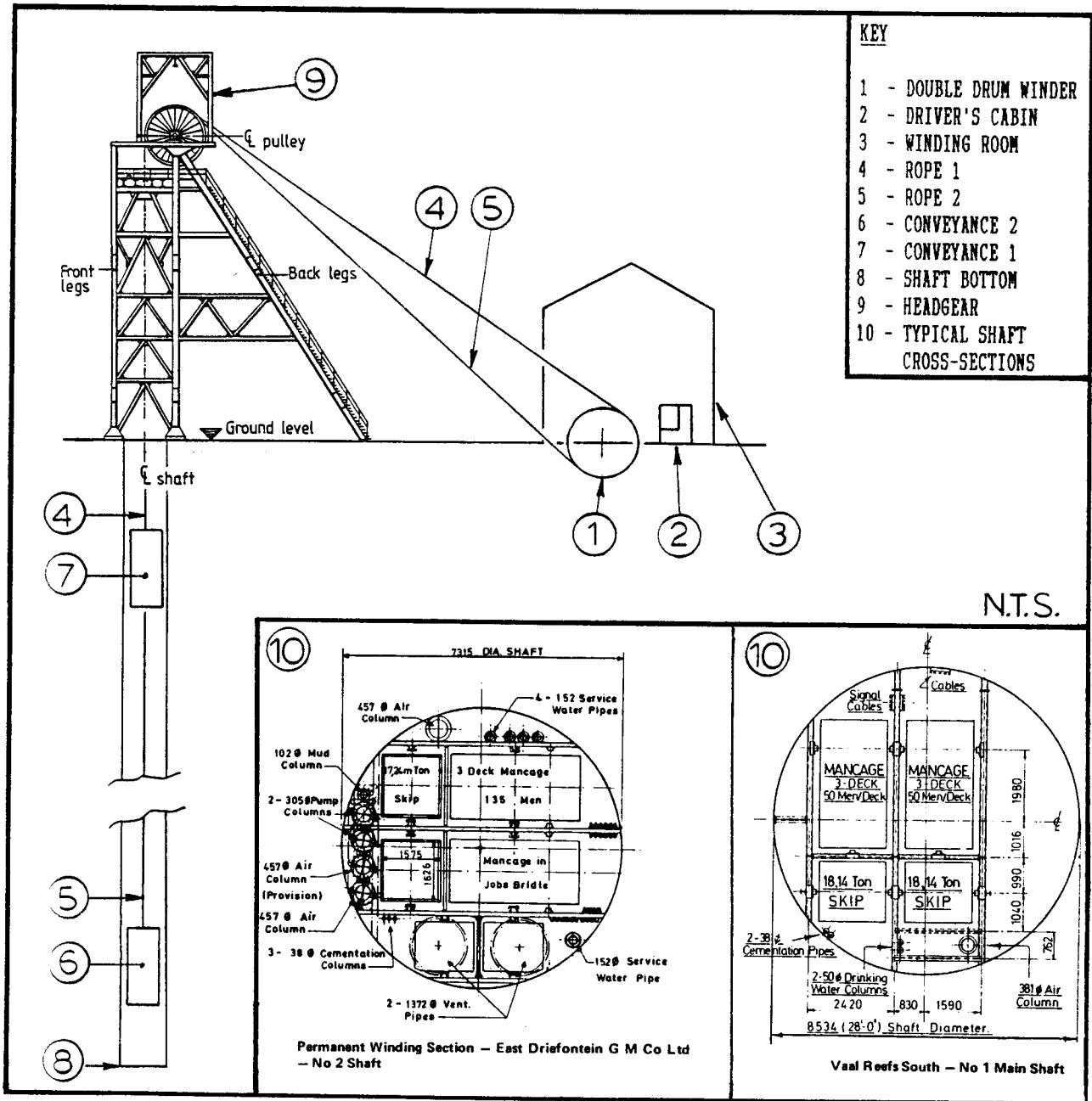


Figure 1.2 - Typical drum winding system in a vertical shaft. Adapted from Walker (1988) and Moll (1973).

## 1.4 LITERATURE REVIEW

In the past the majority of research into torque-tension rotation properties was done on non-spin and spin resistant ropes. These include multi-strand ropes and ordinary lay ropes. The reason for this is that these type of ropes are specifically constructed so that they do not generate high torques or exhibit high rotations upon application of a tensile load. This makes their torque-tension behaviour of particular interest.

In a multi-strand rope an additional layer of strands is wound in the opposite direction around a single layer rope. This gives a torque balance upon load application and prevents the rope from rotating. In spin resistant ropes the strands are wound in the opposite direction to the rope. This also leads to a lower torque being generated and less rope rotation upon load application. Haggie Rand (1987).

Both the CSIR and Haggie Rand were approached for literature on torque-tension rotation properties of TSR's with little success. From discussions with staff at these two organizations it became apparent that TSR torque-tension is not a problem in shafts of depth up to about 2500 m, but it is certainly a problem at depths greater than this. With the increase in the number of deep level shafts in South Africa more attention is being given to the torque-tension rotation behaviour of TSR's.

A literature search was conducted at the Rand Afrikaans University. The computerised version of the Engineering Index, CompEndix was accessed for any literature on torque-tension rotation properties of steel wire rope. In particular, triangular strand ropes. Over 100 different keyword searches were entered but no useful references were found. This was an indication of the lack of literature on this topic.



The literature search conducted on the Haggie Rand Product Development Department base revealed a number of papers on the torque tension rotation properties of steel wire ropes. Most of the literature were either conference papers or CSIR contract reports. There was however no specific work on the triangular strand torque tension rotation properties which would be useful for this project.

The CSIR was able to supply some relevant literature. Borello (1993), in unpublished work, investigated the derivation of torque-tension rotation equations for a rope based on the Torque factor and Torsional stiffness method. A worked example is also given for the rotation behaviour of a rope for full and empty skip loading states.

Van Zyl (1993) discusses torque-tension rotation equations derived from tests don on a 48 mm triangular strand drum winder rope. A different, more direct approach is used to the C and T factor method.

Kollross (1976) derives mathematical equations for torque in terms of load and twist. Tests were also conducted on Langs lay and ordinary lay ropes which showed that for a constant end rotation the Langs lay ropes generate higher values of torque than the ordinary lay ropes. Kollross also identified the fanning out of the lines, of constant rotation, as the load was increased. These torque tension lines were also shifted vertically depending on the end rotation of the specimen. The maximum twists used by Kollross were + and - 5°/m.

Yiassoumis (1992) investigates the torsional rotational behaviour of headgear mounted Koepe winder ropes. Although some of the experimentation is the same as in this work the ropes tested were of the non-spin type. The results of the analysis are therefore not entirely applicable to the topic of this project.

In a two part paper by Feyrer and Schiffner (1986) the

torque and torsional stiffness of wire rope are discussed. Emphasis is placed on predicting the torque in the rope for a given load and twist. Tests of up to  $220^{\circ}/\text{m}$  were conducted on a variety of rope constructions all in the 16 to 20 mm diameter range. Similar characteristic torque-tension rotation curves were obtained. On the Langs lay specimen the lines of torque versus force for constant twist were found to become curved at higher angles of twist.

McKenzie (1987) states that the torsional properties of steel wire ropes are often of significance to their in-shaft performance. Various methods and equipment for determining torque-tension rotation behaviour of ropes are described. One of these is the method of testing and test equipment as used in this work. Mathematical equations describing the rope torque twist and force are explained but the rotation of the rope, in the shaft, under different loading conditions is not dealt with. The accuracy of the CSIR test machine is noted as well as its ability to produce meaningful results for the torque-tension rotation characteristics of steel wire ropes.

According to Haggie Rand (1987) the reason why TSR's are so widely used is that they are highly resistant to crushing due to their compact construction. They also exhibit high resistance to abrasion due to the greatly increased wearing surface as compared with round strand ropes.

The two torque-tension rotation models, Borello (1993b) and Van Zyl (1993b), which are considered by the CSIR as the most accurate to date are described in the section on EXISTING THEORY.

## 2. OBJECTIVE AND PURPOSE OF PROJECT

The objective of this project is to derive an experimental model which can accurately predict the torque-tension rotation behaviour of 48mm diameter TSR operating in vertical shafts of different depths. The model must preferably be computer based and must, in its derivation, take into account actual rope behaviour as measured in a working shaft.

When complete this model could be useful in determining the maximum depth at which a single TSR could be used. According to Van Zyl (1993a) the maximum estimated depth is approximately 2500 m. However, it is not clear to what extent the high torque values will affect the rope performance. With an accurate torque-tension rotation model, more confident predictions of in service rope behaviour can be made.

From the accurate rotation behaviour of the rope a better understanding of the modes of rope degradation may be gained. At present it known that TSR show an even wear pattern around their circumference. This is because of the torque-tension rotation properties of the rope. The variation in applied load as well as dynamic effects cause the rope to rotate differently in each cycle. This results in it passing over the sheave wheel and winding drum with different contact points.

A cross-section of the rope passing over the sheave wheel is shown in the figure below. Knowing that the rope exhibits an even wear pattern, it can be assumed that the position of a single outer wire varies randomly every time the rope passes over the sheave. For example the position of a wire during ten hoisting cycles could be as indicated by the numbers 1 to 10 in the figure.

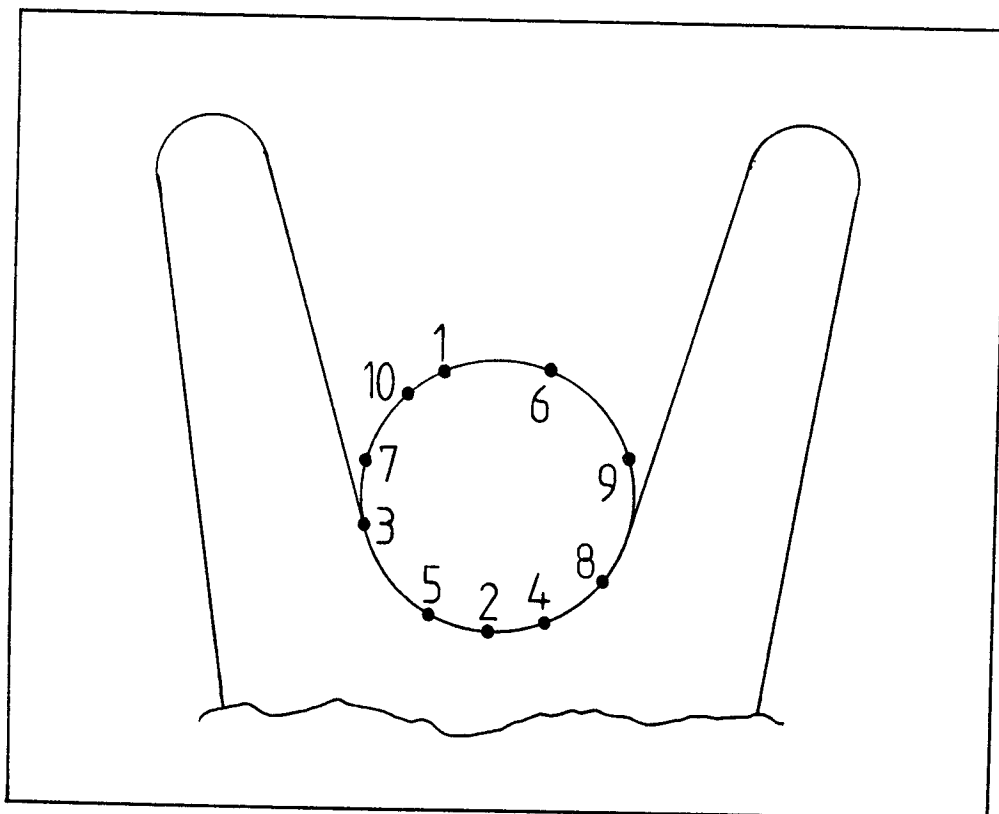


**Figure 2.1** - Rope contact on the sheave wheel.

If the rope rotation is properly understood and modeled then it may be possible to predict the rope degradation more precisely. This is however far beyond the scope of the present project but it allows ample room for further work.

The CSIR in conjunction with external consultants conducted a feasibility study into the possibility of developing a steel wire rope testing machine. It is intended that the machine would accurately simulate rope behaviour in the shaft. In the design of such a machine it would be vital to include the torque-tension rotation effects which a rope experiences in service. To simulate these effects an accurate model of the behaviour is required.

It is important to note that such torque-tension models as described above do already exist, but they do not accurately predict the rotational behaviour of the rope under different loading conditions. Also, when they were derived they did not take into account actual maximum and minimum lay length

variations as found in the shaft.

### 3. OVERVIEW OF EXISTING THEORY

#### 3.1 TORQUE-TENSION ROTATION

Typical torque-tension rotation characteristics of a TSR are shown in Figure 3.1 below. These curves resulted from tests conducted on 44 mm diameter TSR. The torque-tension machine at the CSIR laboratory was used to do the testing. It can be seen from the curves that there is an approximately linear relationship between torque and tension. There is a slight vertical shift in the lines, depending on the end rotation of the specimen and the lines tend to fan out at higher values of torque and tension. The fanning out is believed to be due to the rope being more resistant to twisting at high values of rope tension. This could be as a result of the rope acting more like a unit or solid under higher tension.

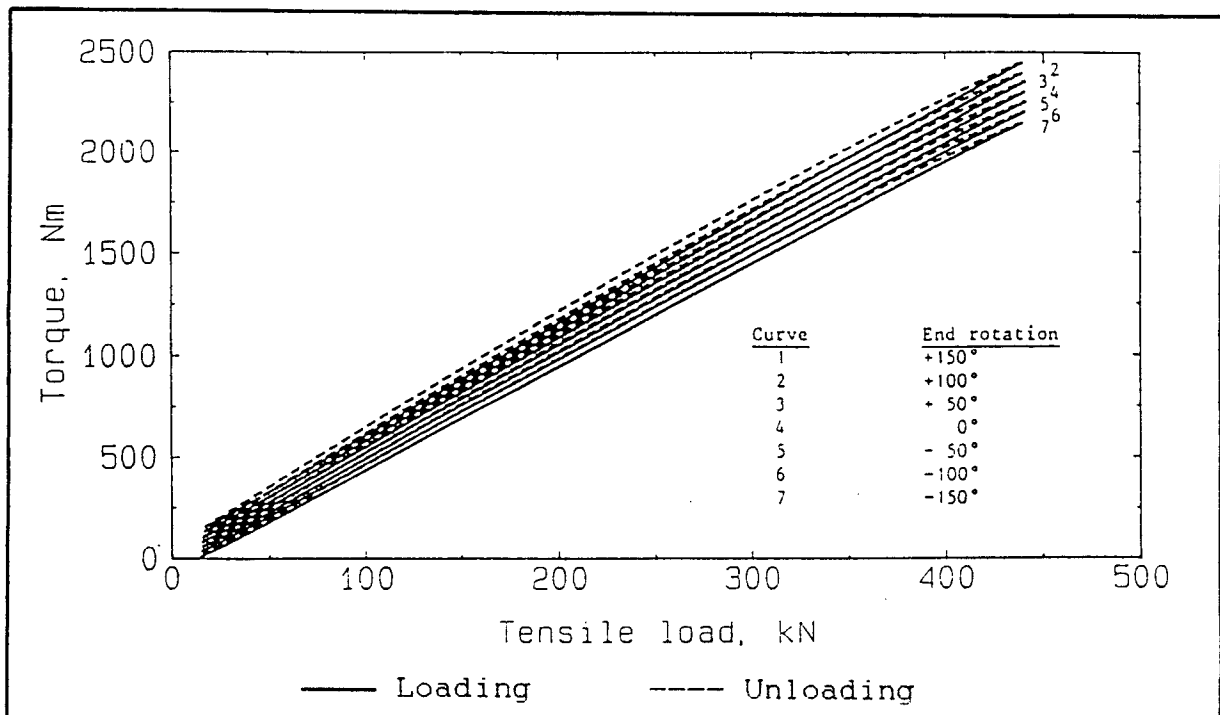


**Figure 3.1** - Torque-tension curves of a 44 mm TSR. Taken from Yiassoumis (1992).

Now in order to determine the rope rotation from these

curves, there are two approaches. The first approach involves fitting an equation directly to the torque-tension rotation curves and then by manipulation of that equation, obtaining the rope rotation.

The second requires the calculation of C and T factors from the raw data which then can be manipulated to give an equation for rotation.

Overviews of these two methods are given below. It is intended that both methods will be applied to the results obtained from the tests conducted in this project.

### 3.1.1 DIRECT DATA FIT METHOD

From torque-tension curves, like the ones illustrated in Figure 3.1 above, it is possible to determine a mathematical model which describes the rope behaviour. In deriving a model there are three components to consider :

- i. The approximately linear relationship between torque and tension.
- ii. The vertical shift of the lines, depending on the initial rope rotation before testing.
- iii. The fanning out of the lines at higher values of torque and tension.

It was found by Van Zyl (1993) that these characteristics of the rope behaviour could be accounted for by an equation of the form :

$$M = a.F + b.R.F + c.R \quad (1)$$

where

M	=	rope torque in Nm
F	=	rope tension in N
R	=	rope twist in °/m

The values of the constants a, b and c depend on the rope

diameter and the rope construction. The values of these constants for a 48mm TSR are given below. Note that these constants were obtained by fitting equation (1) to the results of torque-tension rotation test conducted on a 48mm Langs lay TSR specimen.

$$\begin{aligned}
 a &= 5.37 \times 10^{-3} && \text{m} \\
 b &= 5.20 \times 10^{-6} && \text{m}/(^{\circ}/\text{m}) \\
 c &= 2.64 && \text{Nm}/(^{\circ}/\text{m})
 \end{aligned}$$

Examining equation (1) it can be seen that the first term results in the linear relationship between torque and tension. The second term causes the torque-tension curves to fan out at higher values of torque and tension. The third term shifts the lines vertically depending on the initial rope rotation angle.

Using equation (1) it is possible to calculate and plot the approximate torque-tension rotation curves for a 48mm rope. Table 3.1 below shows the torque values for different rope tensions and twists. Actual tests have only been done up to a maximum of 75°/m but for purposes of illustration it has been assumed that equation (1) holds true for 100°/m and larger angles too.

**Table 3.1** - Torque-tension rotation table for a 48mm TSR.

TENSION F (kN)	TORQUE M (Nm)									
	M = a.F + b.R.F + c.R									
	TWIST R (°/m)									
	100	75	50	25	0	-25	-50	-75	-100	
0	234.0	198.0	132.0	66.0	0.0	-66.0	-132.0	-198.0	-264.0	
50	558.5	466.0	413.5	341.0	266.5	196.0	123.5	51.0	-21.5	
100	858.0	774.0	695.0	616.0	537.0	456.0	379.0	300.0	221.0	
150	1147.5	1062.0	978.5	891.0	805.5	720.0	634.5	549.0	463.5	
200	1442.0	1350.0	1258.0	1166.0	1074.0	982.0	890.0	798.0	706.0	
250	1736.5	1638.0	1539.5	1441.0	1342.5	1244.0	1145.5	1047.0	948.5	
300	2031.0	1926.0	1821.0	1716.0	1611.0	1506.0	1401.0	1296.0	1191.0	
350	2325.5	2214.0	2102.5	1991.0	1879.5	1768.0	1656.5	1545.0	1433.5	
400	2620.0	2502.0	2384.0	2266.0	2149.0	2030.0	1912.0	1794.0	1676.0	
450	2914.5	2790.0	2665.5	2541.0	2416.5	2292.0	2167.5	2043.0	1918.5	
500	3209.0	3078.0	2947.0	2816.0	2685.0	2554.0	2423.0	2292.0	2161.0	
550	3503.5	3366.0	3228.5	3091.0	2953.5	2816.0	2678.5	2541.0	2403.5	
600	3798.0	3654.0	3510.0	3366.0	3222.0	3078.0	2934.0	2790.0	2646.0	



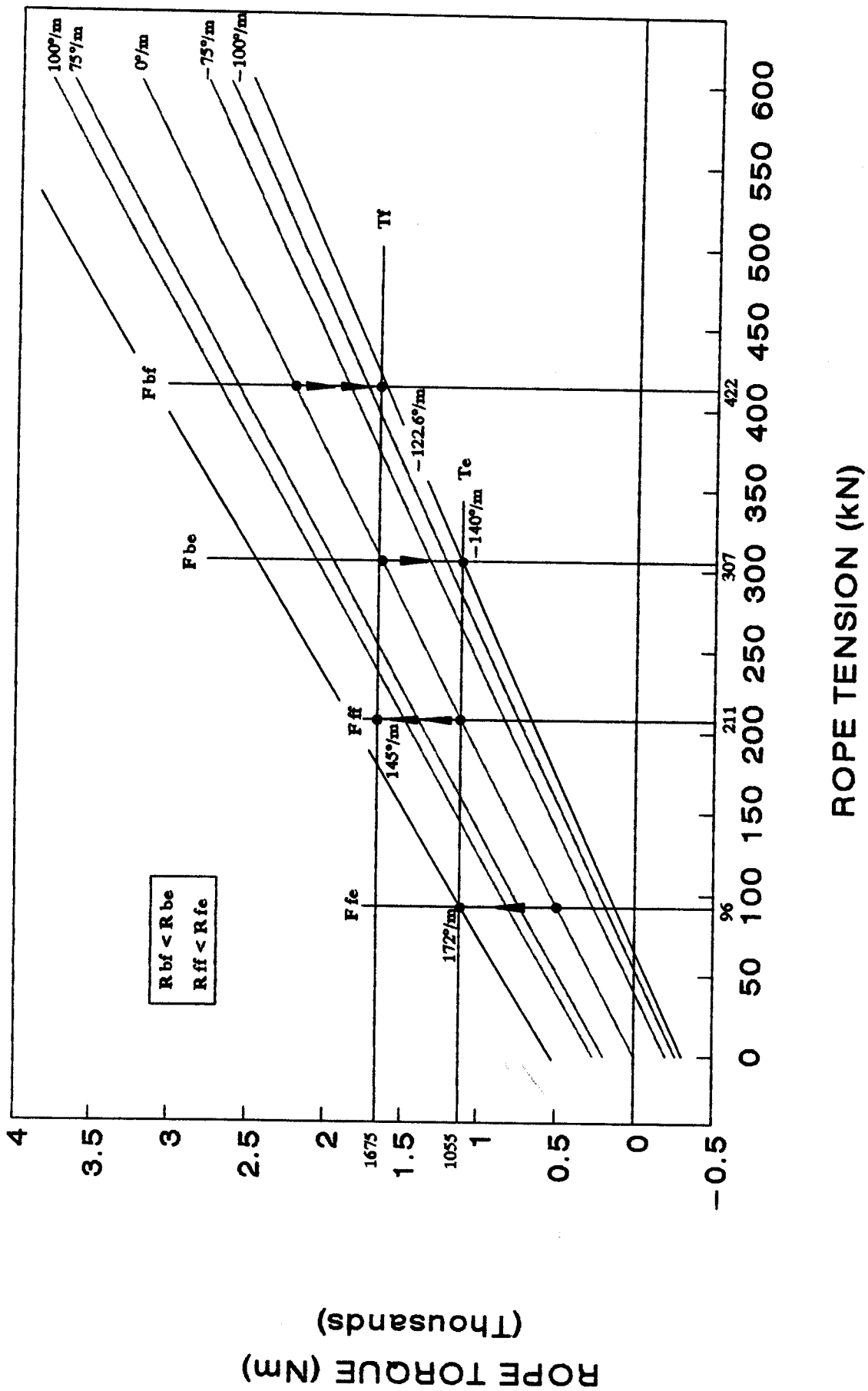


FIGURE 3.2 - TORQUE--TENSION ROTATION CURVES OF A 48mm TSR.

Some of the values in Table 3.1 are plotted in Figure 3.2. In order to demonstrate the nature of the torque-tension rotation characteristics of the rope an example has been plotted on the torque-tension curves. The values assumed in the example are :

Conveyance weight empty	=	96 kN
Conveyance weight full	=	211 kN
Rope length	=	2204 m
Rope weight / metre	=	96 N/m
Rope torque empty	=	1055 Nm
Rope torque full	=	1675 Nm

The various abbreviations on Figure 3.2 are detailed in the key below :

F fe	-	Rope tension front end empty.
F ff	-	Rope tension front end full.
F be	-	Rope tension back end empty.
F bf	-	Rope tension back end full.
Te	-	Rope torque empty.
Tf	-	Rope torque full.
R fe	-	Rope twist front end empty.
R ff	-	Rope twist front end full.
R be	-	Rope twist back end empty.
R bf	-	Rope twist back end full.

When the conveyance is at shaft bottom and is empty it can be seen, from Figure 3.2, that the front end of the rope must wind up from  $0^\circ/\text{m}$  to  $172^\circ/\text{m}$ . The back end must unwind from  $0^\circ/\text{m}$  to  $-140^\circ/\text{m}$ . The winding up of the front end and the unwinding of the back end will result in them reaching the torque equilibrium value  $T_e$ . These rotations are shown by the single arrows in Figure 3.2.

Similarly when the conveyance is loaded the front end must reach an equilibrium twist of  $145^\circ/\text{m}$  and the back end  $-122.6^\circ/\text{m}$ . This will result in the front and back end of the rope both having an equilibrium torque of  $T_f$ . The loaded twists are shown by the double arrows in Figure 3.2.

This rope twist results in considerable changes in lay length. For TSR's operating in deep level shafts, lay lengths of up to 100% longer than the manufactured lay at the back end and 30% shorter at the front end have been observed, McKenzie (1990). For the 48mm TSR with which this project is concerned, the as manufactured lay length would be 361 mm and the lay length should change to approximately 300 mm at the front end and 510 mm at the back end. This is based on data measured on the rope while it was operating in the shaft.

How the values of rope twist were determined will be discussed hereafter. At this point it is however interesting to note that the rope rotates in one direction when installed in the shaft and then when the conveyance is loaded, it rotates in the other direction. This does not seem logical but it occurs. This reverse rotation upon loading is a result of the fanning out of the torque-tension curves. If the curves were parallel then the rope would not rotate at all when the conveyance was loaded.

It can be seen that the reverse rotation occurs by comparing the values of front and back end twist for the empty and loaded skip conditions. In both cases the "empty" twist are larger than the "full" twists.

From equation (1) it is possible to write an equation for the rope twist  $R$  in  $^\circ/\text{m}$ . This has the form :

$$R = \frac{M - a.(q.z + P)}{c + b.(q.z + P)} \quad (2)$$

where  $q =$  weight per unit length of rope

$P$  = weight of the mass attached to the end of  
the rope

$z$  = rope length measured from skip

By integrating equation (2) with respect to  $x$  and then writing the result for torque  $M$  it is possible to calculate the values of  $T_e$  and  $T_f$  given in the previous section. Since  $R$  is  $d\Phi/dz$ , integrating  $R$  with respect to  $z$  gives the rotation  $\Phi$ . Knowing that  $\Phi = 0$  at  $z=0$  and  $z=\text{total length}$  gives  $T_e$  and  $T_f$ . Dividing  $\Phi$  by 360 gives the number of turns which the rope makes in terms of distance from the skip,  $z$ .

Curves can be plotted which will predict the twist of the rope at different distances from the conveyance located at shaft bottom. Figure 3.3 shows these curves. The point of 0 twist is located slightly off centre at 1051 m from the conveyance. The exact centre position is 1102 m from the conveyance. The maximum values of twist at the two ends of the rope are determined from equation (2).

The maximum level of twist,  $\pm 75^\circ/\text{m}$  per meter, to which TSR specimens have been tested are indicated in Figure 3.3. It can be seen from the graph that these values do not cover the whole length of the rope. Only the middle 1247 m of the rope falls into the test limits.

The rope twist curves are not completely linear. This is due to the fanning out of the torque-tension rotation curves shown in Figure 3.1.

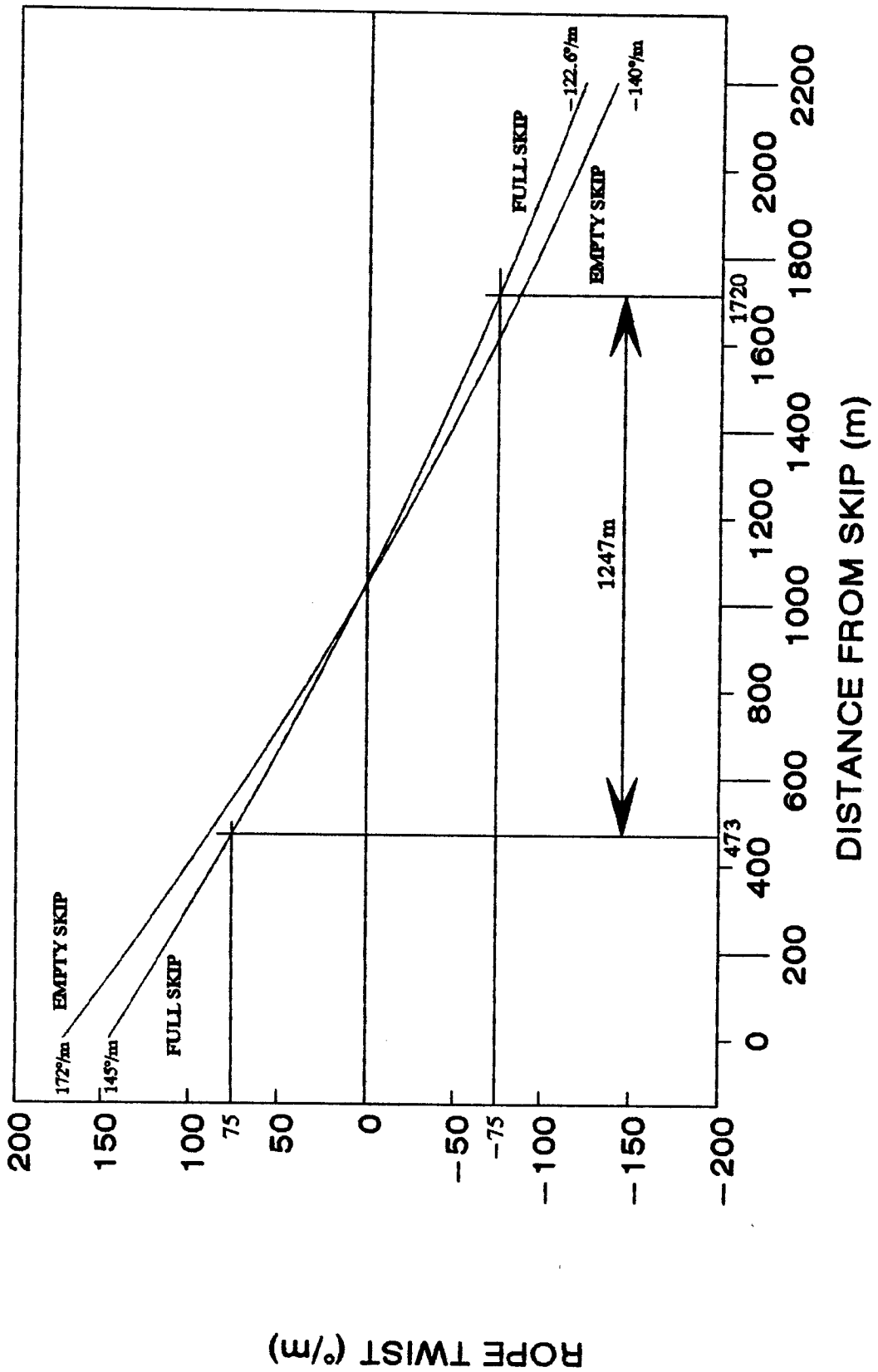


FIGURE 3.3 - ROPE TWIST AS A FUNCTION OF POSITION ALONG THE ROPE.

Note that the rope twist, in the empty and full skip states, is larger at the front end than at the back end. This is associated with the spacing between the torque-tension rotation curves due to the fanning effect. If one examines Figure 3.2 it is apparent that a 10 mm vertical shift in the lower tension range, implies more rotation than the same shift in the higher tension range. As was stated previously the rope tends to act more as a solid unit under higher tension. Therefore its resistance to rotation increase with tension.

Figure 3.4 shows the rope rotation ( $\Phi/360$ ) as a function of distance from the skip. The difference in rotation between empty and full skip conditions is also indicated.

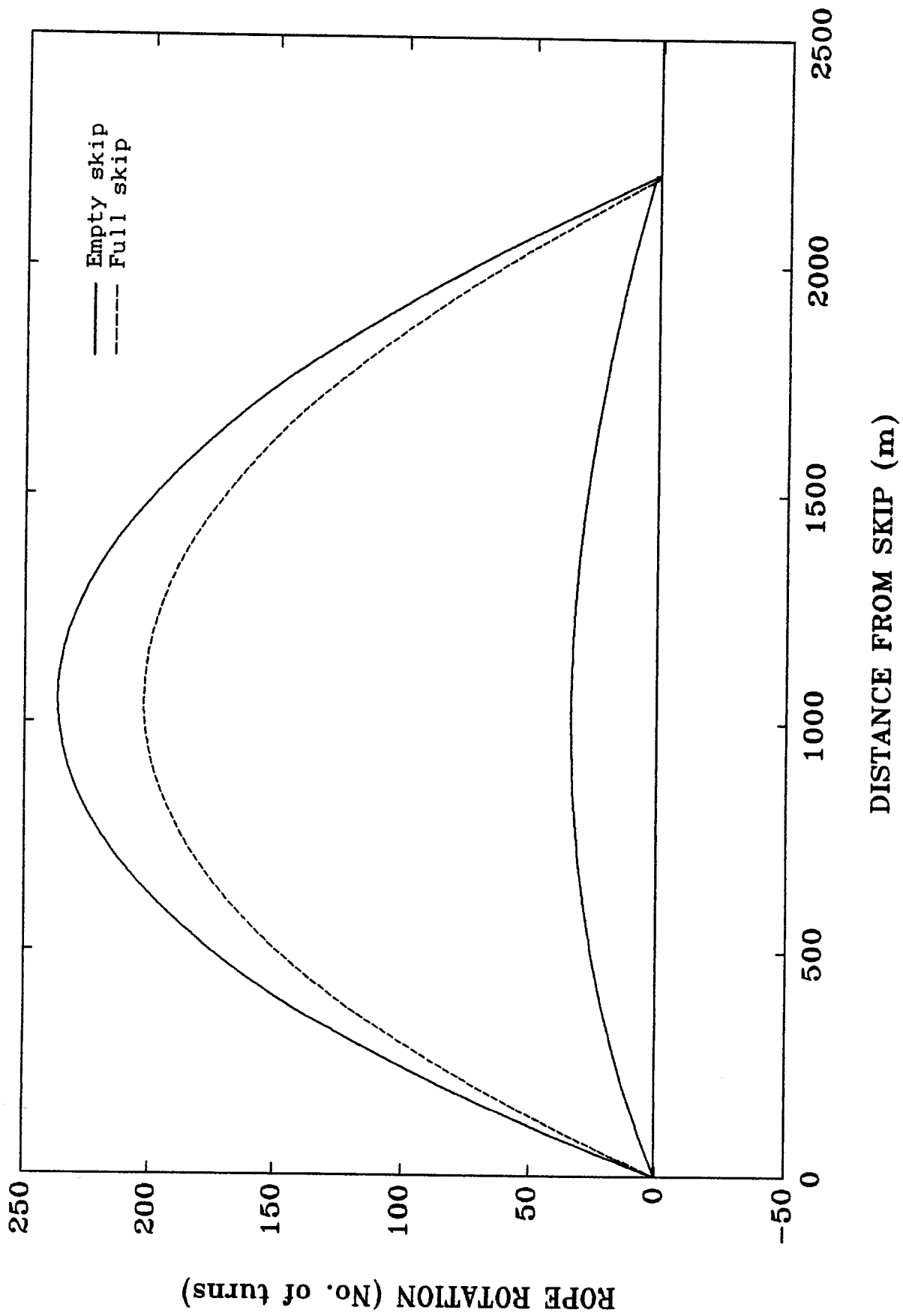
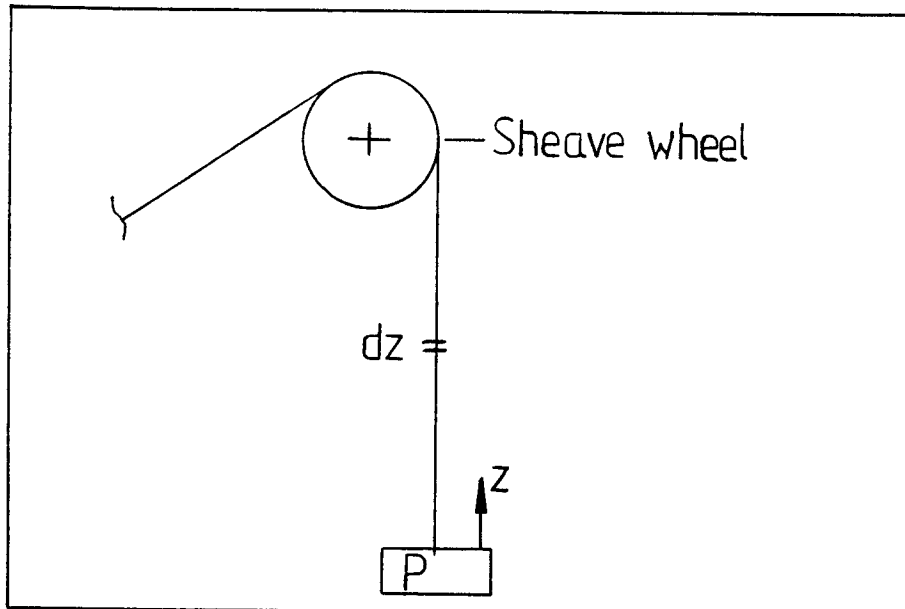


FIGURE 3.4 - IN-SHAFT ROPE ROTATION.

### 3.1.2 C AND T FACTOR METHOD

The rope and load layout as used in this approach is shown below :



**Figure 3.5** - C and T factor rope and load layout.

In this method, the test torque-tension rotation values are used to determine C and T factors where :

$$C = \frac{\Delta \text{ Torque}}{\Delta \text{ Force}} \quad (3)$$

$$T = \frac{\Delta \text{ Torque}}{\Delta \text{ Twist}} \quad (4)$$

According to Borello (1993b) the torque factor, C, is a function of rope force. The torsional stiffness, T, is a function of twist. So, C and T can be described by :



$$C = a_c + b_c \cdot \frac{d\Phi}{dz} \quad (5)$$

$$T = a_t + b_t \cdot F \quad (6)$$

$$F = P + z \cdot q$$

The constants  $a_c$ ,  $b_c$ ,  $a_t$  and  $b_t$  are determined from C and T factor plots for the rope concerned. As in the Direct Data Fit method, the tests were only conducted up to values of + and - 75°/m.

The torque in the rope is given by :

$$M = C \cdot F + T \cdot \frac{d\Phi}{dz} \quad (7)$$

M is a constant torque depending on the end load. If equations (5) and (6) are substituted into equation (7) then an equation for  $d\Phi/dz$  can be obtained :

$$\frac{d\Phi}{dz} = \frac{M - a_c \cdot (P + q \cdot z)}{(b_c + b_t) \cdot (P + q \cdot z) + a_t} \quad (8)$$

Integrating equation (8) with respect to z and applying the boundary conditions  $\Phi=0$  at  $z=0$  and  $z=\text{total rope length}$  yields the constant of integration and the constant torque, M. All the other constants are known. P varies depending on whether the skip is full or empty. ?  $\phi \neq 0$  at  $z=L$

$$\Phi = \frac{M - P \cdot a_c}{q \cdot (b_c + b_t)} \cdot \ln(B + z) - \frac{a_c}{b_c + b_t} \cdot (z \cdot \ln(z+B) - ((z + B) \cdot \ln(z + B) - (z + B))) + C$$

$$\text{Where } B = \frac{P \cdot (b_c + b_t) + a_t}{q \cdot (b_c + b_t)}$$

The integral of equation (8) with respect to  $z$  gives equation (9), the rotation of the rope in degrees. Dividing this rotation by  $360^\circ$  gives the number of turns the rope makes in terms of distance from the skip,  $z$ .

### 3.3 VALIDITY OF THEORY

The most obvious problem with the both methods outlined in the above two sections is that they only considers the middle section of the rope. Tests that have been conducted to  $\pm 75^\circ/\text{m}$  twist do not take into consideration the effects of the front and back ends of the rope. These are however the most critical areas since they show the highest values of twist along the rope length. Also, the front and back ends are where the minimum and maximum lay length variations occur.

In the preceding discussions it was assumed that equation (1) and (7) hold true for all angles of twist. In fact beyond  $\pm 75^\circ/\text{m}$  it is not known whether the equations model the rope torque-tension behaviour at all.

There is a definite need to conduct torque-tension tests which will include twist angles as high as say  $200^\circ/\text{m}$  to  $300^\circ/\text{m}$ . From the results of these tests it will be possible to comment on whether equation (1) holds true for higher values of twist. If it does not hold true then a new torque-tension rotation model can be derived which will cover the full range of twists.

A measurement has been done on a 48mm TSR in service which showed that the rope rotated by -12.5 turns, at 600 m from the conveyance, upon loading of the conveyance. The present model based on the direct data fit predicts that the rope should have rotated -28 turns at this point. The C and T factor model predicts that the should have rotated -43 turns.

After discussion with Borello and Van Zyl it is believed that this high error between the actual and predicted rotation has connection to the inadequate testing which was done in deriving the model.

## 4. EXPERIMENTATION

The steel wire rope, torque-tension rotation testing facility used for the purpose of this project is located at the CSIR Mine Hoisting Technology laboratories in Cottesloe Johannesburg.

### 4.1 EXPERIMENTAL EQUIPMENT

The test apparatus can be categorised into three components namely, the mechanical system, electrical data acquisition and control system the control software.

#### 4.1.1 MECHANICAL SYSTEM

The torque-tension machine consists of a steel frame bolted to the laboratory floor. A general arrangement diagram of the machine is shown in Figure 4.1 below.

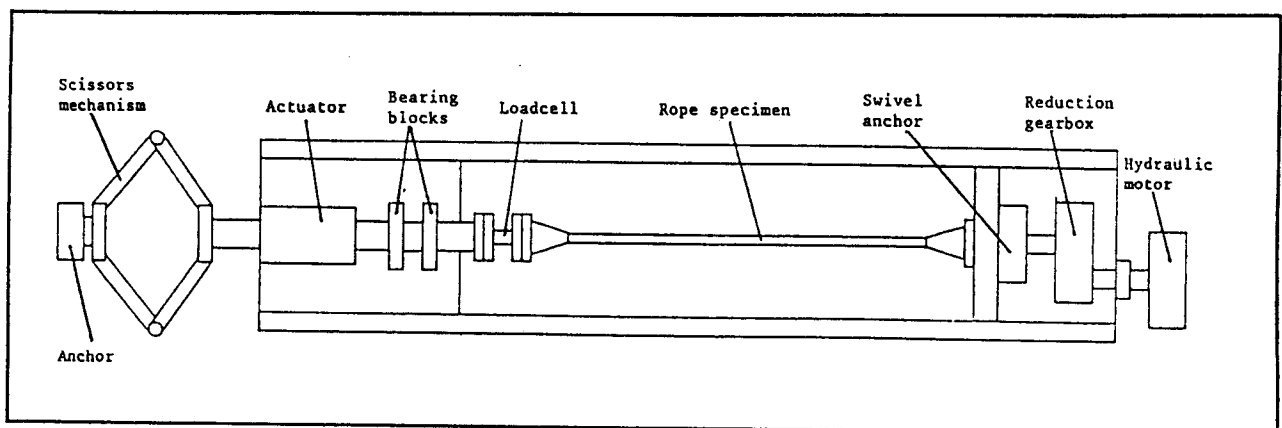


**Figure 4.1** - General arrangement of torque-tension machine. Taken from Yiassoumis (1992).

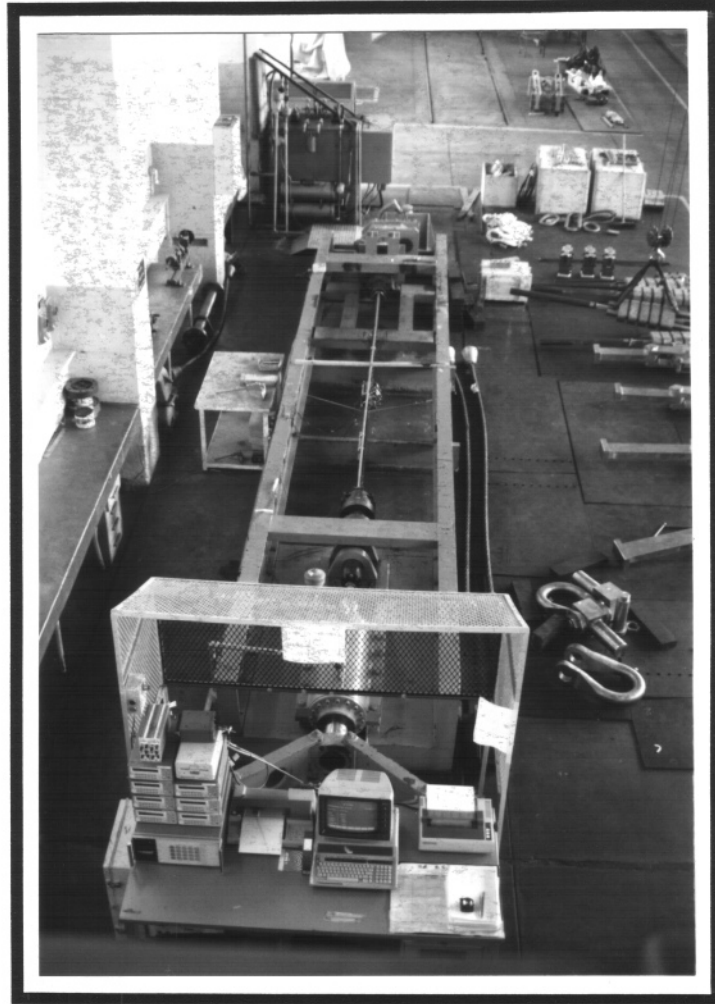


**Figure 4.2** - CSIR Rope torque-tension machine.

The machine can accommodate rope specimens of length 2750 mm and 4050 mm. For this project 4050 mm specimens were used. Conical type grips on either end of the machine secure the rope specimen.

The one grip is attached to a reduction gearbox powered by a hydraulic motor. This allows it to be rotated in both directions. A clamp type friction brake is fitted to the output shaft of the motor. Once a rotation has been set the brake is tightened preventing any rotational movement of the conical grip during testing. The following photograph shows the hydraulic motor, friction brake, reduction gearbox and the swivel anchor at the rotation end of the machine.



**Figure 4.3** - Test machine rotation components.

A rotation gauge is fitted to the rope-side shaft of the reduction gearbox. This indicates to within  $0,5^\circ$  the rope rotation over the specimen length. The rotation gauge arrangement is shown in Figure 4.4.

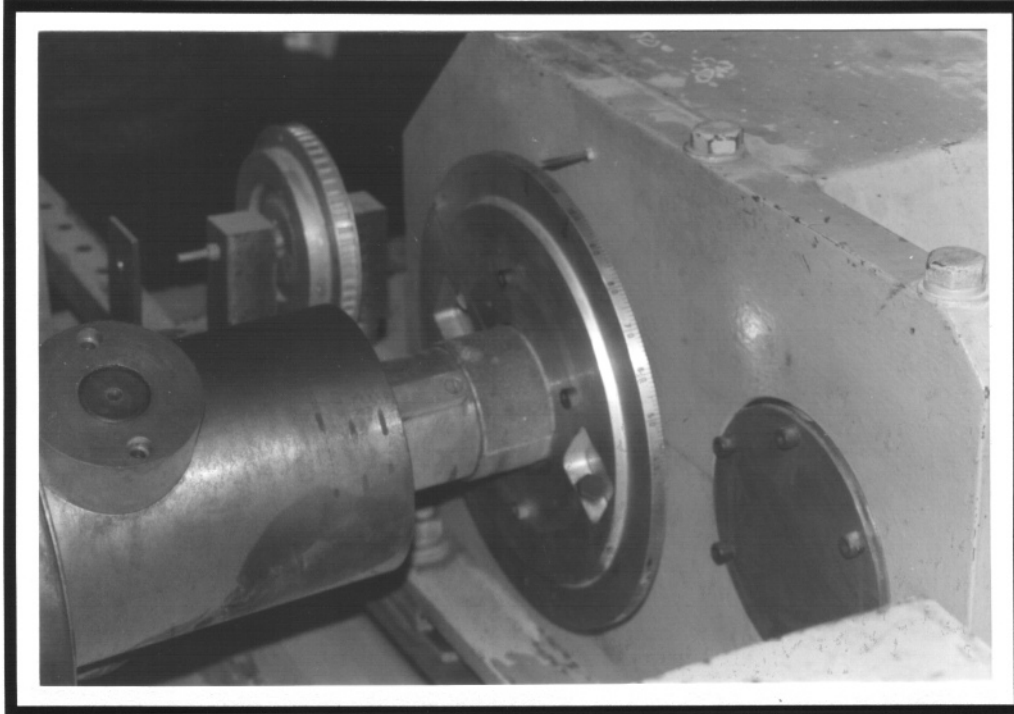


**Figure 4.4** - Rope rotation gauge.

On the loading end the second grip is bolted in series with a torque-tension load-cell to a hydraulic cylinder. This end cannot rotate. Rotation is prevented by a scissor mechanism attached to the rear side of the hydraulic cylinder and fixed to an anchor also bolted to the laboratory floor.

The strain gauge load-cell has a 500 kN / 3000 Nm capacity.

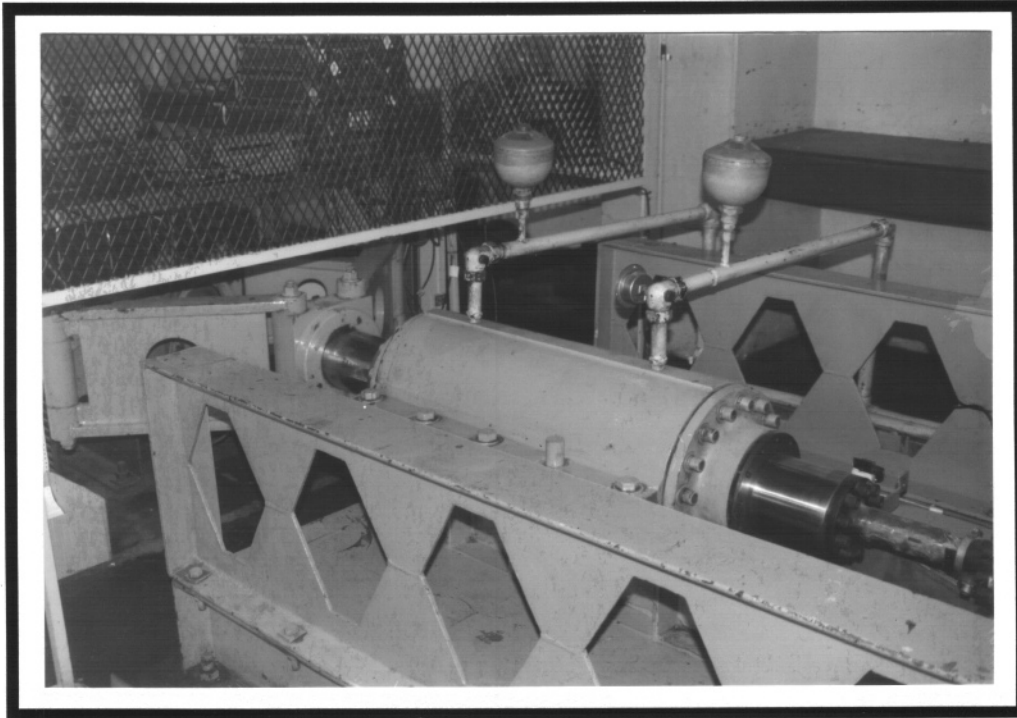


**Figure 4.5** - Scissor mechanism and hydraulic cylinder.

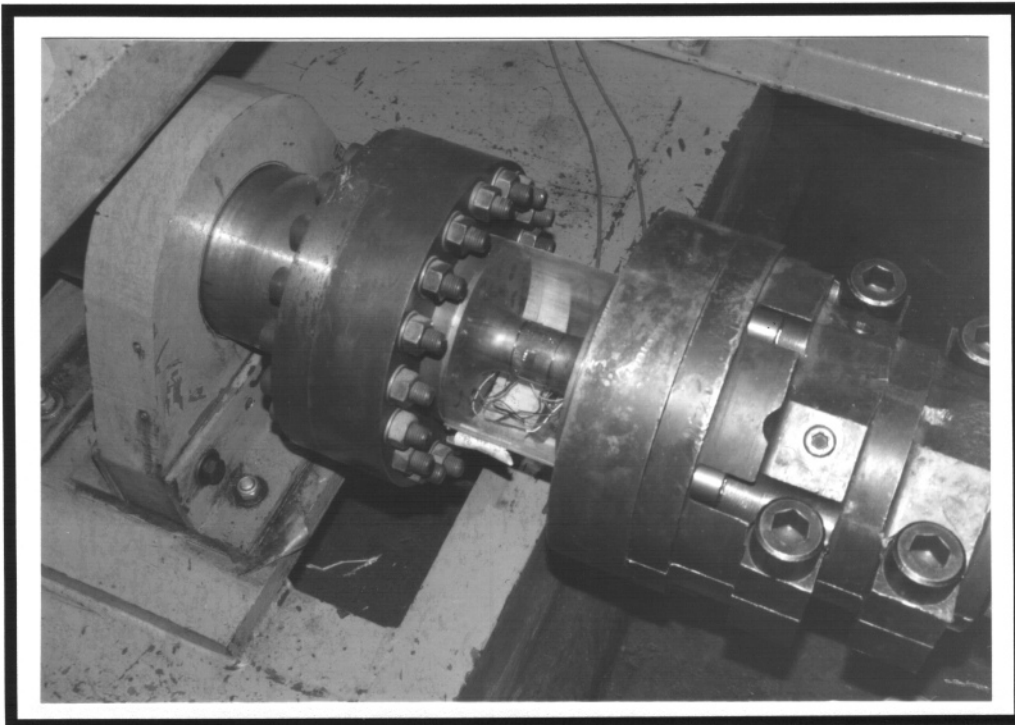


**Figure 4.6** - Load-cell and loading end grips.

Both the hydraulic tensioning cylinder and the rotation motor are powered the hydraulic unit located at the rotation



end of the machine. Hydraulic fluid is passed through a water heat exchanger which is connected to a Sulzer cooling tower located outside the laboratory. Figure 4.7 shows the unit and the electrical control panel. Hydraulic circuit diagrams for the tensioning cylinder and for the rotation motor are included in APPENDIX A.

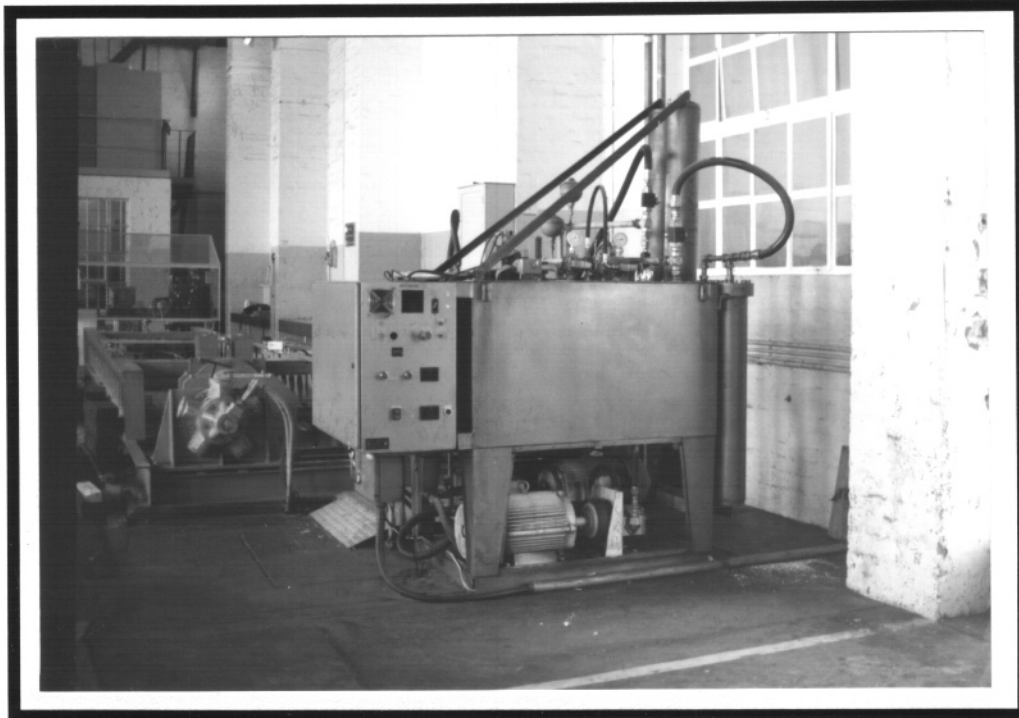


**Figure 4.7** - Test machine hydraulic unit.

An telescoping extensometer bar is attached across the length of the rope specimen. This bar enables the elongation between the two conical grips to be measured. A Linear Variable Differential Transformer (LVDT) is clamped onto the outer tube of the extensometer bar. The LVDT nib rests against a small plate screwed onto the inner tube of the extensometer. When the inner and outer tubes move relative to one another the LVDT senses the change.

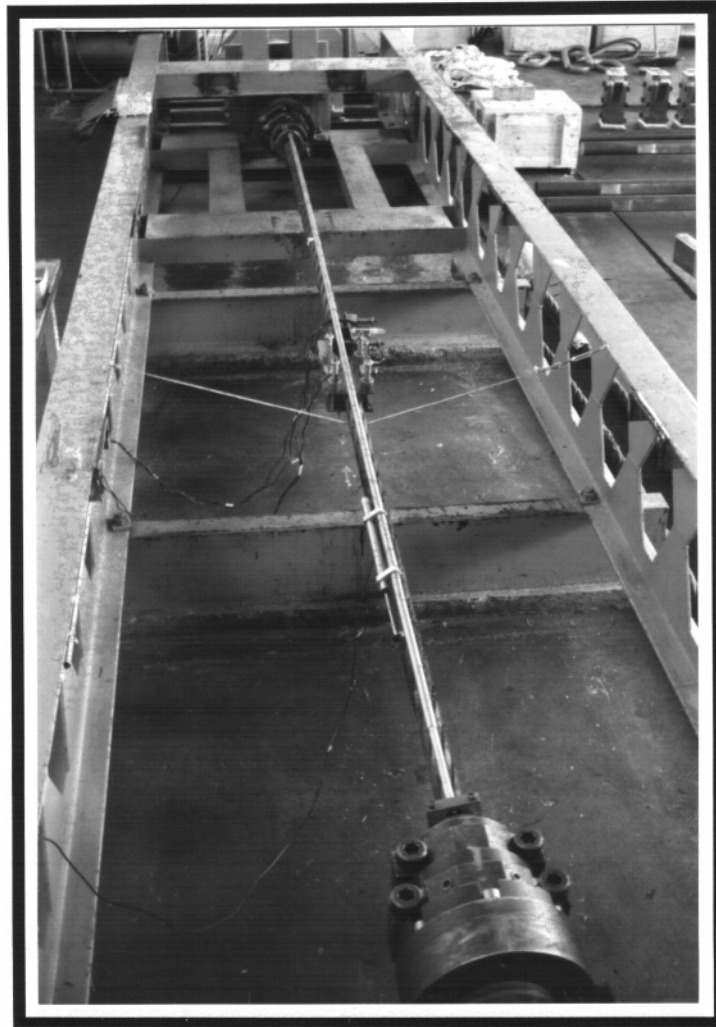


**Figure 4.8** - Extensometer bar between loading and rotation end conical grips.

A diameter measuring bracket is connected to the rope in the centre between the two grips. The bracket consists of two sets of flat plates at  $90^\circ$  to each other. The rope passes in between these sets of plates. In each set the one plate is fixed and the other movable. The moveable plates are pushed onto the rope by four sets of springs. Each plate has two Linear Variable Differential Transformers which sense any change in diameter. In Figure 4.9 the whole bracket and a detail of one set of plates is shown.

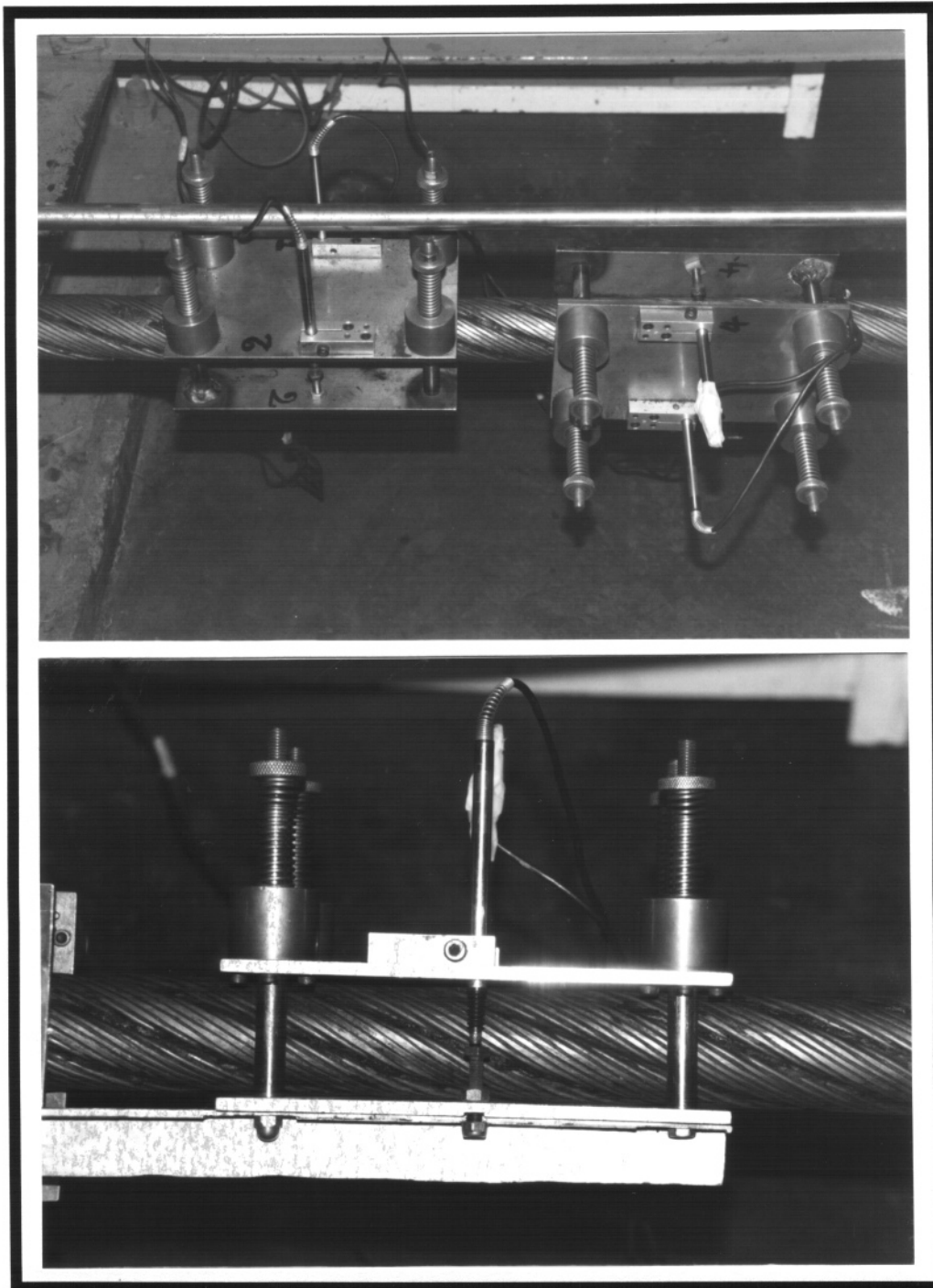


**Figure 4.9** - Diameter measuring bracket.

It is also necessary to accurately measure the diameter of the rope before testing commences. The measurement is taken with a rope vernier as detailed in Figure 4.10.

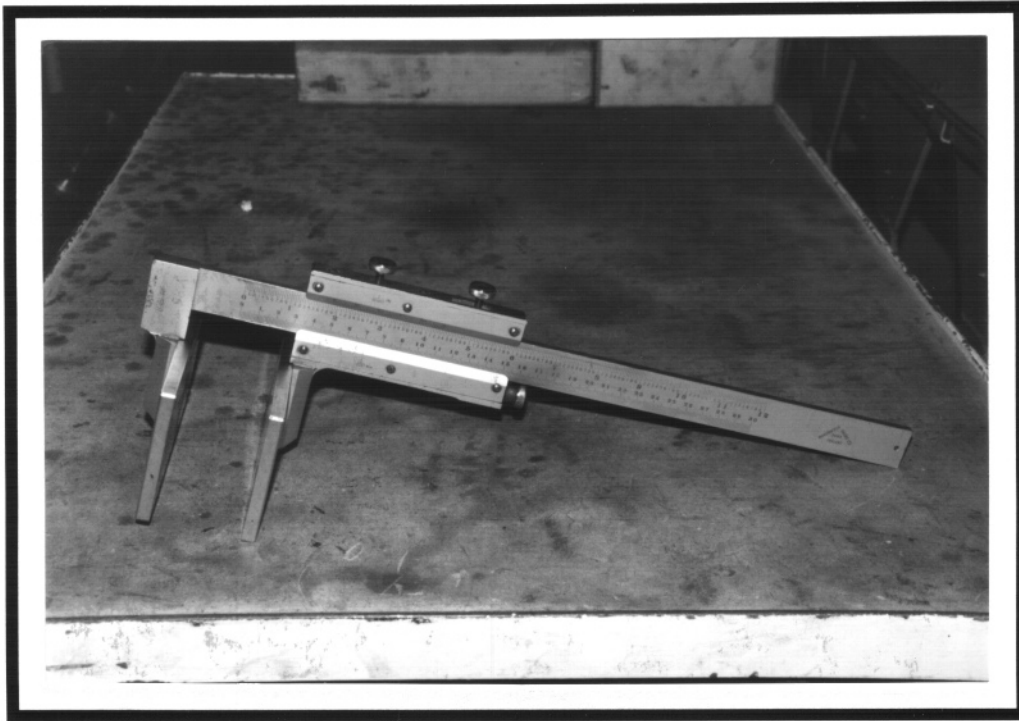
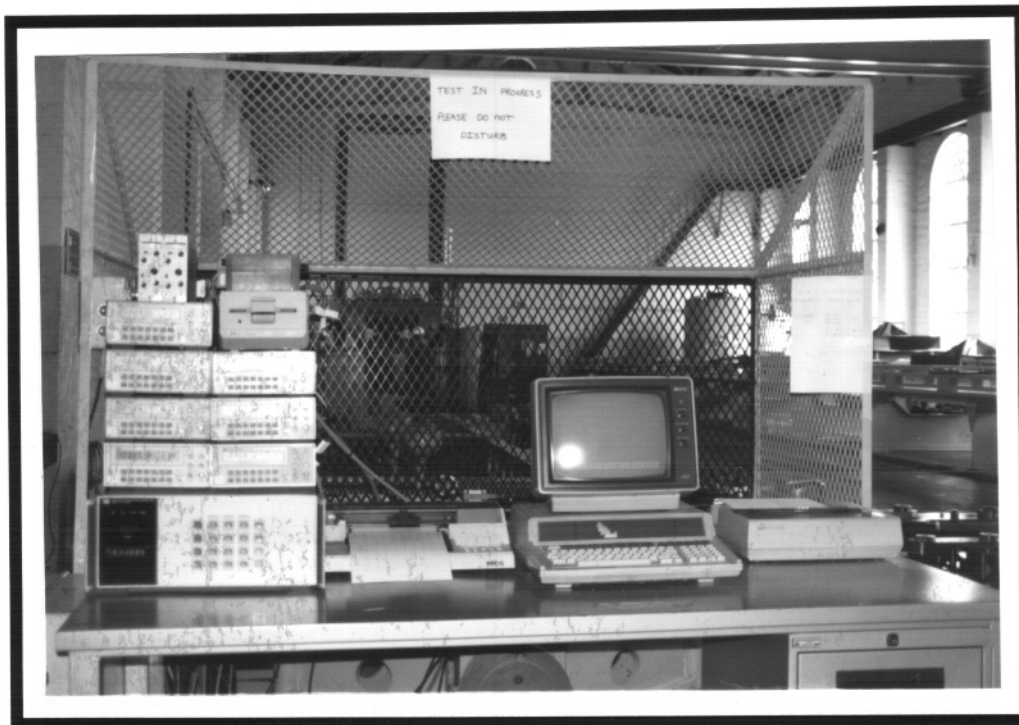


Figure 4.10 - Rope vernier.

#### 4.1.2 ELECTRICAL DATA ACQUISITION AND CONTROL SYSTEM

All the test data acquisition and control of the testing is processed by a Hewlett Packard (HP) 86 computer.



**Figure 4.11** - Test control table.

For data output and storage during testing the HP 86 is equipped with a HP pen plotter, a dot matrix printer and a floppy disk drive. The output voltages of the four diameter LVDT's and the extensometer LVDT are fed directly into five HP 3478 digital multimeters (DVM).

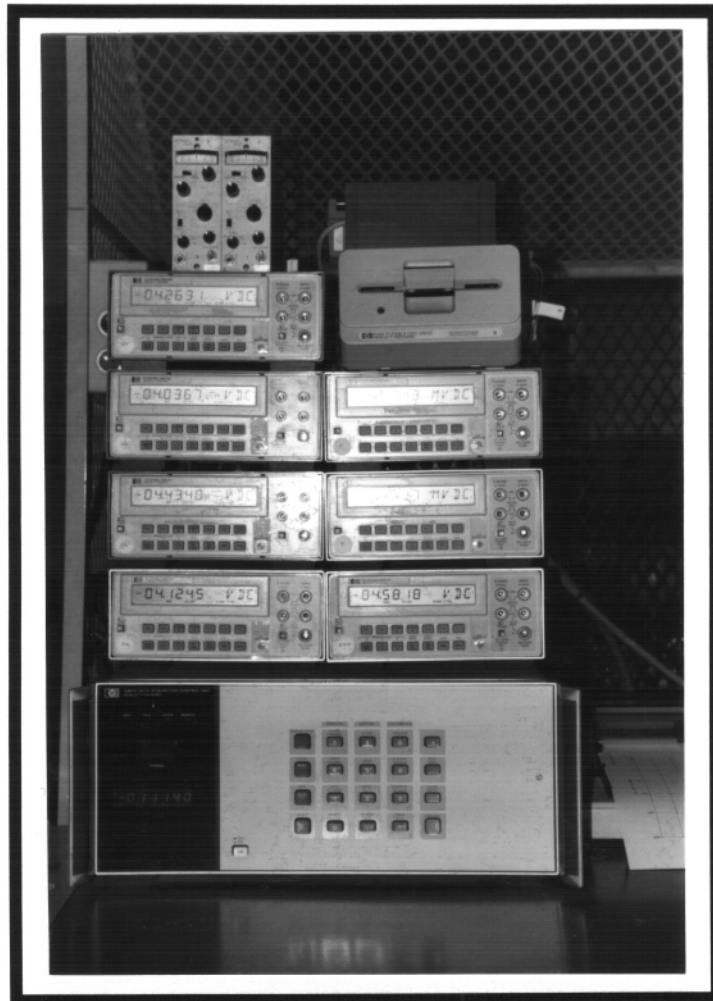


**Figure 4.12** - Strain gauge amplifies, floppy disk drive, DVM's and Data Acquisition/Control Unit.

The voltage outputs from the torque and force strain gauge bridges are first fed through two Kyowa stain gauge amplifies and then into two HP 3478A DVM's.

These DVM's are capable of direct interfacing with the HP 86 computer via an HP-IB (Interface Bus) card. In this manner the computer can access each DVM individually and read the voltage at any instant during a test.

All seven DVM's are connected in series with a Data Acquisition and Control Unit to the HP-IB card inserted into one of the four external card slots at the rear of the computer. Access to each of the DVM's is made possible by an addressing system using DIP switches on the rear of each

DVM. In this way an unique address can be set to enable the computer to identify the DVM's.

Calibration accuracy of the measurement instruments was insured by the fact that they had been calibrated by the manufactures four months prior to the testing.

The Data Acquisition and Control Unit houses the digital to analog card for communication with the proportional valve control card at the hydraulic unit. The D/A card receives a digital signal via the HP-IB and converts it to a analog signal acceptable to the valve control card. This set up allows the computer accurate control of the three position solenoid operated proportional valve.

Manual control of the machine is made possible by a hand control box. This allows the tightening and slacking of the rope during the setting up procedure. Rope rotation can also be adjusted. The bottom two switches enable on/off and directional control of the hydraulic motor.

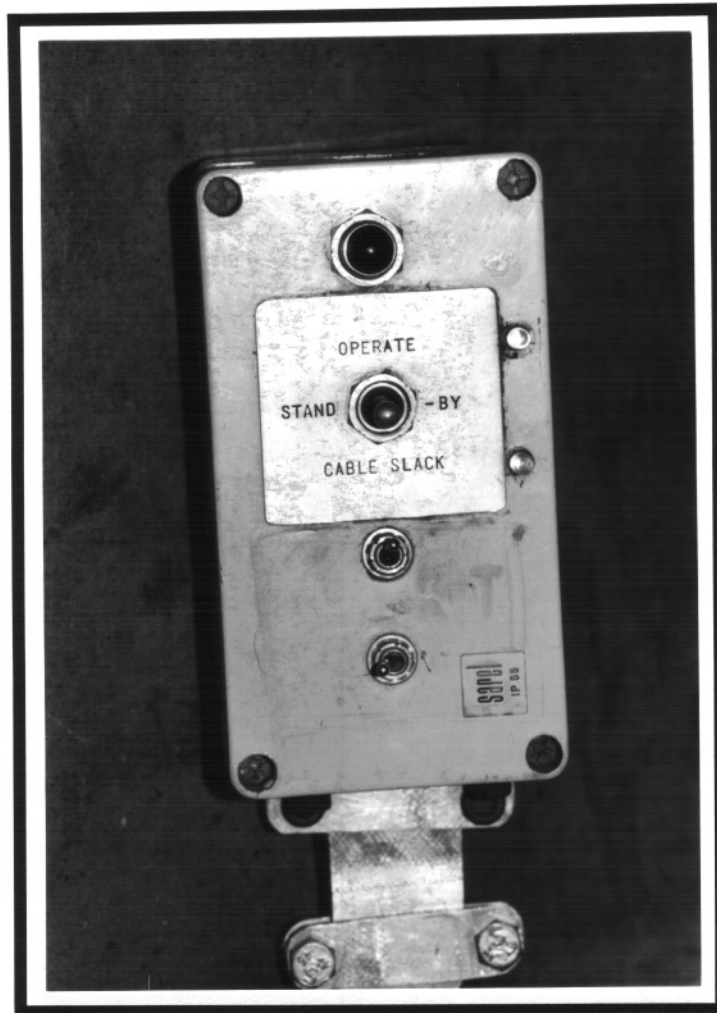


**Figure 4.13** - Manual control box.

Two end of stroke indicator lights on the right of the box light up when the hydraulic cylinder contacts one of the two limit switches located at the physical limits of its stroke.



### 4.1.3 CONTROL SOFTWARE

The program "T\_T\_TEST", is used by the HP computer to run the torque-tension rotation tests. From the start of a test the user is informed by the program as to what actions to take to successfully complete the tests.

First the rope and test information as well as the file name for the test results are entered. Two data files are created, one for general test information and one for the test results. LVDT and load-cell calibration instructions are then given and the calibrations are automatically read by the computer. General test information is printed out and a Torque verses Tension graph frame is plotted.

The user is also prompted for the speed at which the test must be conducted. At this point the actual testing can commence. The program runs two optional bedding in cycles on the rope specimen before the actual test. Here the maximum load is 10% of the rope breaking force. The actual test runs up to 30% of the rope breaking force or 500 kN which ever is smaller. But the torque has a limit of 3000 Nm so if this level is reached before the tensile load limit is reached the load is decreased again.

"T\_T\_TEST" can run up to ten curves or cycles without re-calibration of the equipment. At the end of each cycle the torque verses tension in the rope for the cycle is plotted and the test results stored on disk. The user is then prompted to change and enter a new rope end rotation whereafter the next bedding cycles and test commence.

A more detailed description of "T\_T\_TEST" is contained in APPENDIX B. Due to the confidential nature of the program a complete listing has not been included. The first page of the program is given so that the program structure can be shown. "T\_T\_TEST" was not written completely by the author. It is modified version of a less advanced control program

"Test C&T", originally developed by the CSIR. The modifications made in order to adapt the original software for the purposes of this project are also explained in APPENDIX B.

## 4.2 EXPERIMENTAL PROCEDURE

### 4.2.1 PREPARATION

Six specimens of discarded 48mm 6x32(14/12/6▲)/F rope were supplied by the CSIR. The specimens were originally cut from two ropes, an underlay rope and an overlay rope at the front, middle and back ends. They were cut to a length of 4490 mm. Two white metal collars were then cast onto the specimen ends so as to define a gauge length of 4050 mm.

At this point the ends were unlaidd, cleaned and then white metal conical end caps were cast onto them. This resulted in a specimen as shown in Figure 4.14.

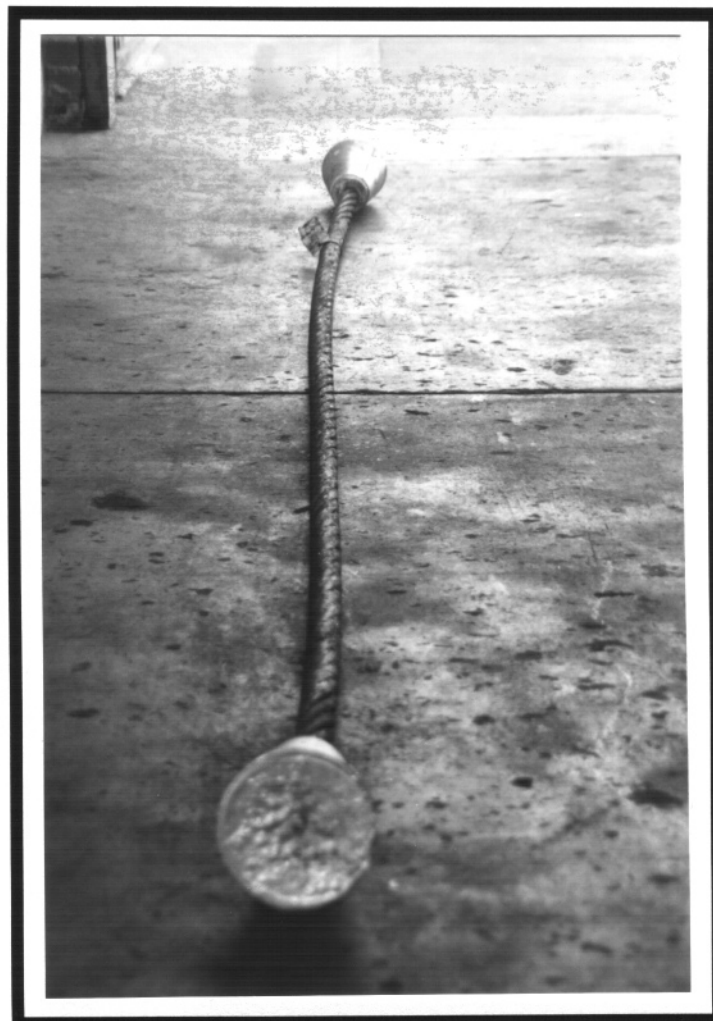


**Figure 4.14** - Rope test specimen (length 4050 mm).

The following six specimens were prepared as above and were ready for testing :

- Underlay and Overlay back
- Underlay and Overlay front
- Underlay and Overlay middle

The conical end grips of the testing machine were then opened up and the first rope's end caps were each placed in a grip. With the rope in the slack position, the grips were closed and tightened completely.

Using the manual control box the rope was pulled tight so that the white metal collars protruded from the grips. The grub screws on top of the grips were then tightened so as to prevent the end caps from rotating inside the grips.

Once the rope was installed the middle section of the rope was cleaned on the surface so that the diameters and lay lengths could be accurately measured. The diameter measuring bracket was attached to the cleaned section of rope.

The telescoping extensometer bar was clamped onto the two protruding white metal collars. When clamping the extensometer LVDT onto the bar care had to be taken to allow for at least 35 mm travel of the LVDT nib so that the extension calibration could be done.

#### **4.2.2 TESTING**

When the rope had been installed and all the equipment attached to the rope, the test program "T\_T\_TEST" was run. The following steps were taken to complete a set of test curves on a rope :

1. It was ensured that the rope was at 0° rotation or at the required starting point and that the friction brake was on.

2. The rope was made completely slack and the strain gauge bridges were balanced.
3. A preload of  $\pm 10\%$  of the rope braking force was placed on the rope and the diameter DVM voltages were set in the range -4 to -4.5 V. This was done by physically adjusting the diameter LVDT's.
4. The file name under which the test data and information was to be stored was entered.
5. If the maximum calculated force was above 500 kN then the new required test force was entered.
6. The rope was made completely slack to allow the reading of the zero force and torque references.
7. The load-cell calibration switches were switched on. This placed parallel resistors of known value across one arm of each strain gauge bridge. The strain gauge amplifier gains were then set to values automatically determined by the program. This ensured precise calibration of the load-cell to match predetermined accurate values.
8. A 30 mm calibration block for the extensometer LVDT and 2 mm calibration plates for the diameter LVDT's were inserted so that the program could determine their calibration values.
9. The required test speed was entered, between 2 and 8, and the first set of bedding in cycles were started. For all the tests a speed of 6 was used.
10. The bedding in cycles were automatically followed by the actual test which was allowed to run to completion. Once the test was complete the torque-tension curve was plotted.
11. At this point the rope specimen lay length was measured and recorded.
12. The friction brake was then unlocked, a new rotation was set and the brake locked again. The new rotation was entered and the next bedding in cycles started.

Steps 10 and 12 were repeated until the desired number of curves had been run or until the tenth curve was run whereafter the program stopped.

#### 4.2.3 ROPE SPECIMEN END ROTATION

One of the main requirements of the testing was to simulate rope lay length changes as found in a working shaft. In fact, lay length is the only parameter which can relate test conditions to in shaft conditions.

Measurements conducted by the CSIR showed that the maximum lay length of the ropes while in the shaft occurred at the back end of the underlay rope, 503 mm. The minimum lay length occurred at the front end of the overlay rope, 303 mm. These measurements were taken approximately every month over the two year working life of the ropes.

For the back underlay specimen a pre-test lay length of 427 mm was measured. This translated to 9,485 lays over a gauge length of 4050 mm. As a rough estimate, the following calculation was used to determine the rotation required to obtain a lay length of 600 mm, which is sufficient to cover any in-service lay length change.

$$4050/600 = 6,75 \text{ lays.}$$

$$\text{Required rotation} = (6,75-9,485) \times 360 = -985^\circ$$

The program "T\_T\_TEST" can handle 10 curves so it was decided to use steps of  $-120^\circ$  resulting in a final rotation of  $-1080^\circ$ .

The back end of a triangular strand Langs lay rope always unwinds and the front end always winds up. It was therefore decided to only unwind the back end specimens from  $0^\circ$  to  $-1080^\circ$  and to only wind up the front end specimens from  $0^\circ$  to  $1080^\circ$ .

On the middle sections a rotation range from  $-600^\circ$  to  $480^\circ$  was deemed adequate since the middle sees less severe lay length changes in-service. Also the middle section of the in-shaft rope experiences both positive and negative twists

so it is necessary for the same during testing.

For the purposes of consistency increments of  $\pm 120^\circ$  were used in all cases.

#### 4.2.4 TEST LIMITATIONS

During the course of the testing certain limitations were encountered with the equipment. These are outlined below :

- On unwinding the back end section of rope the actual gauge length of the specimen becomes greater. It was found that at high angles of rotation ( $-840^\circ$  to  $-1080^\circ$ ) the extensometer ran out of stroke. With one specimen the hydraulic cylinder also ran out of stroke at  $-1080^\circ$ .

The solution to this would be to use an extensometer LVDT with a larger stroke and to have slightly shorter specimens of say 4000 mm gauge length.

- On winding up the front end specimen the gauge length, at high angles of rotation ( $840^\circ$  to  $1080^\circ$ ), became so short that the telescoping extensometer rod ran out of stroke. The extensometer could therefore not be used for these high angle tests.

The extensometer rod would have to be modified if further tests were to be done to high angles of rotation.

- On the front end specimen, at end rotations of above  $240^\circ$  the measured torque went beyond 3000 Nm at which point the program started to decrease the load on the rope. Results could therefore not be obtained in this region. It may be considered to increase the torsional capacity of the load-cell in order to accommodate torques up to say 4000 Nm.

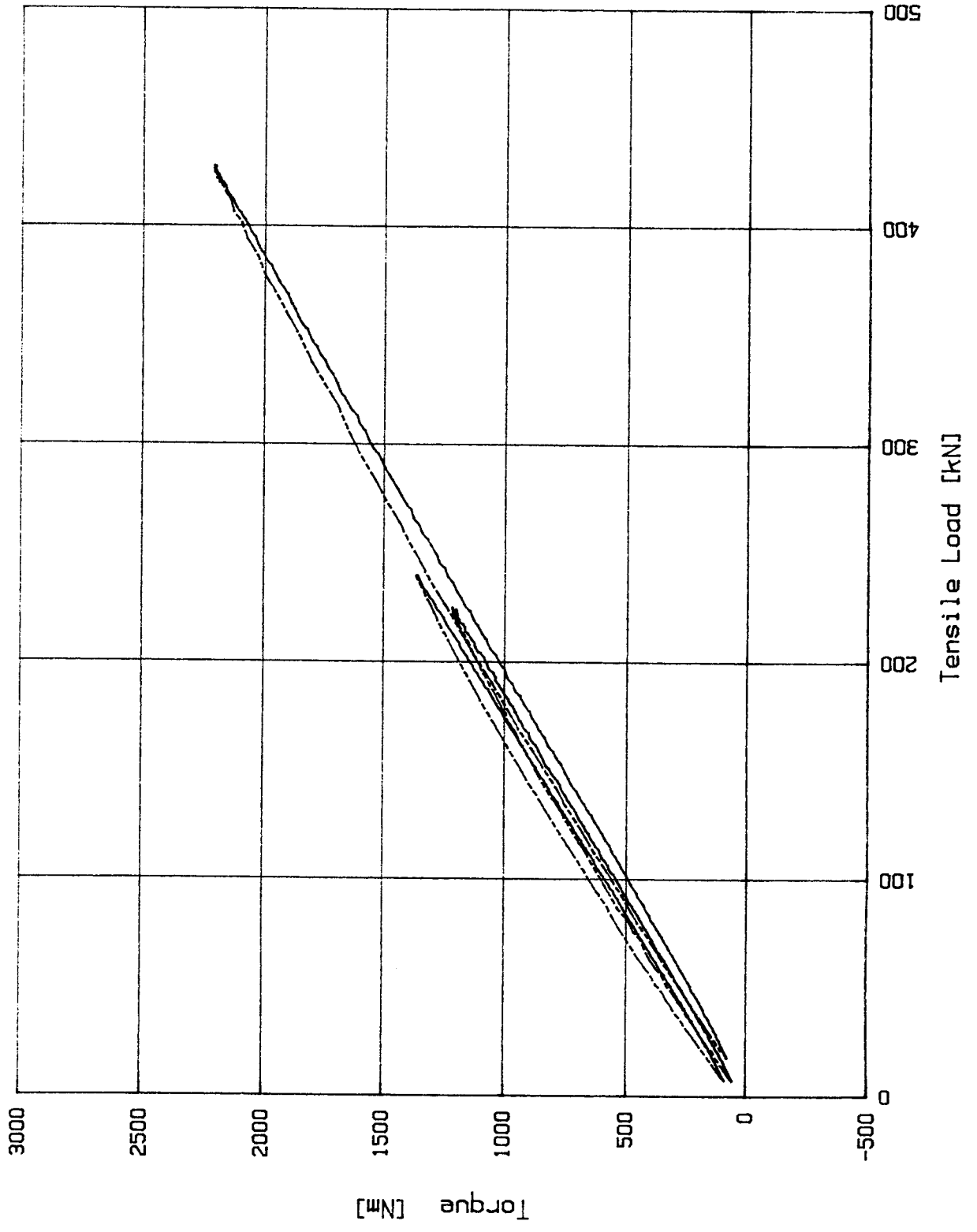
- During some of the torque tension tests it was found that the hydraulic cylinder was not able to tension the rope specimen to the required 500 kN. There was no apparent explanation for this and no pattern. The only fact that was noted was that the components in the hydraulic circuitry were getting particularly hot. Temperature measurements found the outer surface temperatures to be in the range 45 to 55°C.

According to the valve specifications the maximum fluid operating temperature is 70°C. With an outer surface temperature of 45 to 55°C it is quite likely that the fluid temperature is near the operating limit. This could cause the valve to stick and limit the operation of the hydraulic cylinder.

The high temperature of the fluid was caused by one cooling tower being shared with another hydraulic unit in the laboratory. It is also suspected that the heat exchanger of test machine hydraulic unit could be dirty. This would worsen the overheating. Figure 4.15 shows the effect which the overheating had on test results.

At the start of the project, it was intended that all six rope specimens would be tested to give results for front, middle and back ends of an underlay and overlay rope. The problems with the overheating of the hydraulic unit started during the test on the middle underlay specimen.





FNTOL  
 FIG.4.15 - Overheating effect on test results.

It was fortunate that this test could be completed successfully thereby giving a full set of results for the underlay rope.

However the overheating problem worsened with the test on the first overlay rope. Due to the time constraints of the project it was decided to stop the testing since it would take too long to service the hydraulic unit heat exchanger. The other hydraulic unit using the cooling tower could also not be switched off due to CSIR fatigue test contract commitments.

It was felt that the decision to stop testing would not negatively affect the project result because a full set of results for one rope had already been obtained. The results for the overlay rope would have been used for purposes of comparison. It is unlikely that there would be a great difference in torque-tension rotation properties of used underlay and overlay ropes.

**5. TORQUE-TENSION TEST RESULTS**  
**AND ANALYSIS**

**5.1 GENERAL TEST INFORMATION**  
**AND CALIBRATION DATA**

For each test the control program printed out the general information that was entered for the test as well as the instrumentation calibration data as determined during the calibration procedures.

The printouts for the three tests are contained in APPENDIX C. The original CSIR rope test certificate for the underlay rope is also included.

**5.2 LAY LENGTH MEASUREMENTS**

After each curve of a test had been completed the rope lay length was measured. These measurements are shown, with their corresponding end rotations and twist values, in the following three tables.

**Table 5.1 - Back underlay test lay lengths.**

<b>BCKUL</b>			
<b>CURVE No.</b>	<b>END ROTATION (deg)</b>	<b>TWIST (deg/m)</b>	<b>LAY LENGTH (mm)</b>
1	0	0	427
2	-120	-30	445
3	-240	-59	470
4	-360	-89	490
5	-480	-119	500
6	-600	-148	525
7	-720	-178	555
8	-840	-207	580
9	-960	-237	610
10	-1080	-267	660

According to the in-shaft measurements supplied by the CSIR, the underlay back end lay lengths varied from 451 mm to 503 mm. These actual lay lengths clearly fall into the test lay length range of 427 mm to 660 mm.

**Table 5.2** - Middle underlay test lay lengths.

MIDUL			
CURVE No.	END ROTATION (deg)	TWIST (deg/m)	LAY LENGTH (mm)
1	-600	-148	510
2	-480	-119	480
3	-360	-89	470
4	-240	-59	460
5	-120	-30	440
6	0	0	405
7	120	30	385
8	240	59	370
9	360	89	355
10	480	119	345

The in-shaft measurements for the middle section of the rope showed lay length variations of between 380 mm and 408 mm. Once again the test lay lengths more than adequately covered this range.

**Table 5.3 - Front underlay test lay lengths.**

<b>FNTUL</b>			
<b>CURVE No.</b>	<b>END ROTATION (deg)</b>	<b>TWIST (deg/m)</b>	<b>LAY LENGTH (mm)</b>
1	0	0	385
2	120	30	378
3	240	59	354
4	360	89	345
5	480	119	330
6	600	148	315
7	720	178	310
8	840	207	305
9	960	237	295
10	1080	267	290

The in-shaft front end lay lengths were between 308 mm and 336 mm. The test lay lengths covered this range

In all of the above tests it is clear that lay length decreases with positive rotation or twist and increases with negative rotation or twist.

It should be noted that the 0° lay length of the specimens are not all the same. Considering a nominal or as manufactured lay length of 361 mm the back and middle have permanent sets above this value. The front end has a permanent set below 361 mm. This as a result of the permanent negative and positive twist conditions which the rope experiences in the shaft.

### **5.3 TEST DATA MANIPULATION**

The program "T\_T\_TEST" created three data files during the testing period. The files BCKUL, MIDUL and FNTUL contained all the measurements taken for the three specimens.

Data in these files are actual values of tension (kN),

torque (Nm), elongation (mm) and the four diameter changes (mm).

The program "T\_T\_PLOT" was run which read in the test data, one file at a time. Where necessary the data was manipulated by "T\_T\_PLOT" to produce the five output plots namely :

- Torque versus load
- Elongation versus load
- Diameter versus load
- Torque factor versus load
- Torsional stiffness versus load

In all the plots, the curves for different rotations within that test are displayed on the same graph. As with the control program "T\_T\_TEST", "T\_T\_PLOT" was not written completely by the author. It is a modification of a program "Plot C&T" originally developed by the CSIR.

"T\_T\_PLOT" can process a set of ten curves per test. A description of "T\_T\_PLOT" is contained in APPENDIX D. Due to the confidential nature of the program a complete listing has not been included. The first page of the program is given so that the program structure can be shown. The modifications made in order to adapt the original software for the purposes of this project are also explained in APPENDIX D.

Prior to running "T\_T\_PLOT" the data files created by "T\_T\_TEST" had to be made smaller. The reason for this was the limited memory facilities of the HP 87 computer on which "T\_T\_PLOT" was run. The conversion program "FSMALL" was used for this purpose.

"FSMALL" reads the data file into an array and then rewrites the file using every fourth set of data in the array. A listing of this program is contained in APPENDIX E.

## 5.4 TORQUE-TENSION ROTATION CURVES

For all three torque-tension rotation curves the torque increases in the negative direction. This is purely as a result of the test instrumentation set up.

The negative torque also results in negative Torque factors and negative Torsional stiffnesses. As with the torque value, it is the magnitude of the values and not the sign which is important.

### 5.4.1 BACK UNDERLAY

Figure 5.1 shows the torque-tension rotation curves for the back underlay specimen. For each curve the end rotation is indicated on the right hand side of the graph. Examining these curves the following is apparent :

- The lines strongly resemble previous test done on TSR with the typical linear relationship between torque and force. The fanning out effect of the lines at higher values of load is also clear.
- With increasing negative rotations the spacing between the lines decreases. This is due to the rope having a decreasing tendency to generate torque at higher values of negative twist or rotation. The spacing between the lines is larger than in previous tests on the same type of rope. The reason for this is that the step changes in rotation ( $-120^\circ$ ) is larger than any previous steps used.
- The calibration for this test was done at  $0^\circ$ . This is confirmed by the fact that the  $0^\circ$  curve, when extended, would pass through the 0 torque and force origin.

- The hysteresis of the curves between loading and unloading decreases with increasing negative angles of rotation. At  $-1080^\circ$  the hysteresis is almost negligible where at  $0^\circ$  it is much more pronounced. It is not known exactly what the cause of the hysteresis is however it could be a result of inter-wire contact forces in the rope. When the rope is unwound, these contact forces decrease. Therefore the inter-wire friction also decreases and the hysteresis effect is reduced.

It may also be considered that the hysteresis in the results is as a result of the behaviour of the strain gauge torque tension load cell. It may not be a characteristic of the rope.

- The starting points of the curves are shifted up and down depending on the end rotation. Increasing negative rotation decreases the value of the starting torque.

#### **5.4.2 MIDDLE UNDERLAY**

Figure 5.2 shows the torque-tension rotation curves for the middle underlay specimen. From the curves the following features are apparent :

- The lines do not all reach the 500 kN limit. This is partly due to the malfunctioning of the hydraulic system because of the overheating problems mentioned earlier. Also when the magnitude of the torque exceeds 3000 Nm the computer decreases the load. Measurements beyond 3000 Nm are therefore not possible.
- The lines fan out at higher values of load.
- The spacing between the lines increases with an increase in positive rotation.
- The hysteresis effect increases with increasing



rotation

- The calibration for this set of curve was done at - 600°.
- The torque value at the start of each curve increases with increasing rotation and decreases with decreasing rotation.
- The curves for 360° and 480° show a slight curvature at loads below 100 kN.

#### 5.4.3 FRONT UNDERLAY

Figure 5.3 shows the torque-tension rotation curves for the front underlay specimen. These set of curves have the same basic characteristics as the previous two. There are some points which should be noted :

- The hysteresis effect is exaggerated at high positive angles of rotation. The torque value at the end of the unloading does however compare with the value at the start of loading.
- As the positive angle of rotation increases the curvature at low loads becomes more obvious. In fact from around 720° onward the loading lines become curved along their whole lengths. It is therefore fair to say that at high angles of rotation the relationship between force and torque is no longer linear.

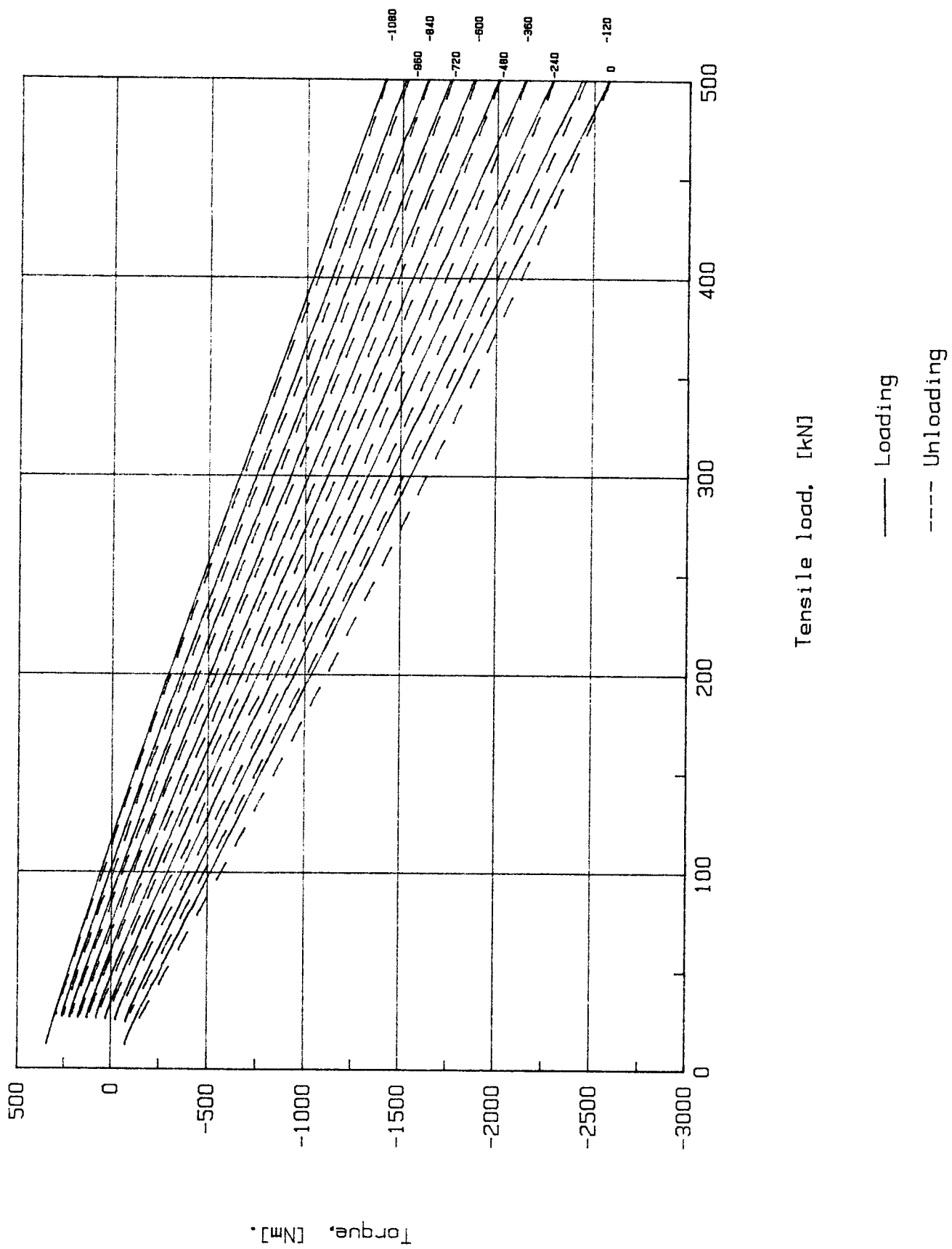


FIG. 51 - Torque-tension rotation curves, back underlay.

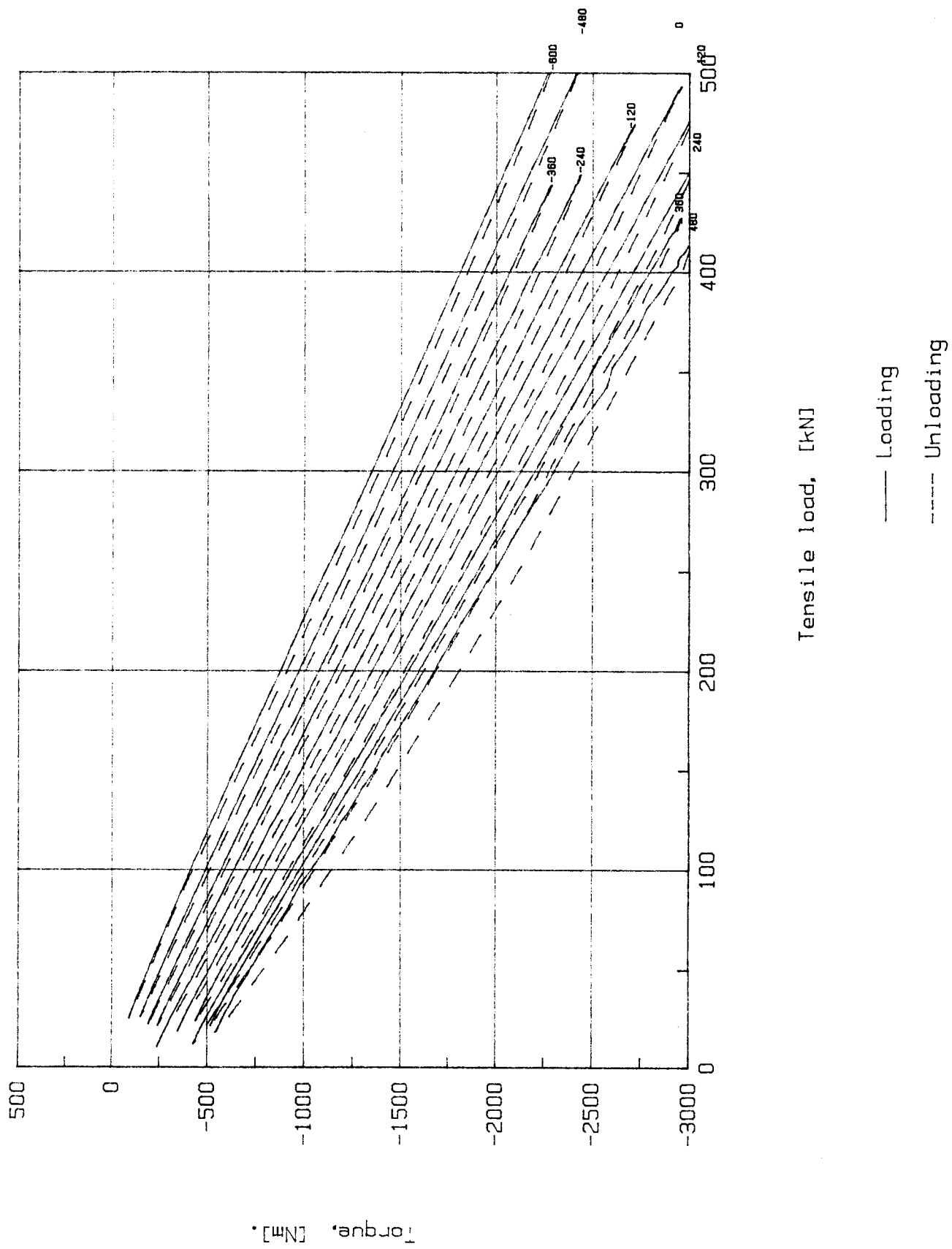


FIG. 5.2 - Torque-tension rotation curves, middle underlay

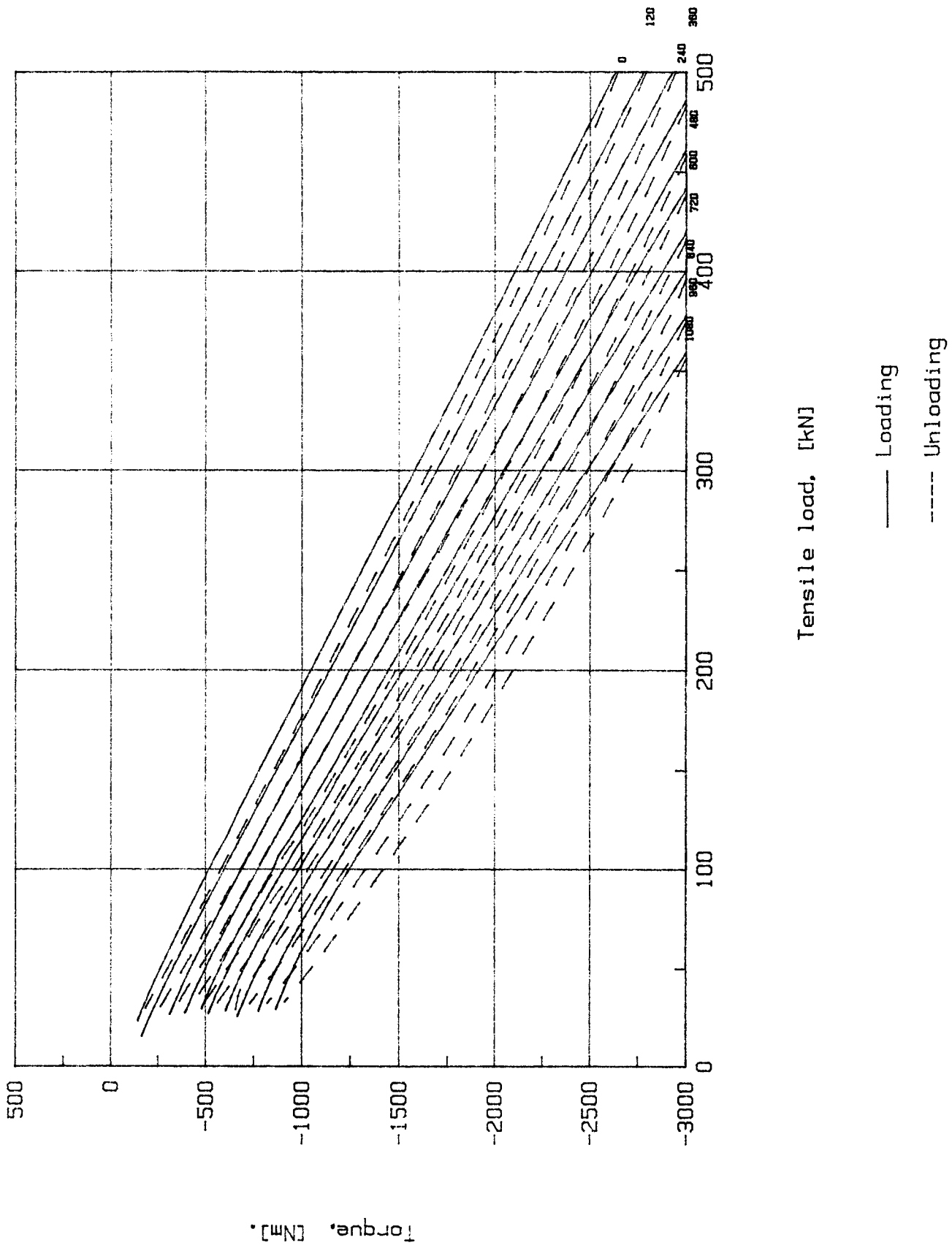


FIG. 5.3 - Torque-tension rotation curves, front underlay

## 5.5 ELONGATION AND DIAMETER CHANGES

Although the elongation of the test specimen and the changes in diameter are not required for determining the torque-tension rotation properties of the rope they were measured and are included for completeness.

### 5.5.1 BACK UNDERLAY

Figure 5.4 shows the elongation versus load curves for the back underlay specimen. For each curve the end rotation is indicated on the right hand side of the graph.

The curves all have basically the same shape and are evenly spaced except for the last curve (720°) where the extensometer ran out of stroke. It is believed that the spacing decreased between the lines because the extensometer LVDT output linearity is affected at the end of stroke.

The hysteresis is also apparent in these curves. It does not appear as if the degree hysteresis is related to the rope end rotation.

As the rope is unwound the starting point of the curves increase. This indicates that the specimen increases in length with an increase in negative rotation.

The diameter changes for four of the ten curves are shown in Figure 5.5. The mean diameter value, 47,45 mm was determined at the start of the test by measuring the rope diameter in perpendicular plains and taking the average. These readings are reflected in the general test information printouts contained in APPENDIX C.

The end rotation of the specimen is indicated on the left

hand side of the graph.

As the negative rotation increases the starting value of the diameter also increases. This is confirmed by the observation that unwinding the rope at low loads tends to open up the strands in the rope.

When the tension in the rope is increased the diameter drops to what seem a constant value which is only slightly dependant on rotation.

### **5.5.2 MIDDLE UNDERLAY**

Figure 5.6 shows the elongation versus load curves for the middle underlay specimen. These curves have the same basic characteristics as those of the back underlay except that the rope specimen gets shorter with increasing positive rotation.

Figure 5.7 shows the diameter changes versus load for the middle underlay rope. The mean diameter value at the start of this test was 48,49 mm. As the rope is wound up the starting point of the diameter curves decreases until 0° is reached and then increases again.

When the tension in the rope is increased the diameter curves seem to converge to constant value which is only slightly dependant on rotation. Hysteresis is also present in the diameter readings. The extent of the hysteresis does not appear to depend on the amount of end rotation.

In both the elongation and diameter curves the lines which do not reach 500 kN are associated with the overheating of the hydraulic unit and the 3000 Nm test torque limit.

### 5.5.3 FRONT UNDERLAY

Figure 5.8 shows the elongation versus load curves for the front underlay specimen. These curves have the same basic characteristics as those of the back and middle underlay.

Figure 5.9 shows the diameter changes versus load for the front underlay rope. The mean diameter value at the start of this test was 47,2 mm. As the rope is wound up the starting point of the diameter curves increase.

When the tension in the rope is increased the diameter curves seem to converge to constant value which is only slightly dependant on rotation. Except for the 1080° curve. Hysteresis is also present in these diameter readings.

It is interesting to note the inconsistency in behaviour of the diameter curves. Consider the following :

- Unwinding the rope increases the starting point of the diameter curves for the back underlay specimen.
- Winding up the rope decreases the starting point of the diameter curves for the middle underlay specimen until 0° is reached. Then the starting point increases with increasing rotation.
- Winding up the rope increases the starting point of the diameter curves for the front underlay specimen.

Therefore, if the rope is unwound from 0° the starting diameter increases. If the rope is wound up from 0° the starting diameter also increases. However, if the rope is wound up from an initial negative rotation (say -600°) then the starting diameter decreases till 0° is reached where after it increases.

More testing would have to be done to determine whether this is just random behaviour or whether it is a repeatable

phenomena .



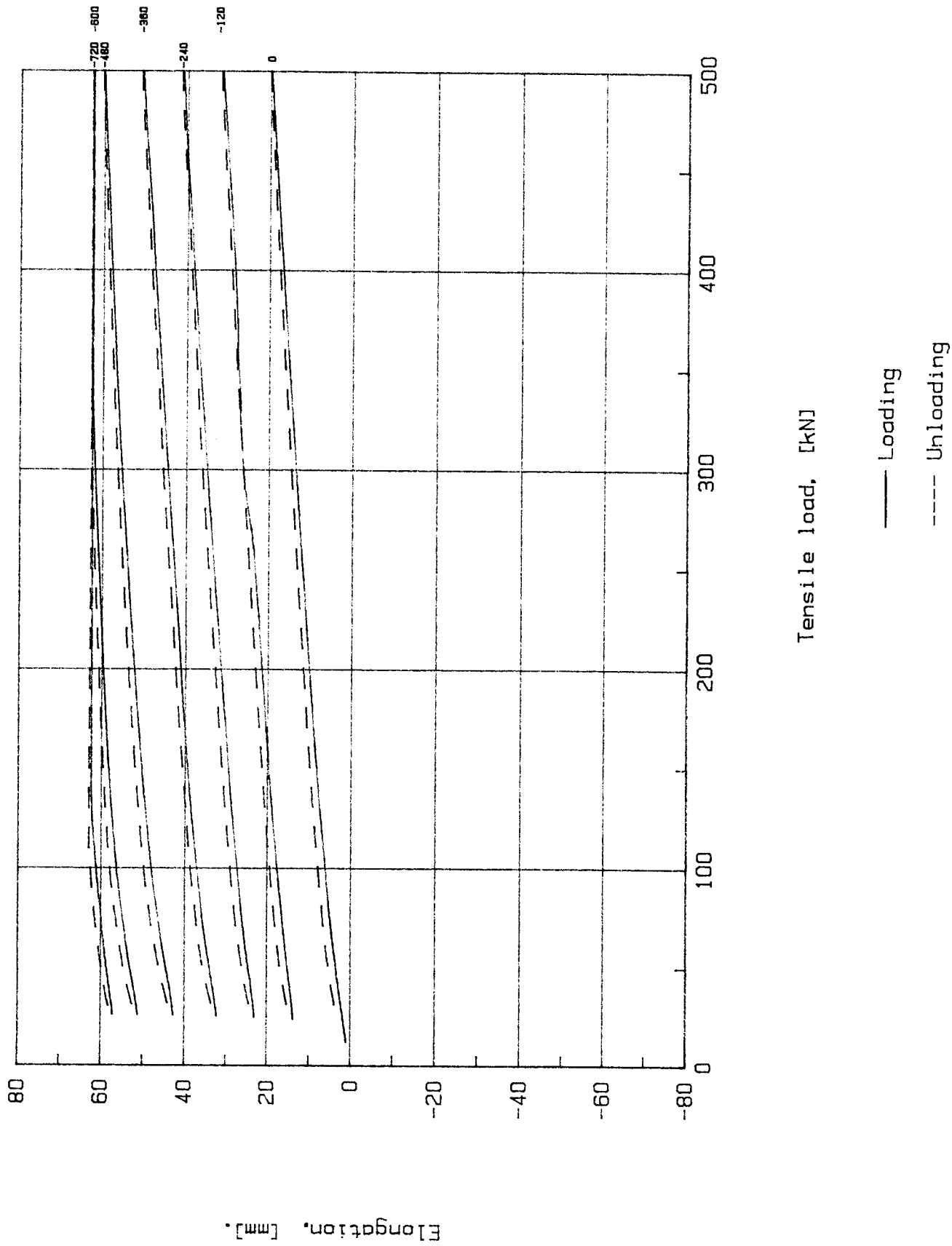


FIG. 5.4 - Elongation curves, back underlay

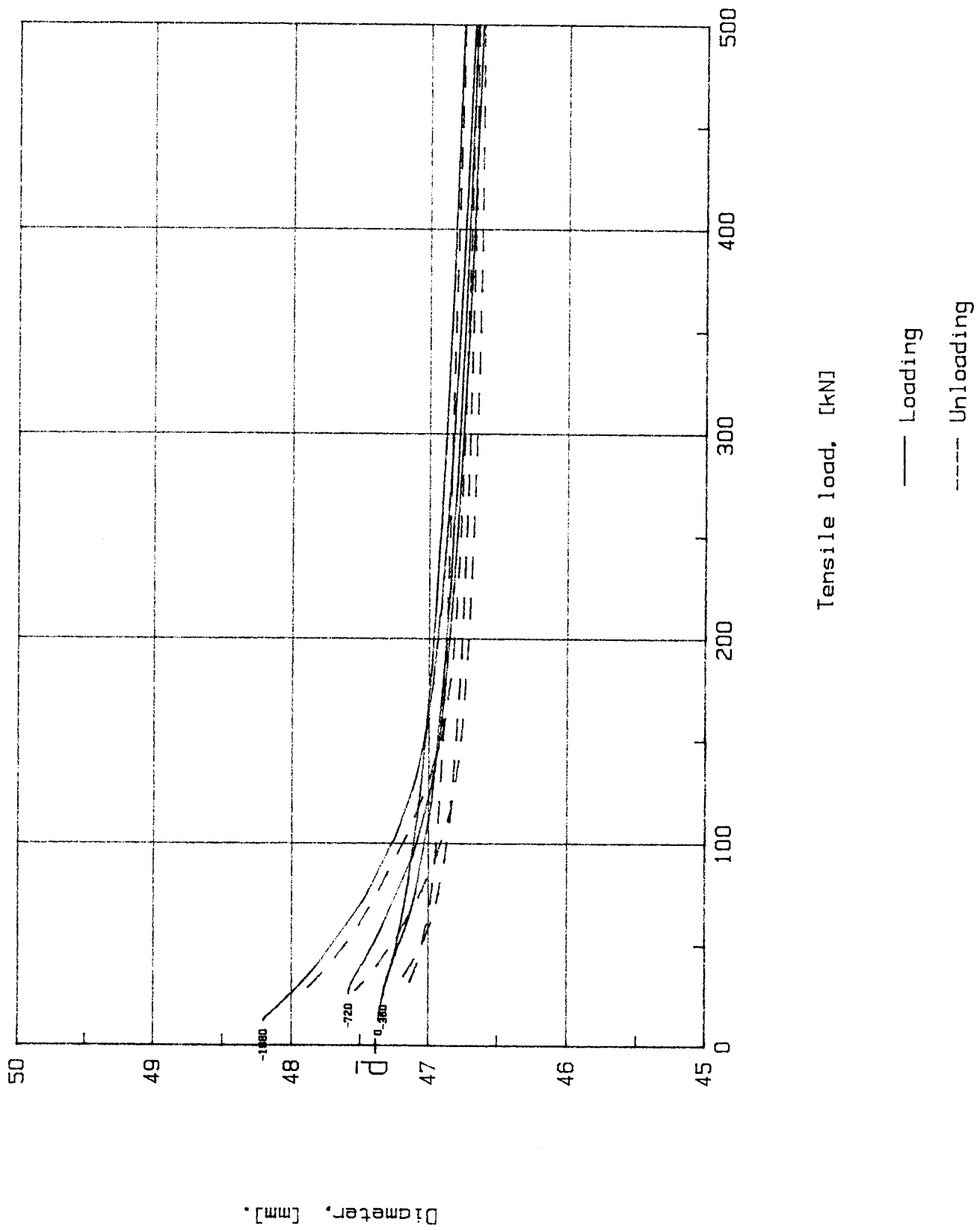


FIG. 5.5 - Diameter curves, back underlay

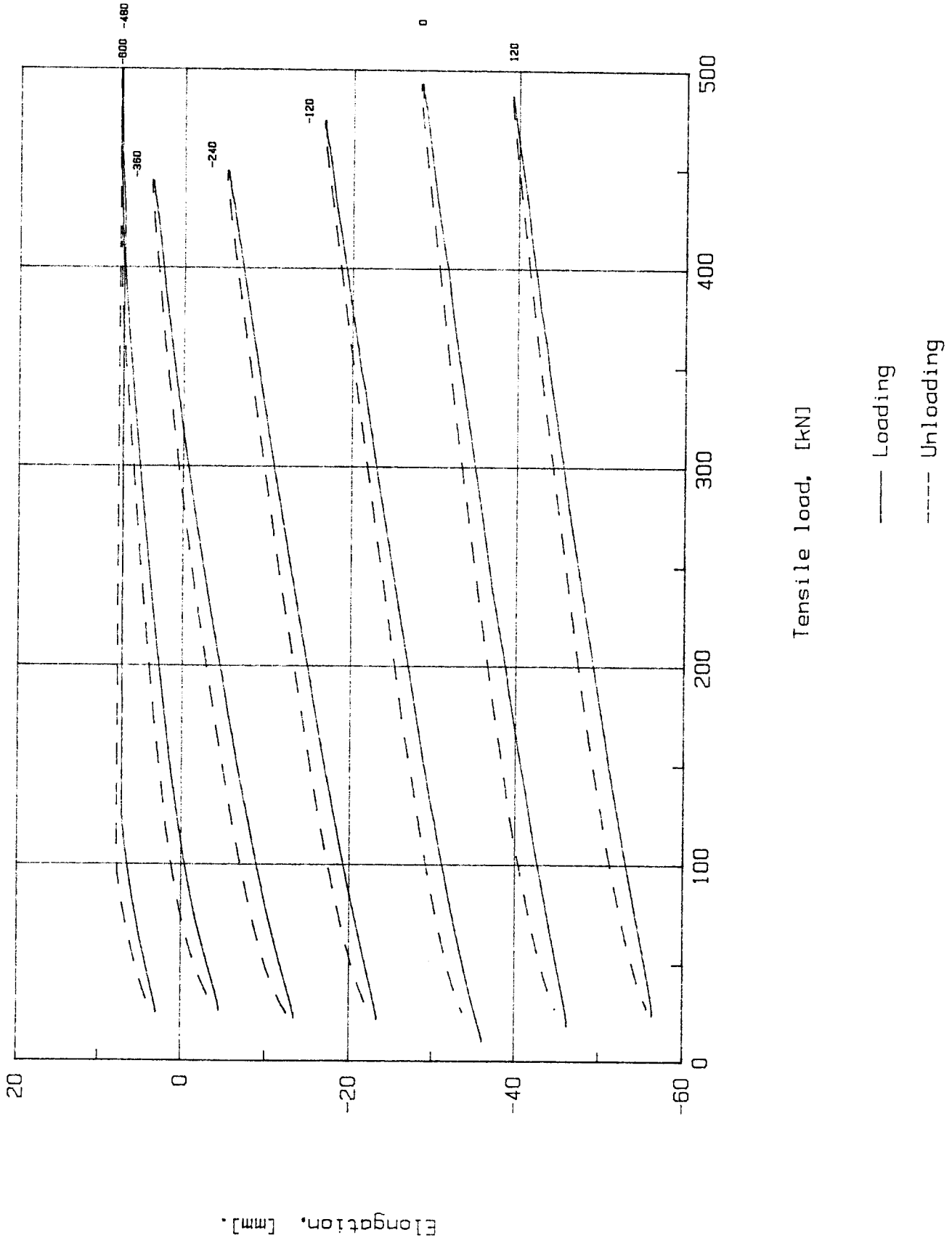


FIG. 56 - Elongation curves, middle underlay

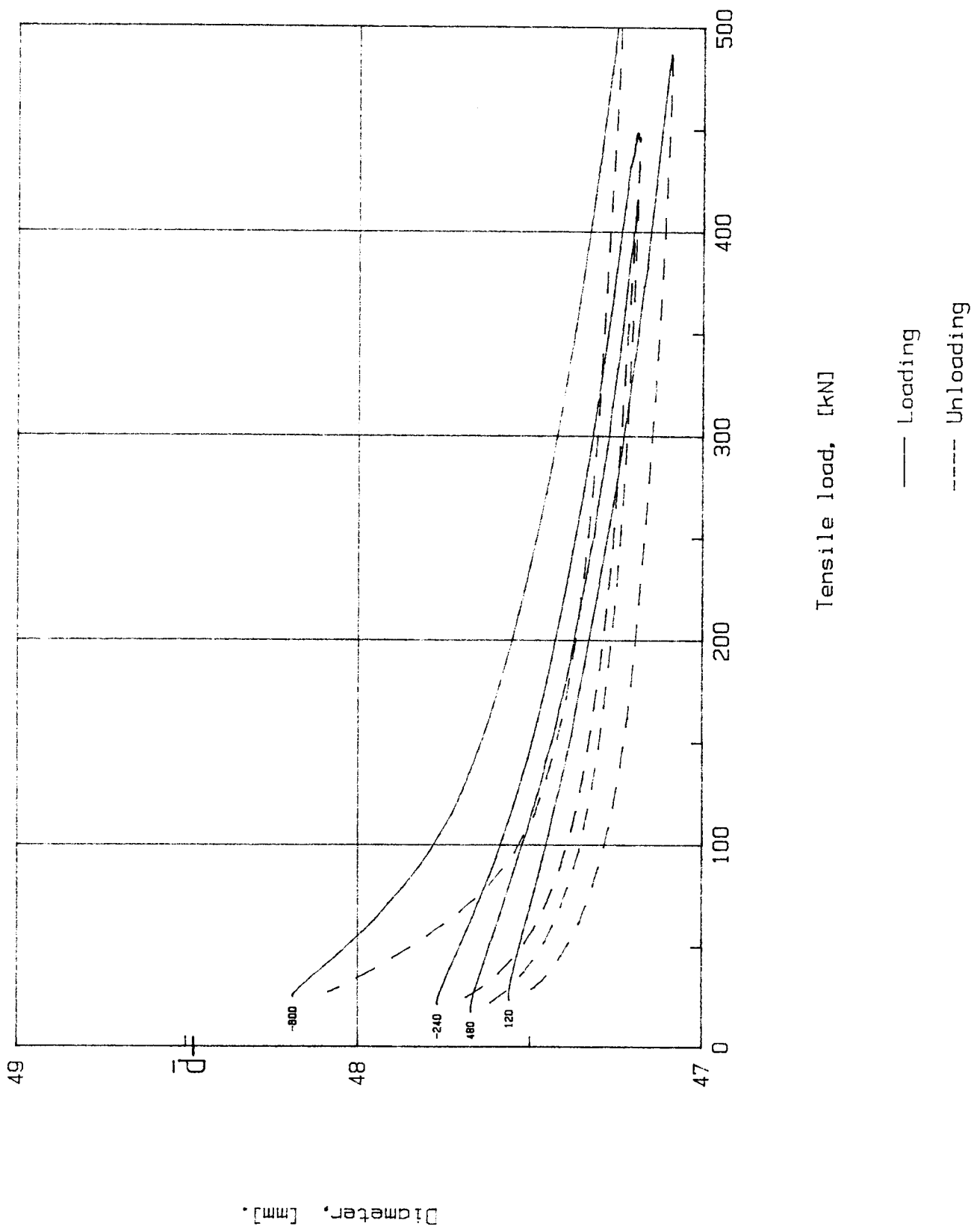


FIG. 5.7 - Diameter curves, middle underlay

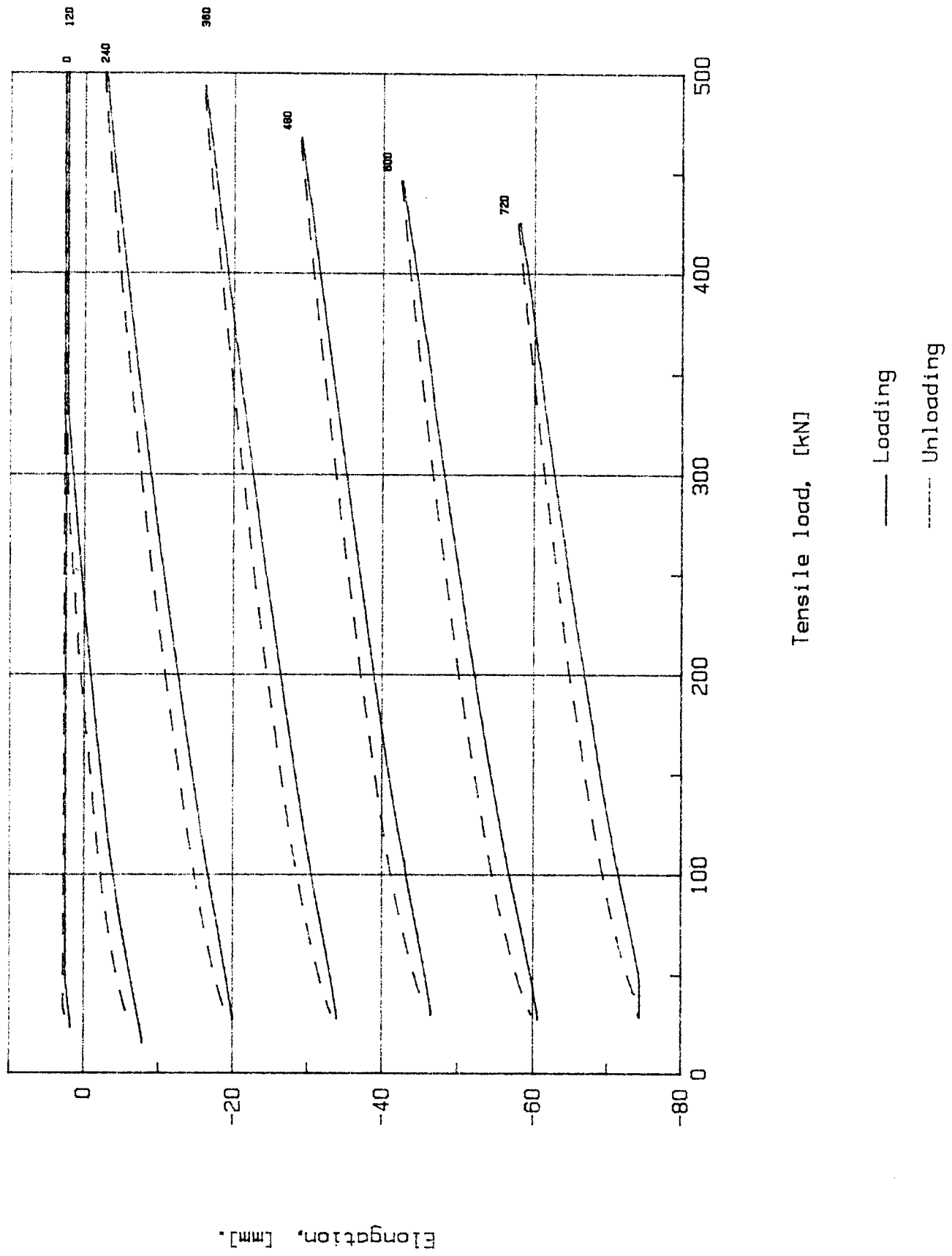


FIG. 5.8 - Elongation curves, front underlay

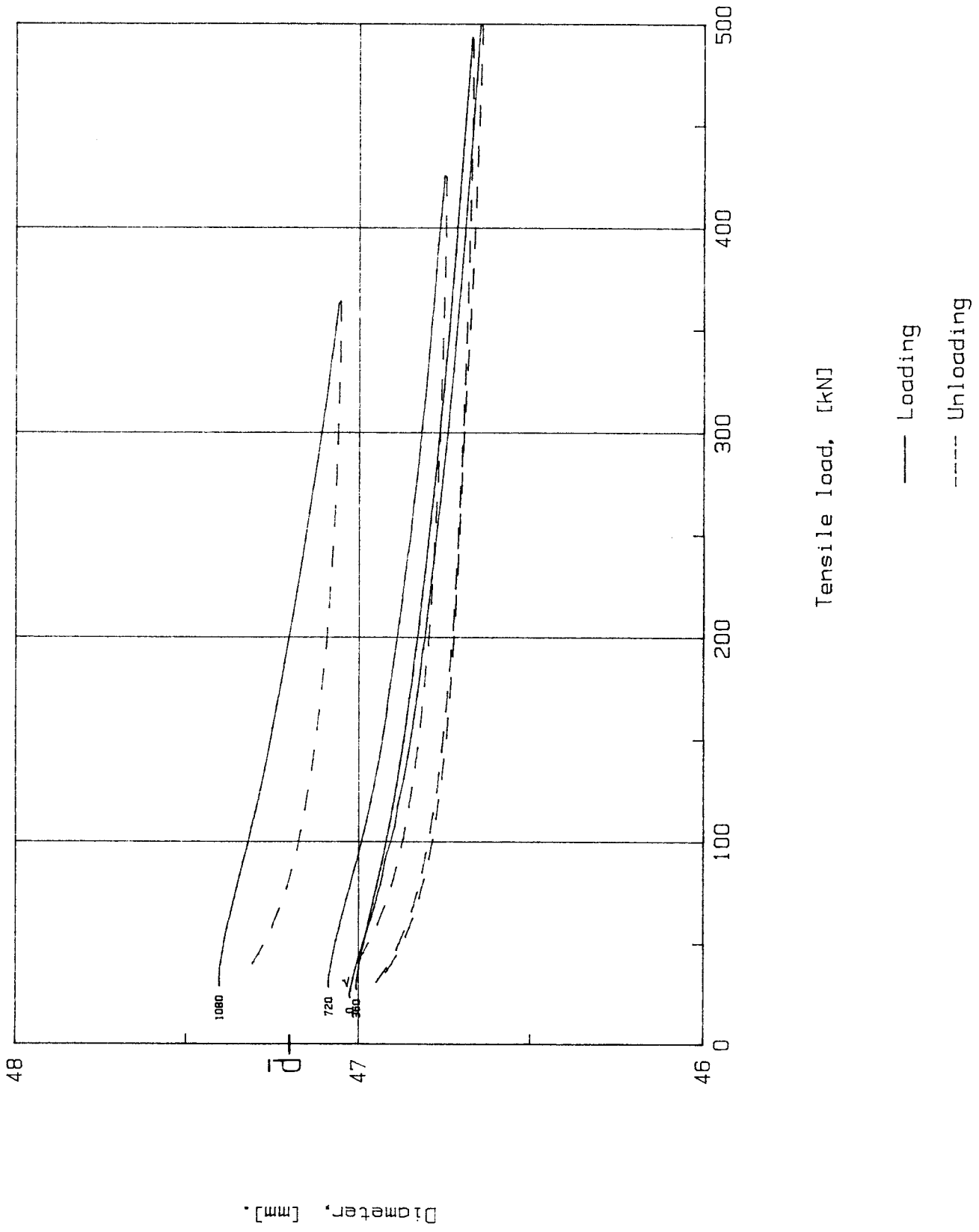


FIG. 5.9 - Diameter curves, front underlay

## 5.6 TORQUE FACTOR - C

The program "T\_T\_PLOT" was set up to automatically generate the Torque factor curves from the raw test data. However, only every second curve for each specimen is plotted. Torque factor is only calculated with the loading values of torque and force.

As was mentioned earlier the Torque factor is the ratio between torque and force for a constant end rotation.

### 5.6.1 BACK UNDERLAY

Figure 5.10 shows the Torque factor curves for the back underlay rope. The peaks at the start of the curves can be ignored. Considering that the a 48 mm TSR sees a minimum load of around 70 kN when installed in the shaft the behaviour of the C factor before this point can be ignored. (With a rope capacity factor of 10 and a skip factor 40% of capacity factor gives,  $1730 \times 0,1 \times 0,4 \approx 70 \text{ kN.}$ )

The C factor lines are approximately evenly spaced and are reasonably constant with increasing force. It would be fair to say that for negative rotations the Torque factor is a function of rotation only.

From the curves it is apparent that Torque factor decreases with increasing negative rotation.

### 5.6.2 MIDDLE UNDERLAY

The Torque factor curves for the middle underlay rope are shown in Figure 5.12. These have similar characteristics to those of the back underlay.

There is an increase of the torque factor with increasing positive rotation. The lines tend to become more curved in the low load regions with increasing positive rotation.

The spikes at the end of the  $-360^\circ$ ,  $-120^\circ$  and  $360^\circ$  curves occurred for no apparent reason.

### 5.6.3 FRONT UNDERLAY

Figure 5.11 shows the Torque factor curves for the front underlay rope specimen. There is a clear difference between this set of curves and those of the middle and back underlay.

The distinct curvature of the of the lines at low load values is observed. From around 200 kN onwards the lines become approximately parallel. Therefore, for positive rotations the Torque factor becomes a function of rotation and force.

The Torque factor also increases with increasing positive rotation.



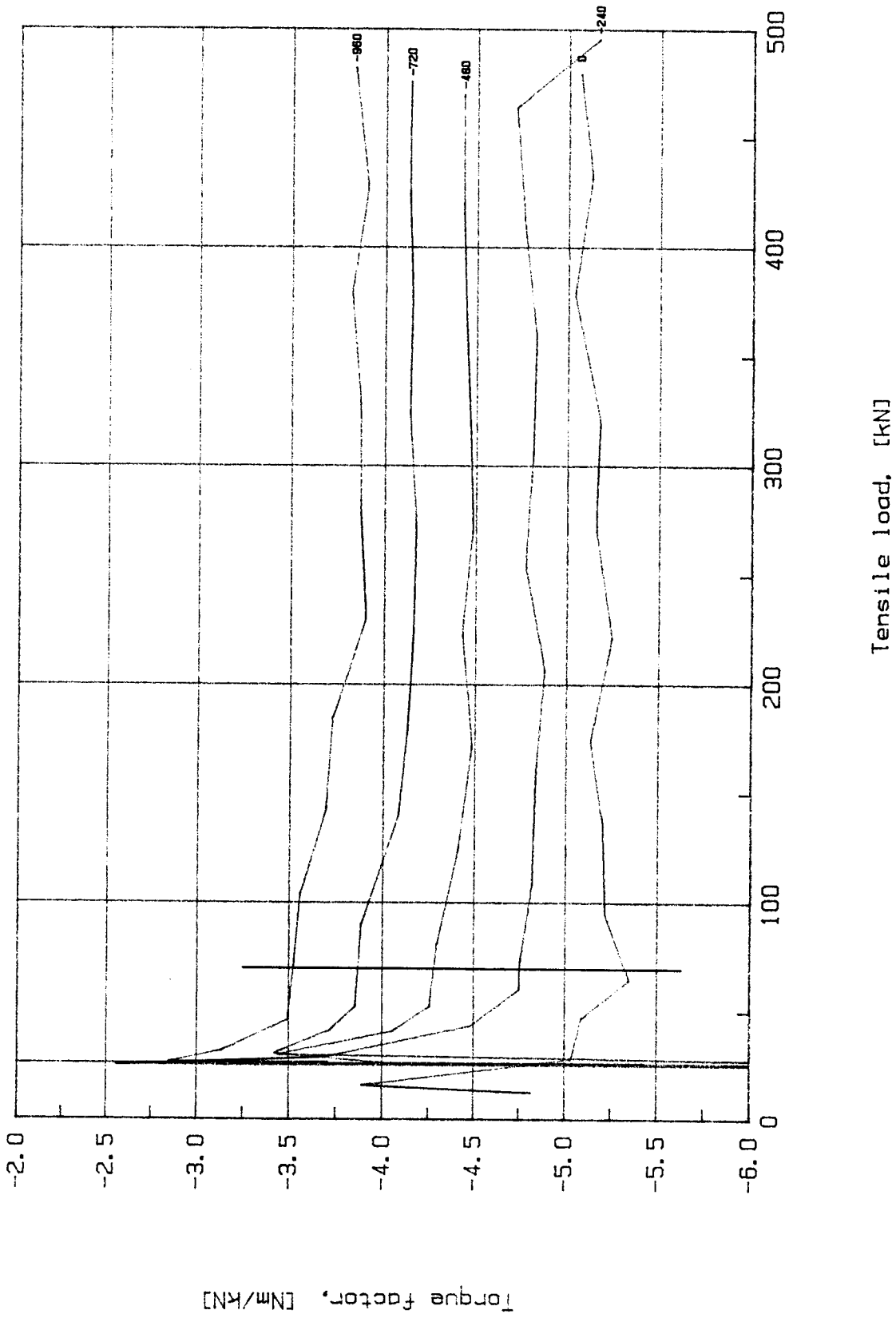


FIG. 5.10 - Torque factor curves, back underlay

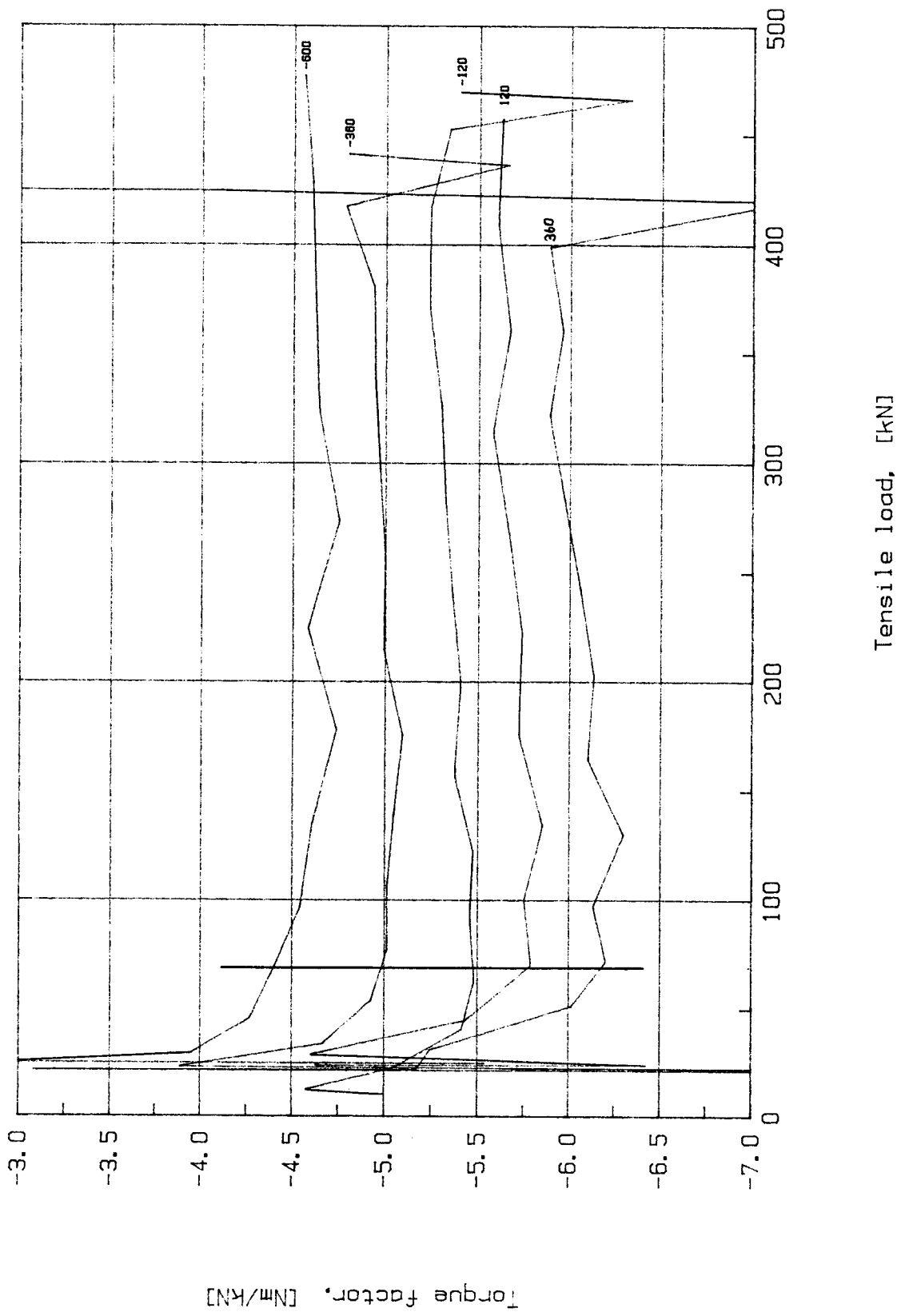


FIG. 5.11 - Torque factor curves, middle underlay

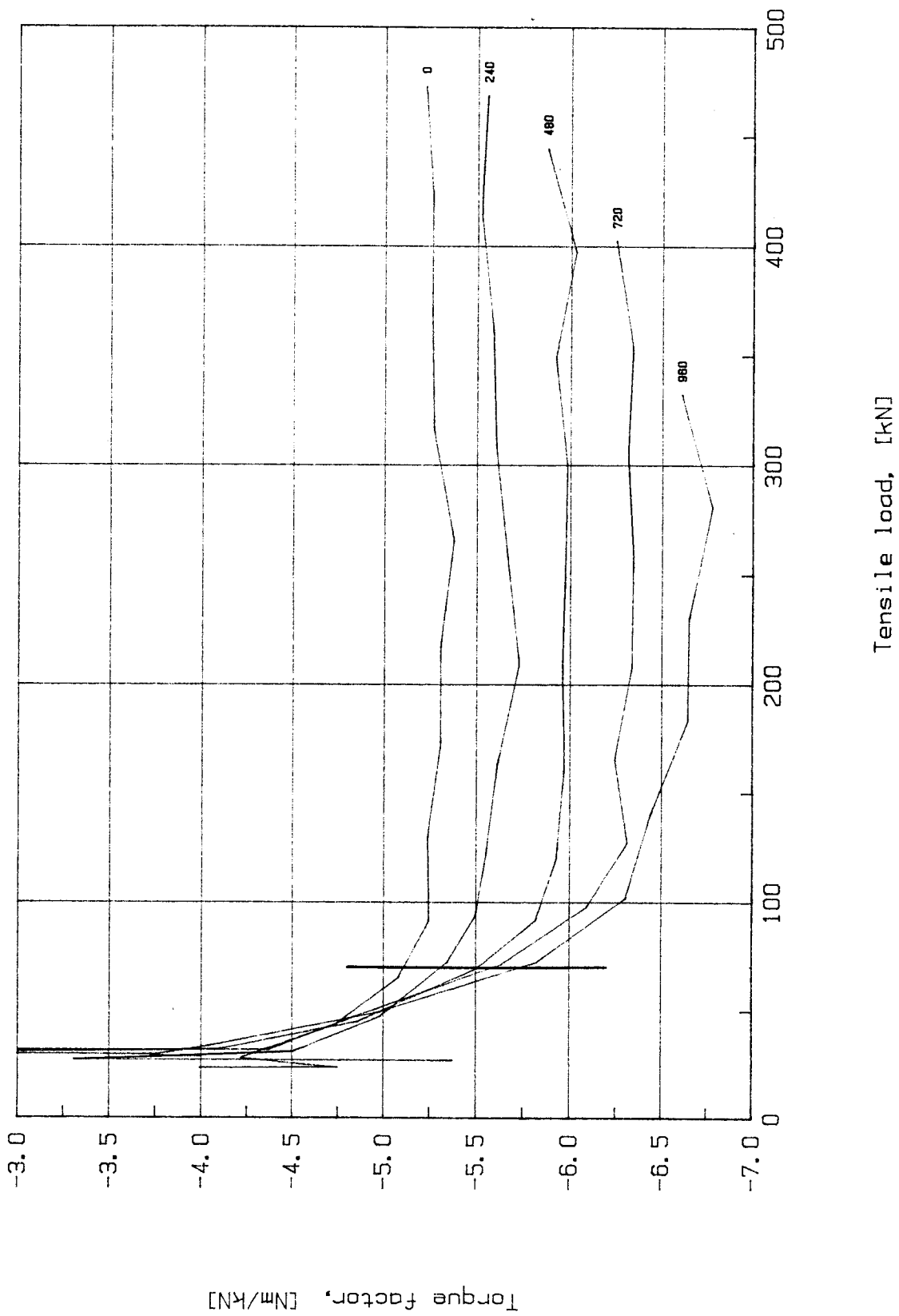


FIG. 512 - Torque factor curves, front underlay

## 5.7 TORSIONAL STIFFNESS - T

Torsional stiffness values are also calculated automatically by "T\_T\_PLOT" and for loading values of torque only. Every second curve in a set of curves is plotted except for the first curve.

T factor is determined, at a constant force, by dividing the change in torque between the curve of interest and the first curve by the change in twist between those two curves.

The first curve is not plotted since the torsional stiffness for that curve is undefined in terms of the above definition.

### 5.7.1 BACK UNDERLAY

Figure 5.13 shows the torsional stiffness versus load curves for the back underlay specimen. From the plot it can be seen that T factor varies linearly with load. The curves are shifted vertically depending on the end rotation.

An increase in negative end rotation decreases the torsional stiffness of the rope specimen. This is because the change in twist is increasing faster than the change in torque.

It is apparent that Torsional stiffness is a function of both force and end rotation.

### 5.7.2 MIDDLE UNDERLAY

In Figure 5.14 the T factor variation with load for the middle underlay section is shown. Here the T factor decreases with an increasing positive rotation. Otherwise it has the same characteristics as the back underlay curves.

### 5.7.3 FRONT UNDERLAY

The front underlay curves as shown in Figure 5.15 are noticeably different to those of the other two specimens. Once again the change comes in the low load region. The lines exhibit a definite curvature whereafter they become straight as before.

It is interesting to note that the Torsional stiffness decreases to a point with increasing rotation and then increases again. The 720° line is below the 960° line. The rate of change of torque must have been greater than the rate of change of twist for this to occur. That is on the 960° line.

Once again the Torsional stiffness is clearly a function of force and rotation or twist.

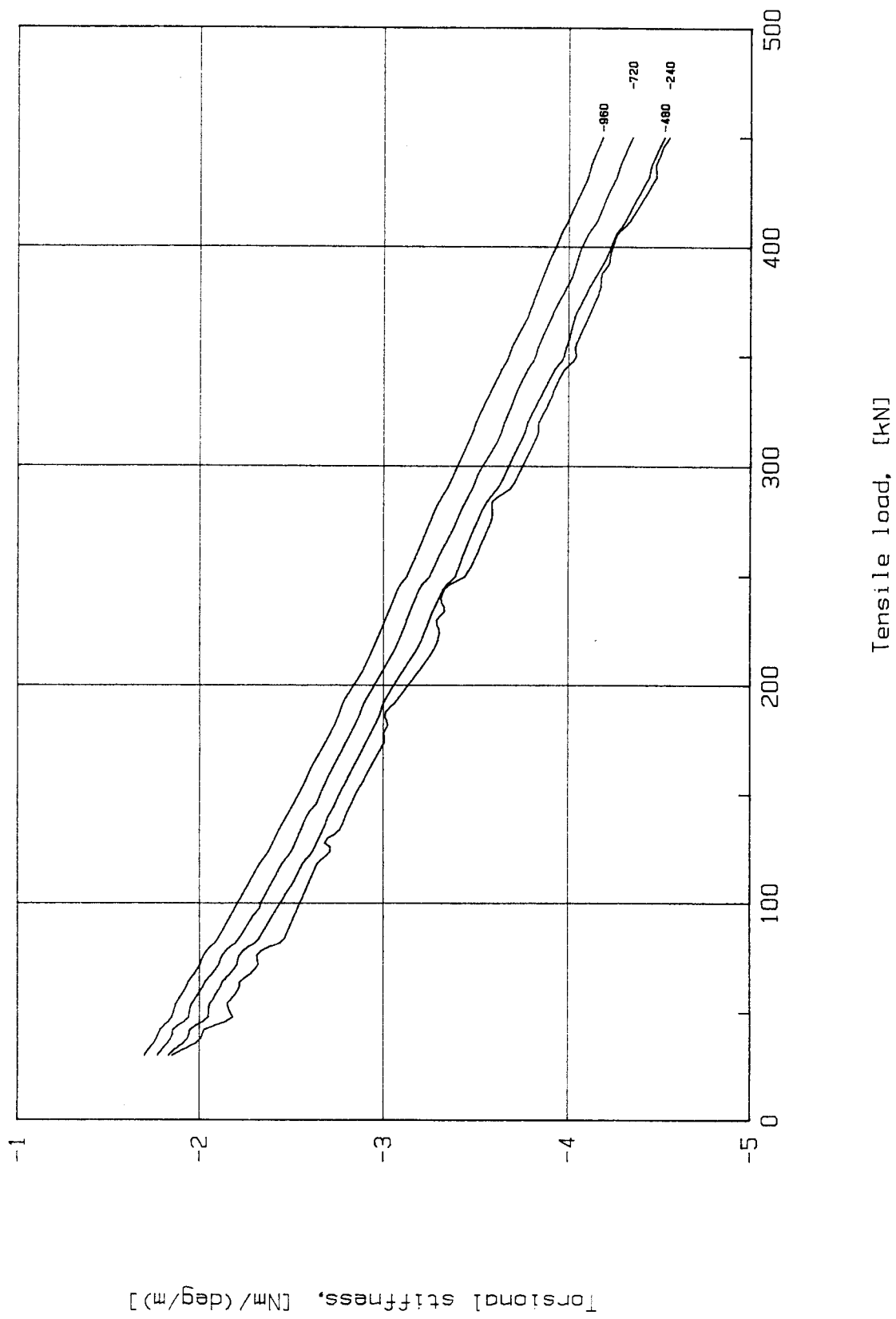


FIG. 5.13 - Torsional stiffness, back underlay

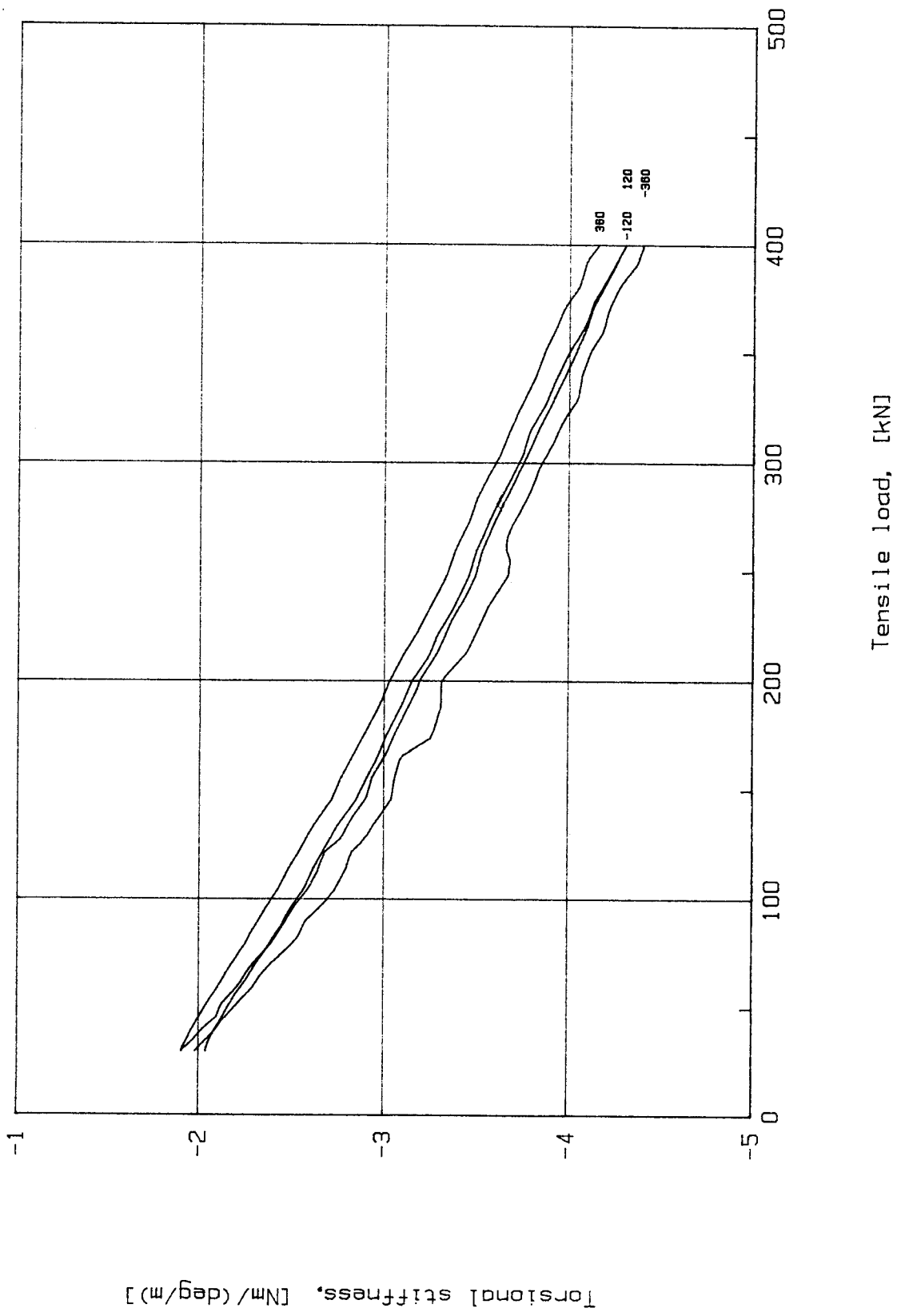


FIG. 5.14 - Torsional stiffness, middle underlay

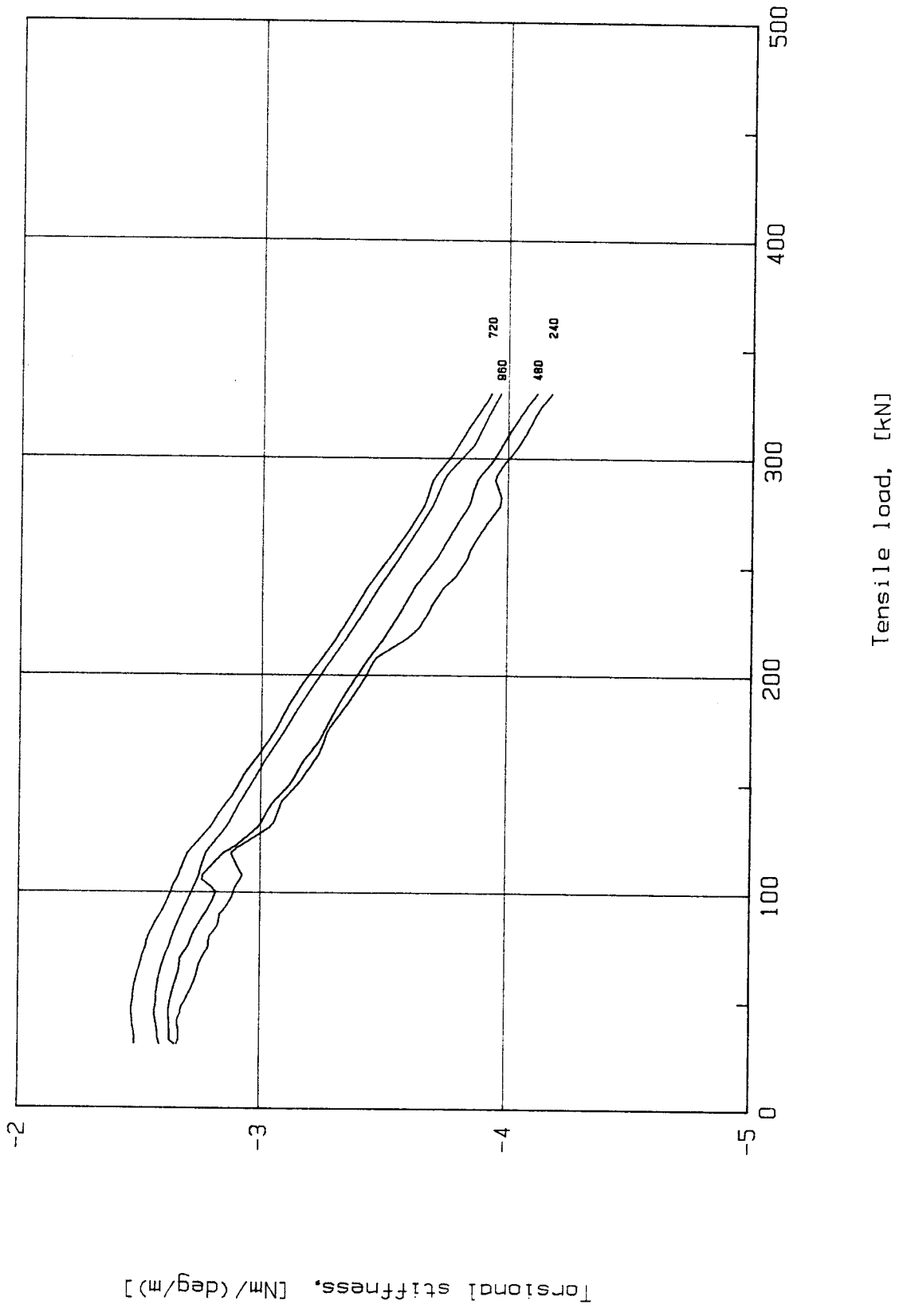


FIG. 5.15 - Torsional stiffness, front underlay



## 6. COMPUTER MODEL

The basic purpose of the computer model is to enable calculation of rope rotation in the shaft. Variables such as rope length, empty and full skip masses and rope mass per metre must be taken into account when calculating the rotation.

At this point it should be noted that in the shaft it is practically impossible to measure total rope rotation. However, it is possible to measure the difference in rotation of the rope for an increase or decrease in end load. With this in mind, the computer models should, as a final result, give a curve showing the difference in rotation of the rope for empty and full skip loads. With this result, the accuracy of the models can be commented on by comparing the predictions with in-shaft rotation measurements.

In this section a basic model of rotation derived from in shaft lay length measurements and test lay length measurements is discussed. Then the Direct Data fit method and the C and T factor methods are applied to the test data.

The numeric computation software package, MATLAB, was used as the main data manipulation and analysis tool throughout this section. Where applicable the MATLAB programs used are appended. Extensive use is made of least squares polynomial fits for describing the data to be manipulated. The general form of an n-th order polynomial in terms of a variable x is :

$$p(x) = a_1 \cdot x^n + a_2 \cdot x^{n-1} + \dots + a_d$$

The number of coefficients for the polynomial is  $d = n+1$ .

## 6.1 ROPE ROTATION IN TERMS OF LENGTH, AN APPROXIMATION

Rope lay length measurements taken in the shaft give a set of values for lay length versus distance from the skip. The lay lengths for the underlay rope, just before it was discarded are shown in the following table.

**Table 6.1** - Lay length as a function of rope length.

Lay length (mm)	Distance from skip (m)
335	0
345	275
370	549
408	1098
448	1647
478	1922
503	2196

Using MATLAB a third order least squares polynomial

$$\text{Lay length} = f_1(\text{Length}) \quad (10)$$

is easily obtained. The data in the above table and the fitted curve are plotted in Figure 6.1.

Data is also available from the torque-tension testing which gives lay lengths for different rope twist values. These are reflected in Table 6.2.

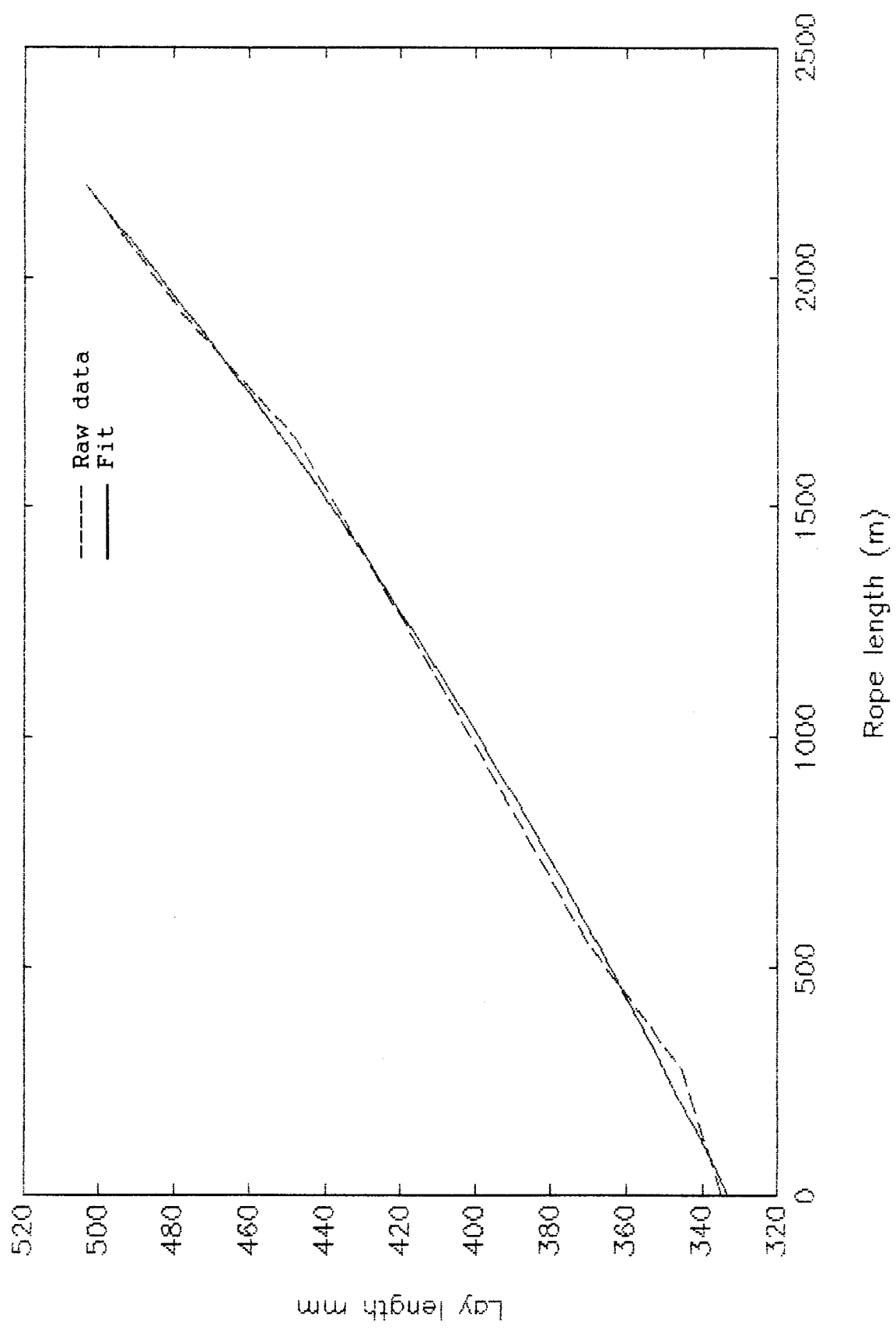


FIG. 6.1 - In-shaft lay length measurements.

Table 6.2 - Twist as a function of lay length.

BCKUL + MIDUL + FNTUL			GAUGE LENGTH = 4050 mm		
END ROTATION (deg)	TWIST (deg/m)	LAY LENGTH BCKUL (mm)	LAY LENGTH MIDUL (mm)	LAY LENGTH FNTUL (mm)	LAY LENGTH COMBINED (mm)
-1080	-267	660			660.0
-960	-237	610			610.0
-840	-207	580			580.0
-720	-178	555			555.0
-600	-148	525	510		517.5
-480	-119	500	480		490.0
-360	-89	490	470		480.0
-240	-59	470	460		465.0
-120	-30	445	440		442.5
0	0	427	405	385	405.7
120	30		385	378	381.5
240	59		370	354	362.0
360	89		355	345	350.0
480	119		345	330	337.5
600	148			315	315.0
720	178			310	310.0
840	207			305	305.0
960	237			295	295.0
1080	267			290	290.0

Here a fourth order least squares polynomial is fitted to the twist and combined lay length data to obtain the equation :

$$\text{Twist} = f_2(\text{Lay length}) \quad (11)$$

The data in Table 6.2 as well as the least squares polynomial for that data are shown graphically in Figure 6.2. With the two preceding equations a third equation can be written as follows :

$$\text{Twist} = f_2 ( f_1(\text{Length}) ) \quad (12)$$

From this equation the plot in Figure 6.3 was obtained.

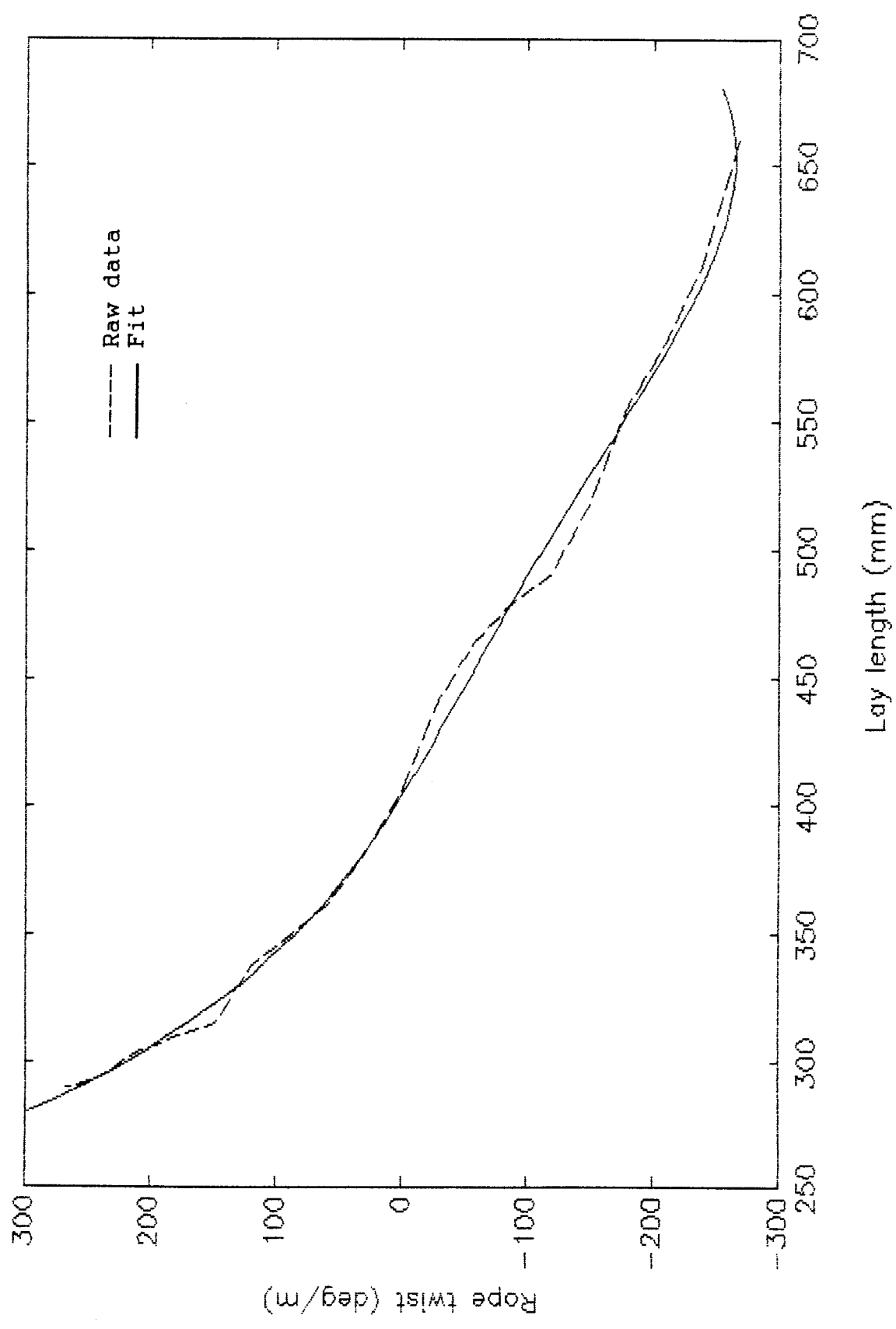


FIG. 6.2 - Test rope twist and lay length.

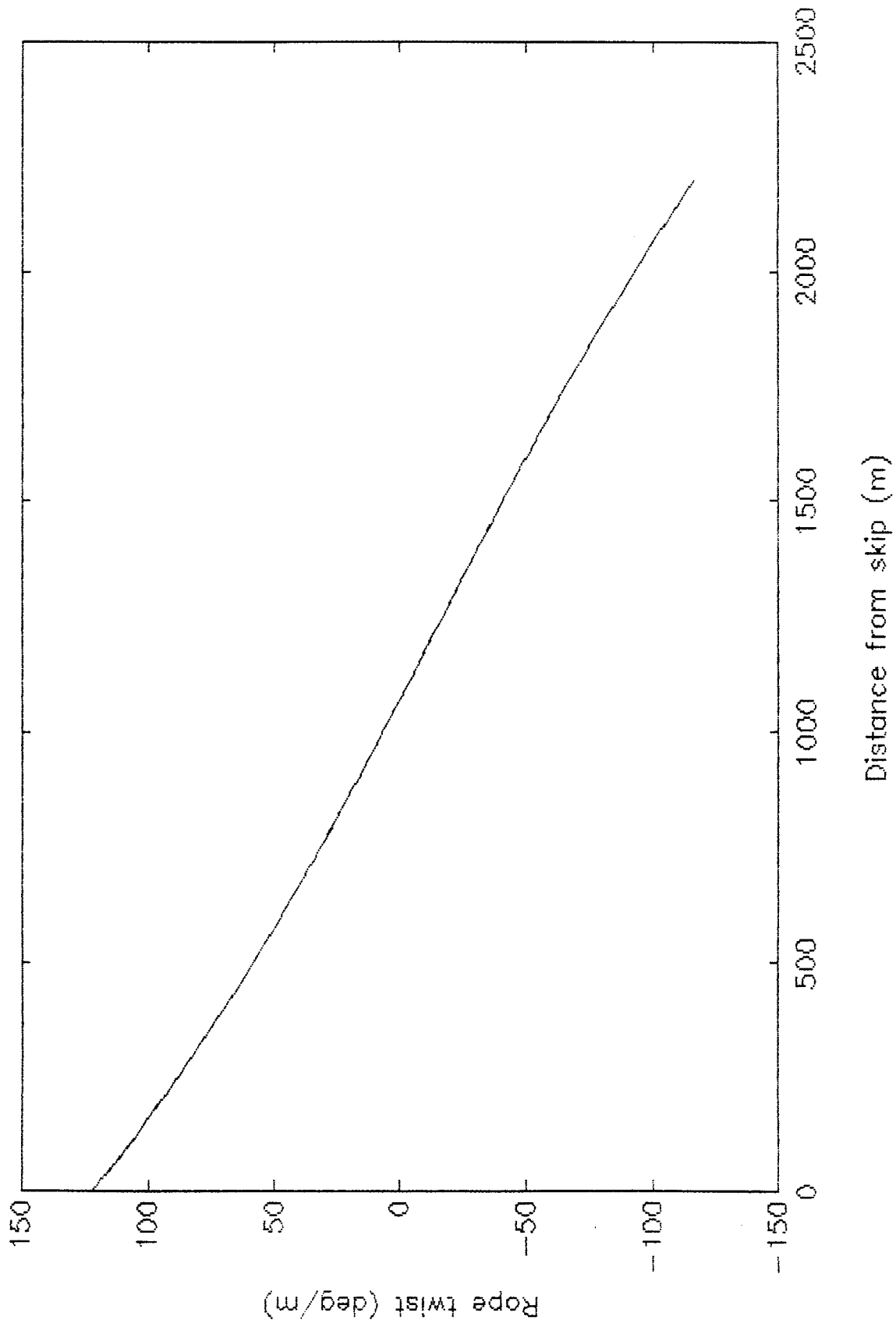


FIG. 6.3 - Rope twist approximation.

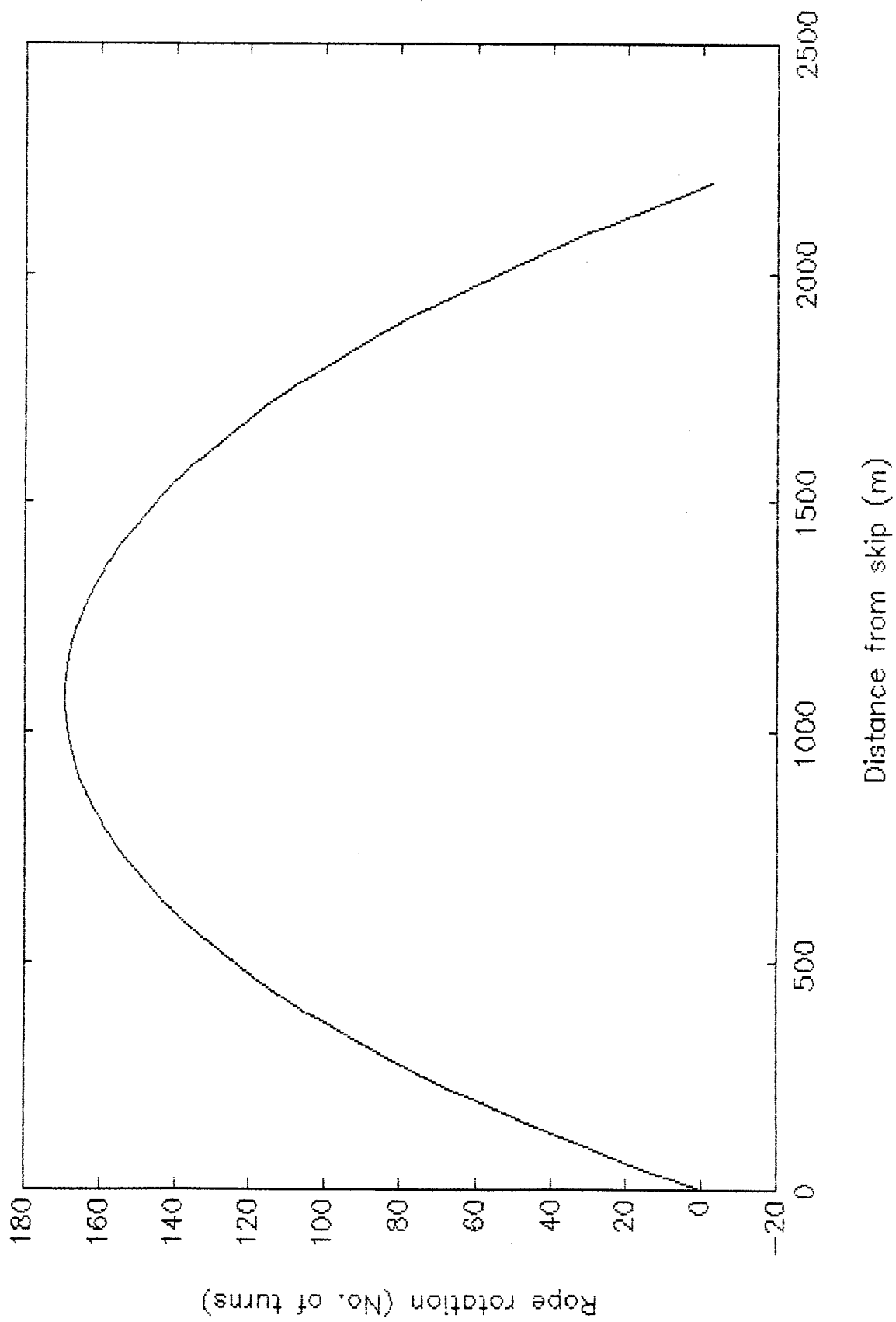


FIG. 6.4 - Rope rotation approximation.

Integrating equation (12) with respect to length gives a formula for rope rotation in terms of length. Applying the boundary condition that rotation = 0 at length = 0 solves for the constant of integration. The resulting function is :

$$\text{Rotation} = f_3(\text{Length}) \quad (13)$$

Where rotation is in degrees. Dividing the above equation by 360° gives an equation for rotation (no. of turns) in terms of rope length. The predicted rotation over the rope length is shown in Figure 6.4.

A MATLAB program which does all of the above data manipulation and generates the necessary graphs is contained in APPENDIX F.

It should be noted that this prediction of rope rotation is end load independent, whereas the other two methods take into account the load on the rope, i.e. full and empty skip loads.

There is however a possibility of expanding this method to include rope end load. This could be done as follows :

- Measure two sets of lay lengths in the shaft, one when the skip is empty and one when the skip is full.
- On the torque-tension machine, measure the lay lengths for a constant load. An average load can be used, say corresponding to the tension in the rope half way up the shaft plus the average between the full and empty skip loads. For the 4050 mm test specimen lay length is varies much more with a change in end rotation than with a change in tension.
- From the measurements described above, it will be possible to formulate the following equations :

$$\text{Lay length} = f(\text{Length}) \quad [\text{empty skip}]$$

$$\text{Lay length} = f(\text{Length}) \quad [\text{full skip}]$$

$$\text{Twist} = f(\text{Lay length}) \quad [\text{constant load}]$$



Combining and integrating will gives :

$$\text{Rotation} = f(\text{Length}) \quad [\text{empty skip}]$$

$$\text{Rotation} = f(\text{Length}) \quad [\text{full skip}]$$

Dividing by  $360^\circ$  will yield the number of turns the rope makes, for an empty and full skip, along the rope length. These two values can be subtracted and the difference compared to in shaft rotation measurements.

## 6.2 DIRECT DATA FIT METHOD

This approach is based on the work by Van Zyl (1993b). Torque-tension rotation data can be taken directly off the test result curves, Figures 5.1 and 5.3. Values of torque for rotations from  $-1080^\circ$  to  $1080^\circ$  ( $-267^\circ/\text{m}$  to  $267^\circ/\text{m}$ ) with forces from 0 to 500 kN are recorded. These values are shown graphically in Figure 6.5 which is basically a combination of Figures 5.1 and 5.3.

The  $0^\circ$  line data is taken as an average between the back and front  $0^\circ$  lines. Only the loading values of torque are used.

From this data it is possible to determine equations for torque in terms of force and rotation. This involves fitting third order least squares polynomials to all 19 curves. Then fitting four fourth order polynomials to the 4 sets of 19 coefficients of the 19 third order polynomials. This results in one equation of the following form :

$$\text{Torque } M = p_1(R) \cdot F^3 + p_2(R) \cdot F^2 + p_3(R) \cdot F + p_4(R) \quad (14)$$

with  $F$  in (kN) and  $R$  in (deg/m) gives  $M$  in (Nm).

$p_1$ ,  $p_2$ ,  $p_3$  and  $p_4$  are fourth order polynomials in terms of  $R$ . Note that  $F$  varies linearly with the distance from the skip,  $z$ .

This is now the same type of equation as Van Zyl had except that it more accurately represents the torque-tension rotation curves. The MATLAB program to determine this equation exactly is contained in APPENDIX G.

The next step in Van Zyl's method is to write equation (14) in the form :

$$R = f(M, F(z))$$

Considering the complexity of equation (14) this is not

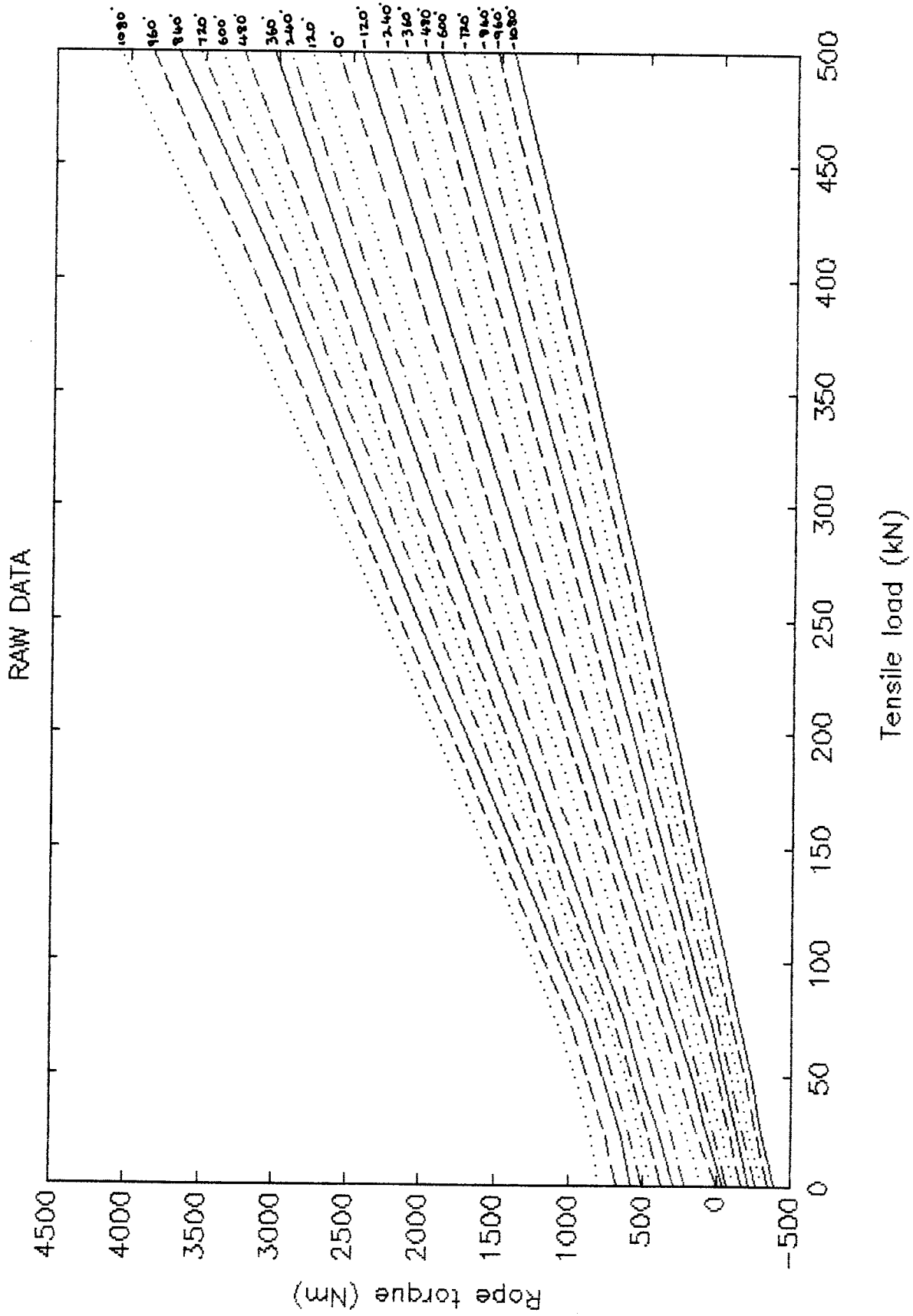


FIG. 6.5 - Combined BCKUL and FNTUL torque-tension rotation curves.

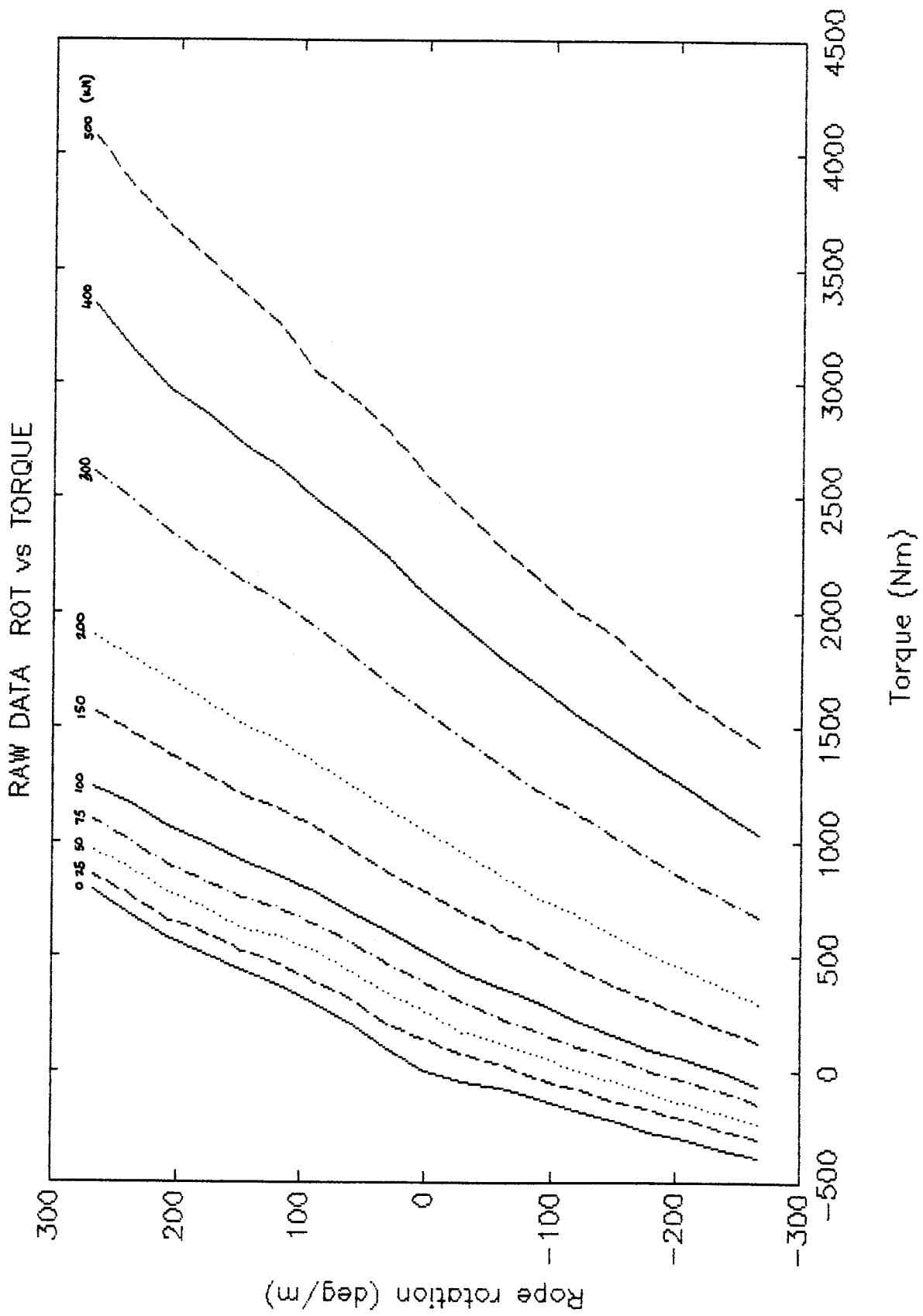


FIG. 6.6 - Rope twist and torque for constant force.

easily achieved. However, since the raw data is available, it is just as feasible to find an equation  $R = f(M, F(z))$  as it is to find equation (14) which is in the form  $M = f(R, F(z))$ .

The data used to generate Figure 6.5 can also be used to plot twist versus torque for lines of constant force. Figure 6.6 shows these curves.

A MATLAB program using the curves in Figure 6.6 was written to determine the following equation for rotation.

$$R = c_1(F) \cdot M^3 + c_2(F) \cdot M^2 + c_3(F) \cdot M + c_4(F) \quad (15)$$

with  $M$  in (Nm) and  $F$  in (kN) gives  $R$  in (deg/m).

$c_1$ ,  $c_2$ ,  $c_3$  and  $c_4$  are fifth order polynomials in terms of  $F$ .  $M$  is a constant which changes depending on the rope end load  $P$ .

The program to generate equation (15) is contained in APPENDIX G.

All that has to be done to determine the actual rotation of rope in number of turns is to integrate equation 15 with respect to  $z$  and divide the result by  $360^\circ$ . It must be remembered that equation (15) has four fifth order polynomials in terms of  $F$ . Where :

$$F = (P + q \cdot z) \quad (16)$$

A third MATLAB program was written which determines  $R = f(M, z)$  in the form :

$$R = d_1(z) \cdot M^3 + d_2(z) \cdot M^2 + d_3(z) \cdot M + d_4(z) \quad (16)$$

with  $M$  in (Nm) and  $z$  in (m) gives  $R$  in (deg/m).

$d_1$ ,  $d_2$ ,  $d_3$  and  $d_4$  are fifth order polynomials in terms of  $z$ .  $M$  is a constant which changes depending on the rope end load

P. APPENDIX G also contains a listing of this program.

From equation (16), for twist, the rotation of the rope,  $\Phi$ , can be determined ( $R = d\Phi/dz$ ). For the integration,  $M$  is a constant so only the polynomials  $d_1$ ,  $d_2$ ,  $d_3$  and  $d_4$  need to be integrated with respect to  $z$ . This will result in four sixth order polynomials containing four unknown constants of integration.

The boundary conditions for the integration are :

- i.  $\Phi = 0$  at  $z = 0$
- ii.  $\Phi = 0$  at  $z = \text{total length}$ .

By making the four constants of integration 0 the first boundary condition is satisfied and the following equation results :

$$R = e_1(z) \cdot M^3 + e_2(z) \cdot M^2 + e_3(z) \cdot M + e_4(z) \quad (17)$$

with  $M$  in (Nm) and  $z$  in (m) gives  $R$  in (deg/m).

$e_1$ ,  $e_2$ ,  $e_3$  and  $e_4$  are sixth order polynomials in terms of  $z$ . The seventh coefficient (= 0) of the four sixth order polynomials is the constant that arose when polynomials  $d_1$ ,  $d_2$ ,  $d_3$  and  $d_4$  were integrated with respect to  $z$ .

Now the only unknown in the equation is the rope torque  $M$ . If the correct value of  $M$  is chosen the boundary condition ii will be satisfied. Alternatively  $M$  can be found by applying boundary condition ii.

With the structure of the MATLAB program it was found to be more suitable to enter a torque and check whether the boundary condition is satisfied. If not the torque is adjusted until it is satisfied.

This process of iteration resulted in the following final torque values :

$M_e = 1025 \text{ Nm}$             (Empty skip)  
 $M_f = 1619 \text{ Nm}$             (Full skip)

Once the correct values of  $M$  are determined the rope twist and rotation versus length can be plotted. Equation (16) is plotted, for  $z = 0$  to 2200, in Figure 6.7. Curves for both an empty and full skip are shown. Equation (17) /  $360^\circ$  is plotted in Figure 6.8.

At 600 m from the skip the difference between empty and full rotations is 58 turns.

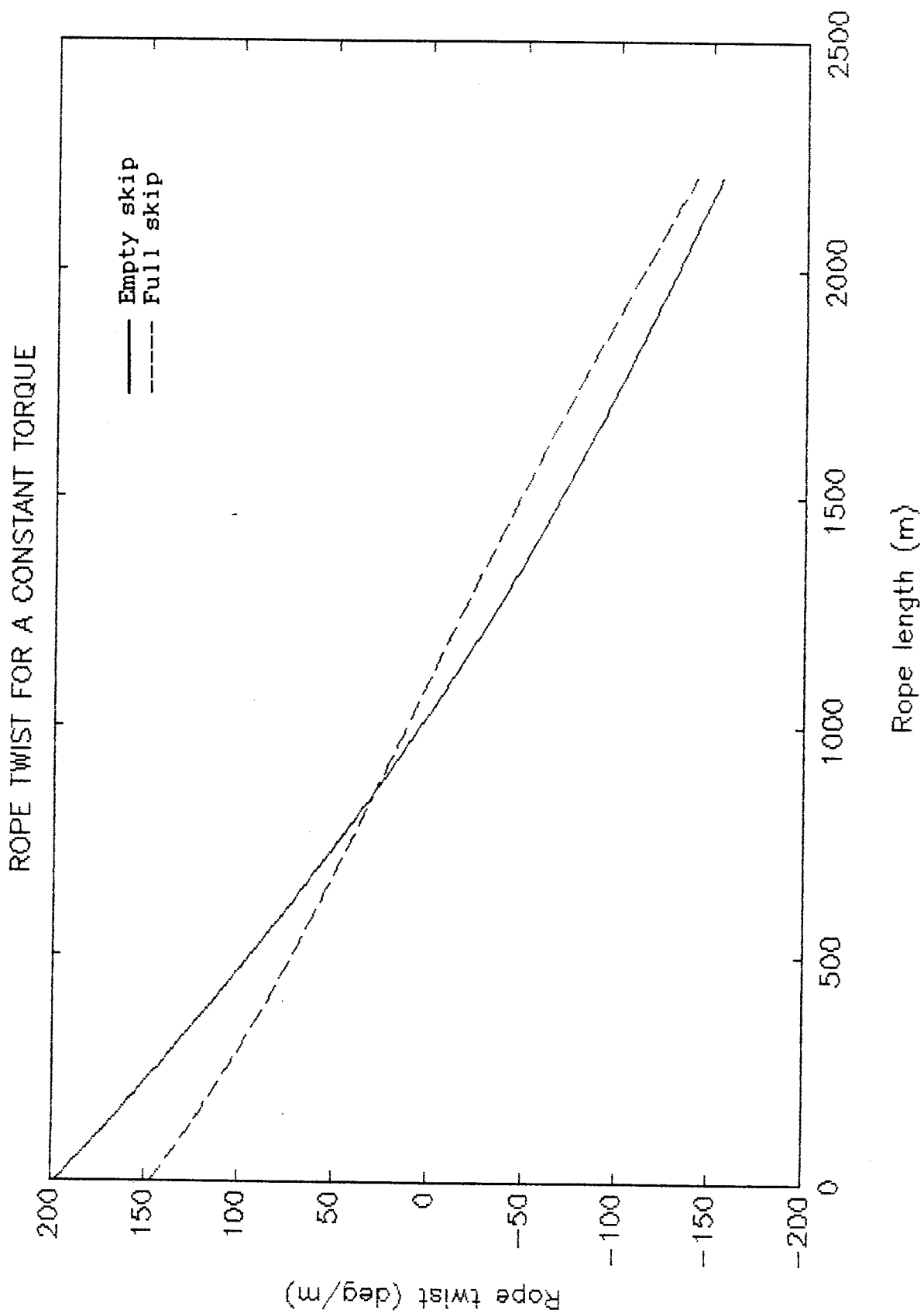


FIG. 6.7 - Direct Data Fit rope twist and rope length.



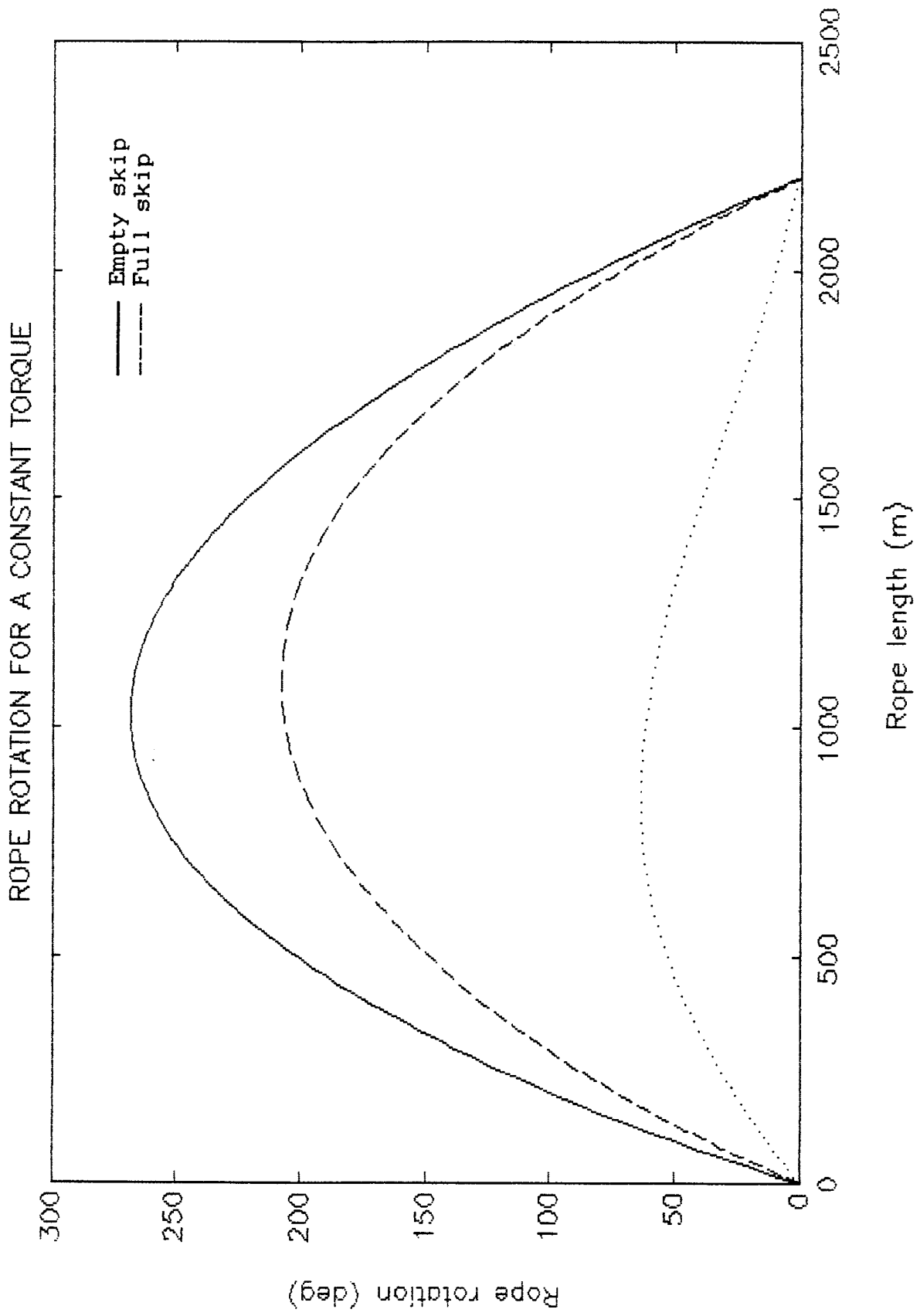


FIG. 6.8 - Direct Data Fit rope rotation and rope length.

### 6.3 C AND T FACTOR METHOD

The work by Borello (1993b) is used as the basis for this method. Using the C and T factor curves, Figures 5.10 to 5.15, equations can be written which describe the shape of these curves for different values of twist and force.

The difference is that this method takes into account the fact that both Torque factor and Torsional stiffness are functions of force and twist. At this point it is important to note that the positive domain is being used for this method, i.e positive torque, C factors and T factors.

$$\text{Torque factor} \quad C = a_c + b_c.R \quad (18)$$

$$\text{where} \quad b_c = f(F) = f(P + q.z) \quad (19)$$

$$\text{Torsional stiffness} \quad T = a_t + b_t.(P + q.z) + c_t.R \quad (20)$$

$a_c = 5,25$  (Nm/kN) from Figure 5.10 and 5.12. C value at  $0^\circ$ .

$b_c =$  fifth order polynomial in terms of F (Nm/kN/( $^\circ$ /m)) see APPENDIX H for MATLAB fit program. Spacing between C factor curves.

$a_t = 2,05$  (Nm/( $^\circ$ /m)) from Figure 5.13. Intercept at theoretical  $0^\circ$  line.

$b_t = 5,90.10^{-3}$  (Nm/( $^\circ$ /m)/kN) from Figure 5.13. Slope of lines.

$c_t = 1,70.10^{-3}$  (Nm/( $^\circ$ /m)/( $^\circ$ /m)) from Figure 5.13 spacing between lines of constant rotation.

$$\text{Torque in rope} \quad M = C.(P + q.z) + T.R \quad (21)$$

Substituting (18), (20) into (21) gives :

$$M = c_t.R^2 + [b_c.(P+q.z) + a_t + b_t(P+q.z)].R + a_c.(P+q.z) \quad (23)$$

Now let

$$\begin{aligned}
 A &= c_t \\
 B &= b_c \cdot (P+q \cdot z) + a_t + b_t(P+q \cdot z) \\
 C &= a_c \cdot (P+q \cdot z) - M
 \end{aligned}$$

Then

$$A \cdot R^2 + B \cdot R + C = 0 \quad (24)$$

or

$$R = [ -B \pm \sqrt{B^2 - 4 \cdot A \cdot C} ] / 2 \cdot A \quad (25)$$

Equation (25) has two answers. One will be a meaningful twist and the other can be discarded. This is easily determined using the MATLAB root finder on equation (24).

Now from equation (25) it is possible to determine the rope twist for a chosen M and a range of z values. With a set of data, twist versus z, a third order polynomial can be determined which gives  $d\Phi/dz = R = f(z)$ . This polynomial is easily integrated with respect to z resulting in a rotation equation,  $\Phi = f(z)$ . This is in the form of a fourth order polynomial.

There is a constant of integration which can be solved by applying the boundary conditions :

- i.  $\Phi = 0$  at  $z = 0$
- ii.  $\Phi = 0$  at  $z = \text{total rope length}$

Boundary condition i is satisfied if the constant of integration is 0. Boundary condition ii is only satisfied if the correct torque was selected.

A MATLAB program was written to process all of the above equations for full and empty skip loads. The program is contained in APPENDIX H. When the program is run it asks for estimates of the rope torque corresponding to the empty and full skip states. From this point on it automatically adjusts the value of the torque until the boundary condition ii is satisfied.

For the constants as detailed above, the program returned

the following final torque values.

$M_e = 1013 \text{ kN}$  (Empty skip)

$M_f = 1629 \text{ kN}$  (Full skip)

Once the program has determined the correct values of rope torque the rope twist and rope rotation curves can be plotted. Figure 6.9 and 6.10 show these two plots. The difference between the empty and full rope rotations at 600 m from the skip is 44 turns.

In Figure 6.11 the actual C factors as used in the in the calculations of rope twist are shown. The solid and the dashed line represent the C factor variation along the rope with an empty skip and the rope with a full skip. Rope force can be related directly to rope length i.e.  $F = P + q.z$  or  $z = (F - P)/q$ .

The C factor curves as described by equations (18) and (19) are plotted for constant rotations or twists. The rotations indicated on the right can be converted to twists by dividing by 4,05. The dotted lines compare favourably to the C factor curves in Figures 5.10 and 5.12. Only in the region marked by the lines 'a' are the curves not representative. However this is not serious since, for the masses and length of rope used in this project, negative rotations are not experienced below loads of 180 kN.

Figure 6.12 shows the actual Torsional stiffness values as used in the calculation of rope twist. The solid and the dashed line represent the T factor variation along the rope length with an empty skip and the rope with a full skip.

The T factor curves as described by equation (20) are shown for constant rotations (dotted lines). These rotations can be converted to twist by dividing by 4.05. The T factor curves do not compare very well with those in Figures 5.13 and 5.15. This is because of the decision made to make T factor increase with positive rotation and decrease with

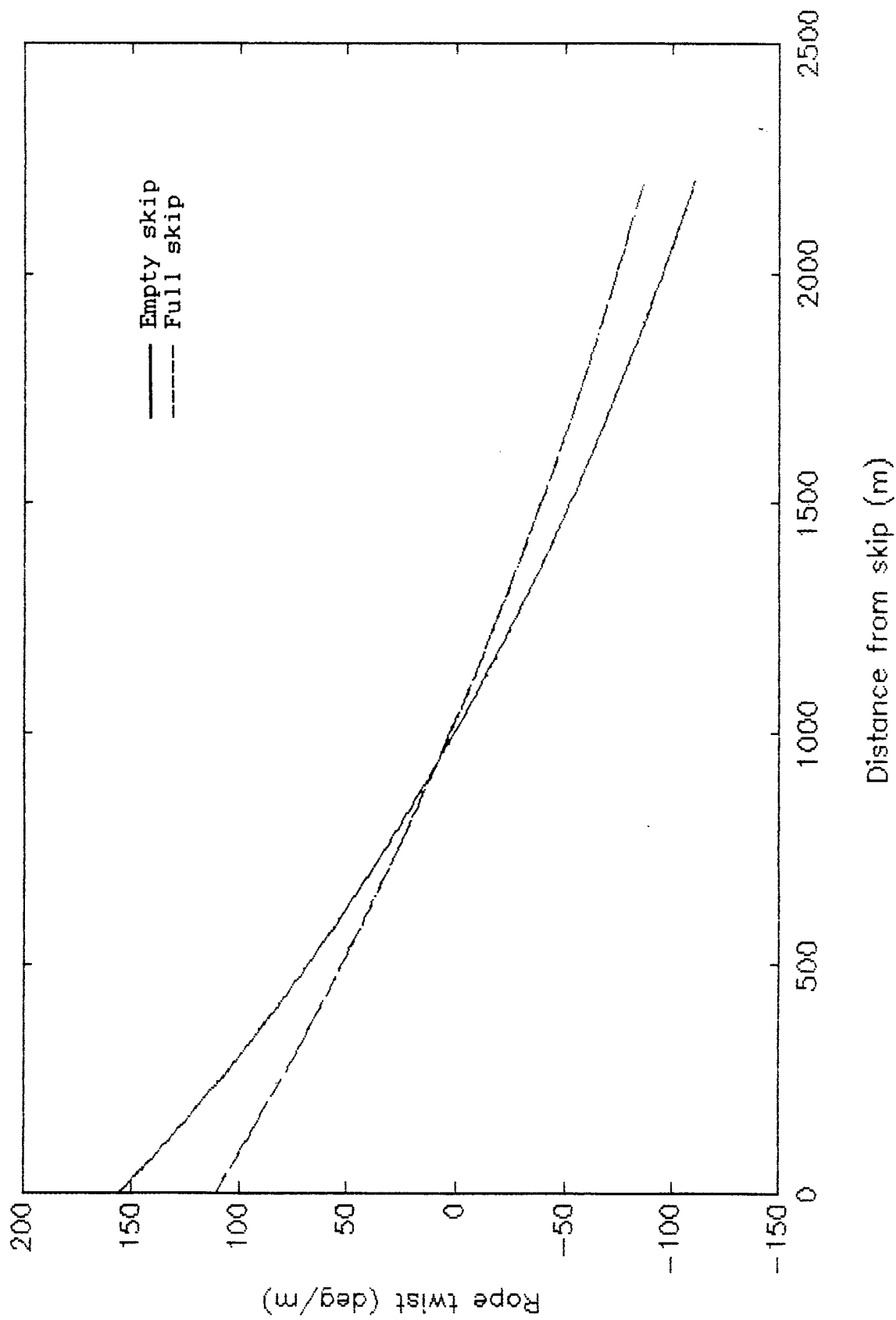


FIG. 6.9 - C and T rope twist and length.

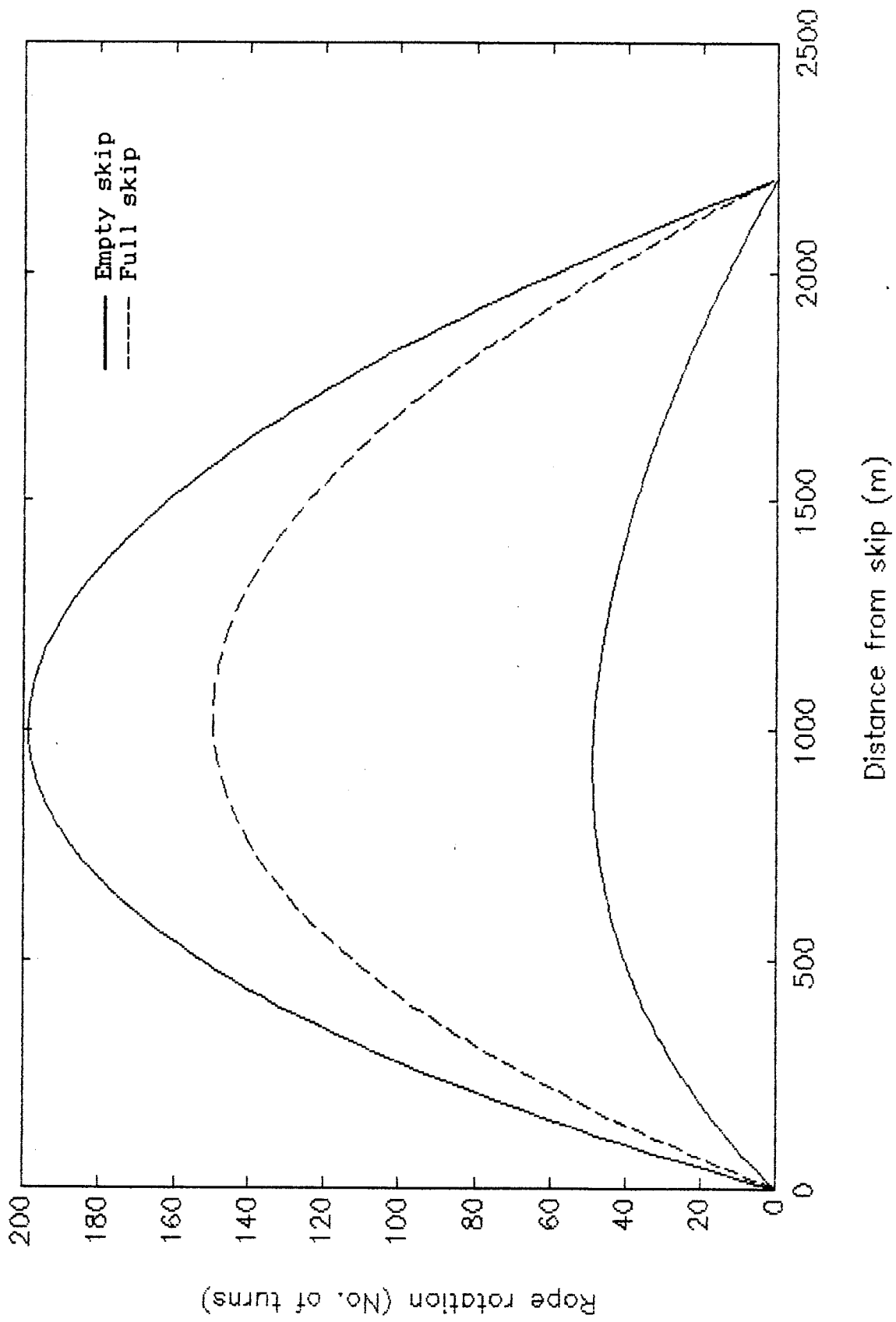


FIG. 6.10 - C and T rope rotation and length.

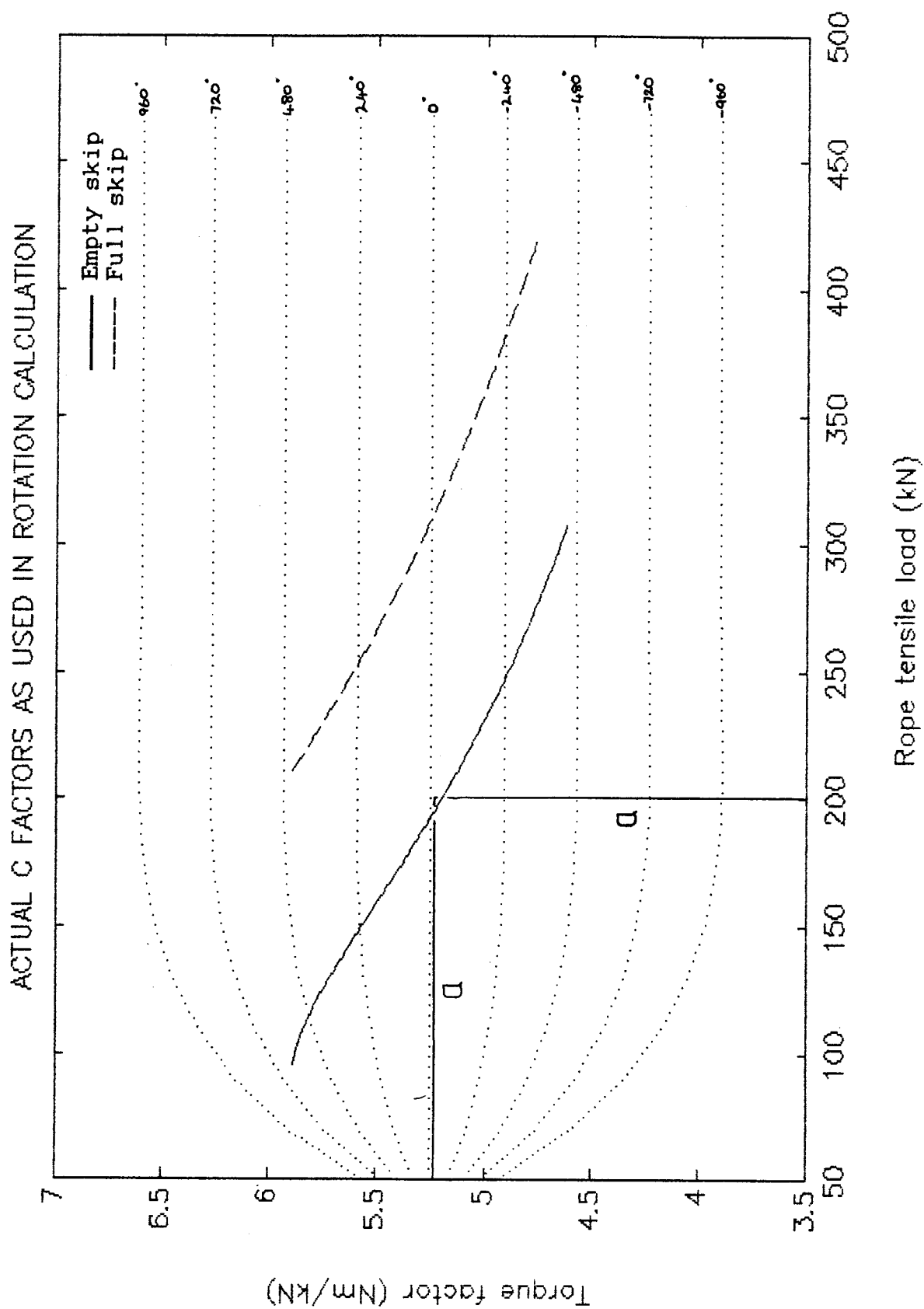


FIG. 6.11 - Actual C factors along rope length.

ACTUAL T FACTORS AS USED IN ROTATION CALCULATION

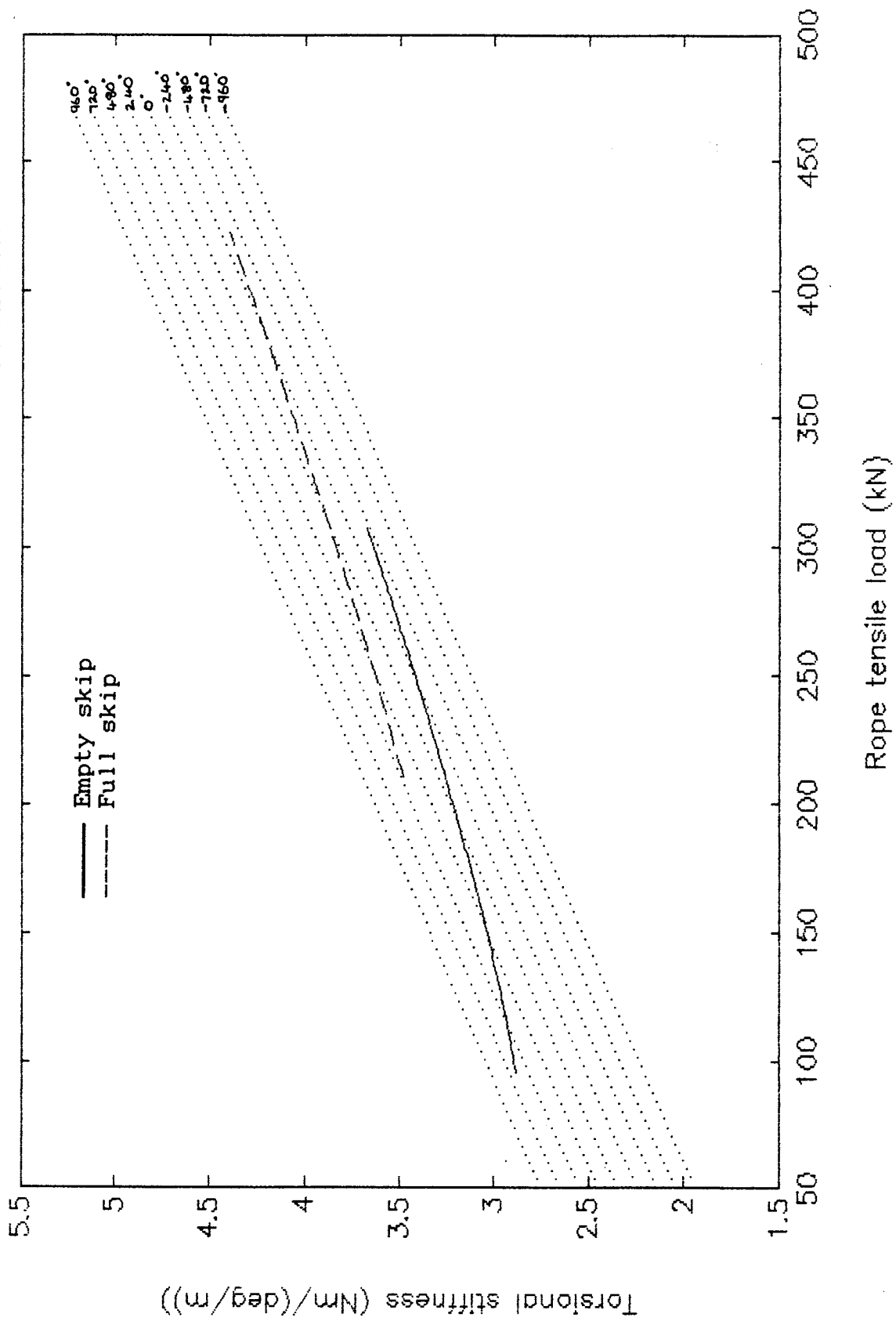


FIG. 6.12 - Actual T factors along rope length.



negative rotation. Rather than increase with both, and then sometimes decrease. Refer back to Section 5.7 for discussion on this.

Finally, in Figure 6.13 the torque curves as described by equation (21) are plotted as dotted lines. These compare reasonably to those in Figures 5.1 and 5.3 however they do not show the same curvature at higher angles of rotation. The accuracy of this method could be improved upon.

The empty and full torque lines are also indicated in Figure 6.13. Referring back to the explanation for Figure 3.2 it can be seen that these lines are in the correct position relative to one another.

The reason why these plots were labelled with degrees is that they could be easily compared with the corresponding lines in the plots of Section 5.

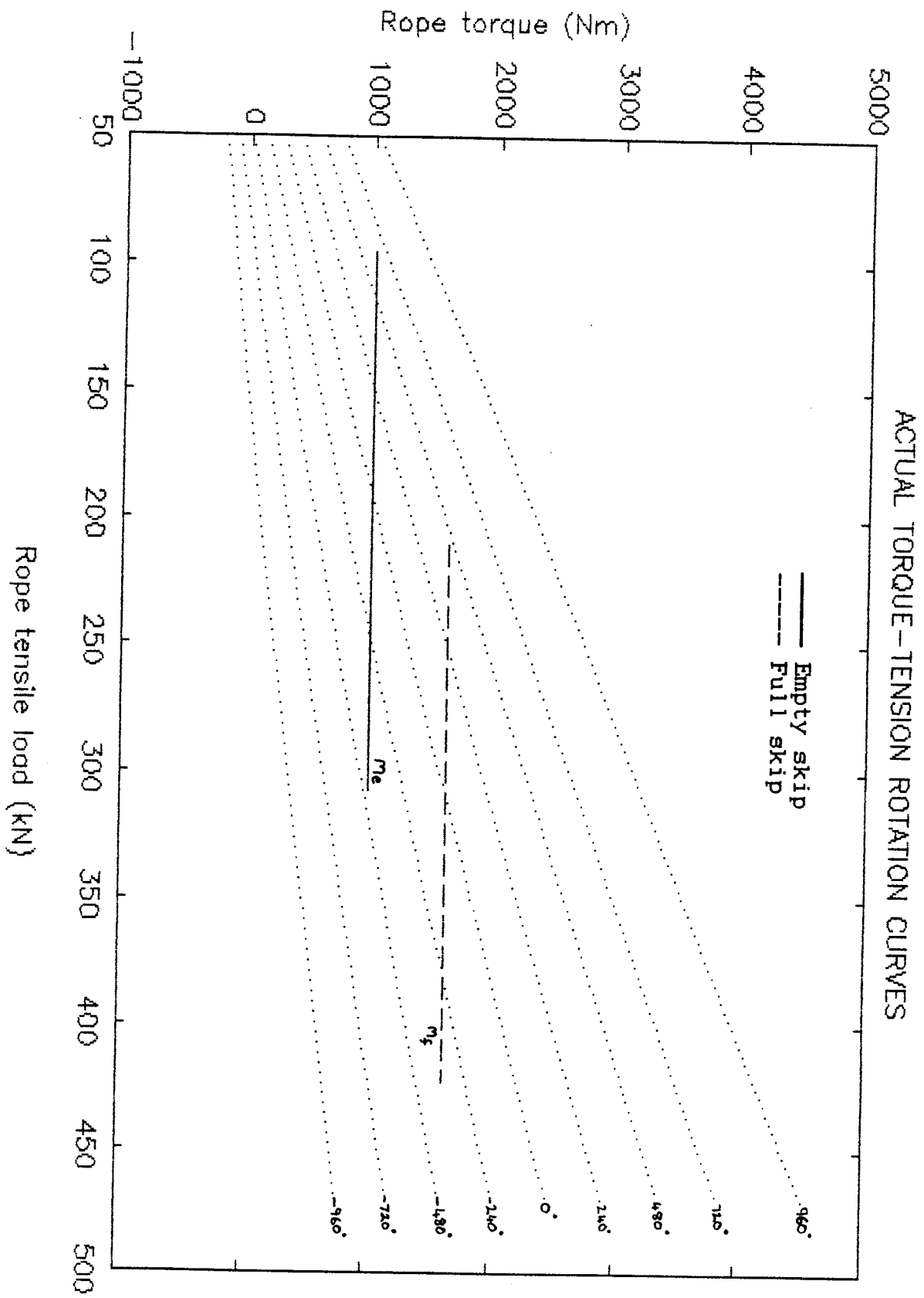


FIG. 6.13 - Actual torque-tension rotation curves.

### 6.3.1 ADDITIONAL NOTE

The C and T factor method presented above was not the first attempt at applying this method. The author and his co-worker developed a HP 87 computer based model to predict the rope rotation as a function of length using the C and T factor approach. It was however realised within the final week of the project that this model was wrong from the point of view of its derivation. The following error was made :

$$\text{Given :} \quad M = C.(P + q.z) + T.R$$

$$\text{Therefore :} \quad d\phi/dz = R = [ M - C.(P + q.z) ] / T$$

$$\text{Integrating :} \quad \phi = (M-C.P)/T.z + (C.q)/(T.2).z^2 + \text{const}$$

$$\phi = 0 \text{ at } z = 0 \quad \text{therefore} \quad \text{const} = 0$$

$$\text{Now :} \quad \phi = (M-C.P)/T.z + (C.q)/(T.2).z^2$$

This is totally incorrect because both C and T are functions of F which is a function of rope length z. So when integrating, these functions of z must be taken into account. With this error the entire model becomes inherently incorrect.

Much time was spent in developing the HP computer program, "T\_T\_CURVE", for the prediction of rope rotation. Some of the equations in the program may be incorrect but the structure is correct and meaningful. It may even be useful to any further development in this field. For these reasons it has been included in APPENDIX I. A basic description of the operation of the program is also included as well as some of the output plots.

## 7. CONCLUSIONS

1. At the start of the project it was intended to do torque-tension rotation tests on six used rope specimens. A back middle and front end section of an underlay and an overlay drum winder rope.

Overheating problems with the hydraulic equipment resulted in considerable time delays and it was therefore decided to stop the testing after the three underlay specimens had been tested. It was felt that this would not negatively affect the results of the project.

2. The torque tension tests, for the first time, took into account actual lay length changes as experienced by the rope in the shaft. Maximum and minimum angles of rotation of  $1080^\circ$  and  $-1080^\circ$  were applied to the 4050 mm long test specimens. The back end was unwound from  $0^\circ$  to  $-1080^\circ$ , the middle wound up from  $-600^\circ$  to  $480^\circ$  and the front end wound up from  $0^\circ$  to  $1080^\circ$ . Steps of  $120^\circ$  were used in all cases.
3. From the data manipulation conducted on the test results it was found that the Torque factor and Torsional stiffness both depend on the rope twist and rope force. This is contrary to previous indications that Torque factor depended only on twist and the Torsional stiffness only on force. It is believed that this came to light because of the high angles of rotation used during the testing. Rope force is linear function of the suspended rope length so the C and T are also functions of length.
4. The results for the back and front underlay specimens were easily combined since the calibrations for the tests were both done with the rope specimens at  $0^\circ$  end rotation. The middle underlay test calibration was done

at  $-600^\circ$  so it was not possible to relate the results to the results of the other two tests.

5. The traditional C and T factor method of determining rope rotation is not the only method that can be used. There is the Direct Data Fit method where an equation is fitted to the torque-tension rotation curves yielding twist  $R = f(M, F) = f(M, z)$ . Integrating this equation with respect to  $z$  gives the rope rotation  $\Phi = f(M, z)$ .

There is another method where the lay length measurements along the length of the rope in the shaft, the test lay lengths and test twists are combined to result in an equation for twist in terms of length. This equation is then integrated with respect to  $z$  to yield rotation.

6. At the start of the project it was planned to base the model of rope rotation on an HP 86 or HP 87 computer. A model was developed in this form but at a late stage it was realised that the assumptions made in determining the model was incorrect. From that point on extensive use was made of the numeric computation software package MATLAB for all three methods of predicting rope rotation. It was found to be extremely useful and powerful and far more suitable to the modelling than the HP computers.
7. In the modelling of the rope rotation much use was made of the least squares polynomial fit approach. This was found to be very accurate since the majority of data curves are near straight lines or lines with slight curvature.
8. Whenever a curve was fitted to data the fit was plotted with the raw data to check for accuracy of fit. The optimum order of polynomials used in the models was determined in this way.

9. This entire project was conducted from a static point of view. The dynamic behaviour of the rope was not taken into account. A MATLAB based model would however simplify the incorporation dynamic effects into the model at a later stage.
10. The main result from the models is the prediction of the difference in rope rotation between the full and empty skip end load conditions. The following results are available. Delta  $\Phi$  is taken at 600 m from the conveyance. :

**Table 7.1 - Rope torques and rotations for different models.**

Method	Me (Nm)	Mf (Nm)	Me/Mf	delta $\Phi/360$
Direct Data Fit ( Van Zyl )	1055	1675	0.630	28
Direct Data Fit ( Rebel )	1025	1619	0.633	58
C and T factor ( Borello )	N/A	N/A	N/A	43
C and T factor ( Rebel )	1013	1629	0.622	44

The actual rotation of the rope as counted in the shaft was 12,5 rotations at 600 m. This is the only value that the models can be judged by. Based on this one in-shaft reading the models are not adequate.

11. If the one in shaft measurement is assumed to be a good indication of the rotational behaviour of the rope then there are a number of areas in the modelling process where errors could have occurred. Reading the data manually of the curves generated by "T\_T\_PLOT" is

definitely inaccurate.

Also, the rope twist values for the testing were always determined by dividing the end rotation by 4.050 m. This is in fact not correct since the gauge length changes with rotation. Each twist value should be calculated using the actual gauge length associated with that rotation..

12. It appears as if there is an almost constant ratio between the full and empty rope torques for the three of the models in Table 7.1. There may be some significance to this. Possibly for a rope with a certain length and empty to full load ratio there may be a set and predictable ratio between the empty and full rope torques.
13. In terms of the objective of the project, an accurate model of the in-shaft rotation of the rope has not been achieved. However, the validity of this remark is dependant on the validity of the one in-shaft rotation reading.
14. The models presented in this report can easily be altered to take into account different shaft depths and rope end loads.
15. A better overall understanding of the processes required to accurately predict the rotational behaviour of the rope has definitely been achieved. This is reflected in the extensive recommendations which follow.

## 8. RECOMMENDATIONS FOR FUTURE WORK

There many aspects which have to be considered in accurately solving the torque-tension rotation behaviour of a triangular strand steel wire rope. In the author's opinion, the solution does not lie in a purely mathematical approach. Rather in an extensive in-shaft measurement and laboratory testing program followed by accurate data manipulation and analysis to describe the measured rope behaviour. Below are some points to consider :

1. Many more in shaft rope rotation measurements are required so that the accuracy of later models can be commented on. It is not feasible to judge a model's accuracy on one measurement.
2. Thought should be given to the measurement of in-shaft rope torque and tension. This could be achieved by attaching a torque tension load cell in between say the rope thimble and the Humble Hook. A conveyance mounted data recorder could then be used to record torque and tension fluctuations in the rope for different conditions during a winding cycle. This would lead to a better understanding of the relationship between in-shaft rope torque and tension.
3. The empirical method of predicting rotation as described in Section 6.1. should be investigated in more detail.
4. For the laboratory testing, new lubricated rope specimens should be used. These will have a neutral lay length unlike the specimens used in this project which showed certain amounts of permanent set. The control program should be modified to process a total of 19



curves so that one rope specimen can be tested from say  $-1080^{\circ}$  to  $1080^{\circ}$  with steps of  $120^{\circ}$ . The tests can also be done from  $1080^{\circ}$  to  $-1080^{\circ}$  for purposes of comparison.

This type of testing will give a full combined set of torque tension rotation data for the rope with a single test calibration procedure.

If tests are done on different rope specimens the calibration should always be done at the same end rotation so that the results can later be related and combined.

5. Accurate data processing requires increased computer hardware facilities above that of the HP 86 and HP 87 computers. The HP 86 computer which controls the test machine is sufficient. From here on it is recommended that the test data be converted to a IBM PC based format. Once this is achieved, MATLAB or an equivalent numeric computation software package could be used for all the computational requirements.

This will eliminate the errors in manually transferring data from the test result curves.

6. The hysteresis in the torque-tension rotation curves should be investigated to determine whether it is a rope characteristic or whether it is caused by the instrumentation.
7. It may also be considered to modify the torque-tension test machine so that it would be capable of maintaining a constant torque in the rope for varying tensile loads. The idea being that the torque, of the rope in the shaft, for a certain end load would be entered into the control computer. The computer would then increase the load on the rope till it equalled the front end load in the shaft.

At this point the end rotation would be automatically adjusted until the torque in the rope equalled the in-shaft torque. By increasing the tension and constantly changing and measuring the end rotation it would be possible to determine curves of force versus rotation for lines of constant torque. Since a load range can be directly related to in-shaft rope length, equations for rope twist in terms of rope length will result from these tests.

Once equations for twist in terms of length are found it is possible to find rope rotation by integration.

## 9. REFERENCES

Due to the sensitivity surrounding the manufacture and operation of steel wire ropes in South Africa, and the confidentiality of certain contract reports, some of the references below may not be completely detailed.

BORELLO M., (1993a), TECHNICAL DISCUSSION, MECHANICAL ENGINEER, CSIR, MAY 1993.

BORELLO M., (1993b), C AND T FACTOR CALCULATIONS FOR A TRIANGULAR STRAND ROPE, CSIR, MAY 1993.

FEYRER K., SCHIFFNER G., (1986), TORQUE AND TORSIONAL STIFFNESS OF WIRE ROPE, WIRE 36(1986), 37(1987).

HAGGIE RAND LIMITED, (1987), STEEL WIRE ROPES FOR MINE HOISTING, JOHANNESBURG, NOVEMBER 1987.

KOLLROSS W., (1976), THE RELATIONSHIP BETWEEN TORQUE, TENSILE FORCE AND TWIST IN WIRE ROPES, WIRE, JANUARY 1976.

McKENZIE I.D., (1987), THE TORSIONAL PROPERTIES OF STEEL WIRE ROPES, Pr.ENG. DISSERTATION, UNIVERSITY OF THE WITWATERSRAND, JOHANNESBURG, 1987.

McKENZIE I.D., (1990), ASPECTS OF THE DESIGN OF STEEL WIRE ROPES, M.Sc. DISSERTATION, UNIVERSITY OF THE WITWATERSRAND, JOHANNESBURG, 1990.

MOLL C., (1973), MODERN SHAFT SYSTEMS IN THE REPUBLIC OF SOUTH AFRICA, INTERNATIONAL CONFERENCE ON HOISTING MEN MATERIALS AND MINERALS, SOUTH AFRICAN INSTITUTE OF MECHANICAL ENGINEERS, OCTOBER 1973.

VAN ZYL M., (1993a), EXTERNAL ENGINEERING CONSULTANT TO THE

CSIR, JULY 1993.

VAN ZYL M., (1993b), INFORMATION ON TORQUE TENSION AND ROTATION IN A DRUM WINDER ROPE, JUNE 1993.

WALKER S.C., (1988), MINE WINDING AND TRANSPORT, ADVANCES IN MINING SCIENCE AND TECHNOLOGY 4, ELSEVIER, 1988.

YIASSOUMIS J.M., (1992), TORSIONAL BEHAVIOUR OF WIRE ROPES FOR KOEPE WINDERS, M.Sc. DISSERTATION, UNIVERSITY OF THE WITWATERSRAND, JOHANNESBURG, 1992.

## APPENDIX A

Test machine hydraulic circuits.

# HYDRAULIC CIRCUIT FOR THE TENSIONING CYLINDER

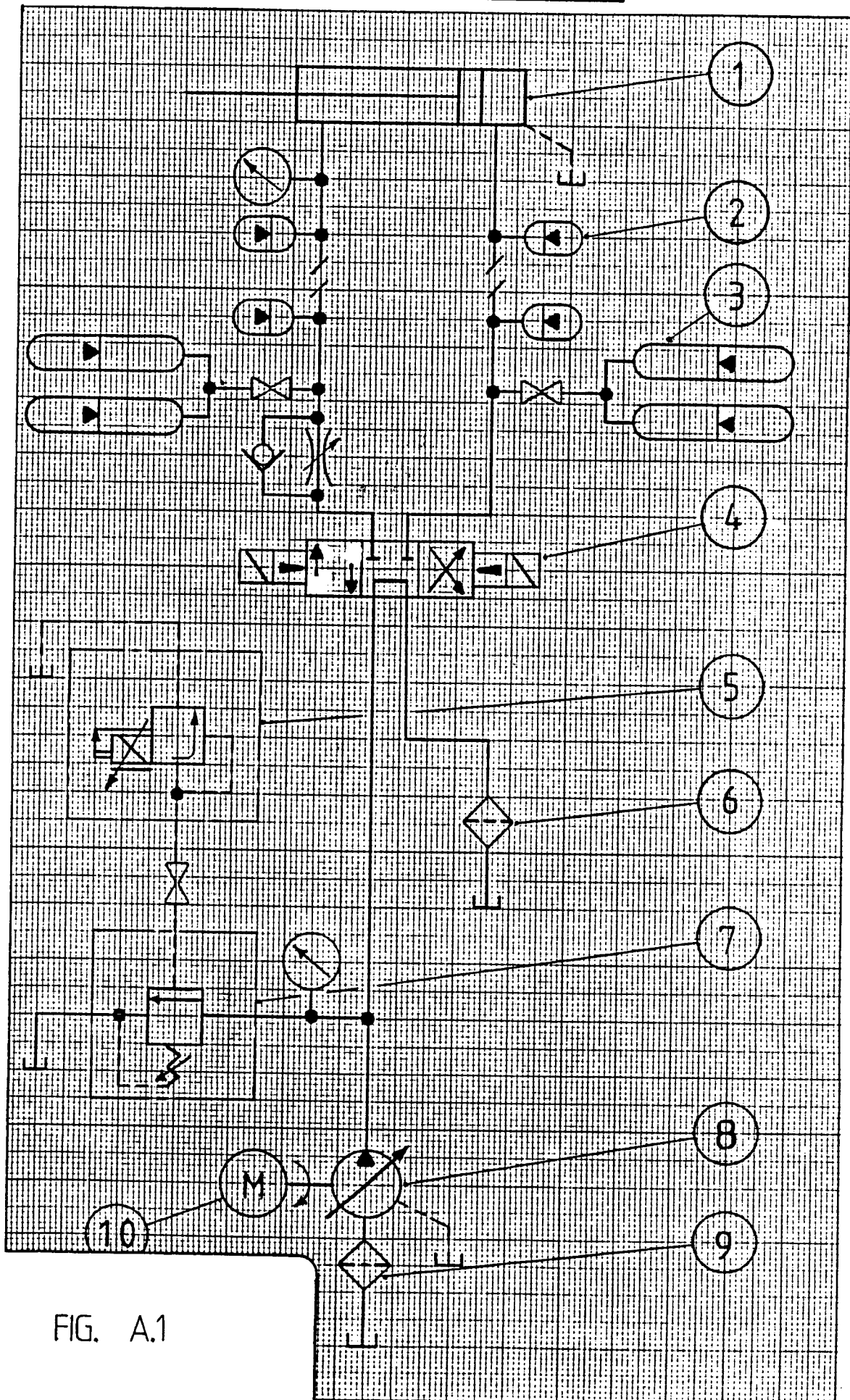


FIG. A.1

HYDRAULIC CIRCUIT FOR THE TENSIONING CYLINDER

PART NO.	DESCRIPTION	CATALOG NO.
1	TENSIONING DOUBLE ACTING CYLINDER	
2	INLINE ACCUMELATOR N <sub>2</sub> PRECHARGED	LANGEN & CO D075-1315-054-615
3	LARGE DOUBLE ACCUMELA- TOR	
4	THREE POSITION SOLENOID OPERATED VALVE	WANDFLUH - A4D203
5	PROPORTIONAL PRESSURE RELIEF VALVE	REXROTH - DBETR/10
6	FILTER 10 MICRON	
7	PRESSURE RELIEF VALVE	CT-06-F-40 - VICKERS
8	VARIABLE DISPLACEMENT PUMP (MANUAL SETTING)	REXROTH - PV2A111/63 RE ... M.
9	FILTER 125 MICRON	
10	ELECTRIC MOTOR - 3 PHASE	SIEMENS - 43 kW - 380 V

# HYDRAULIC CIRCUIT FOR ROTATION

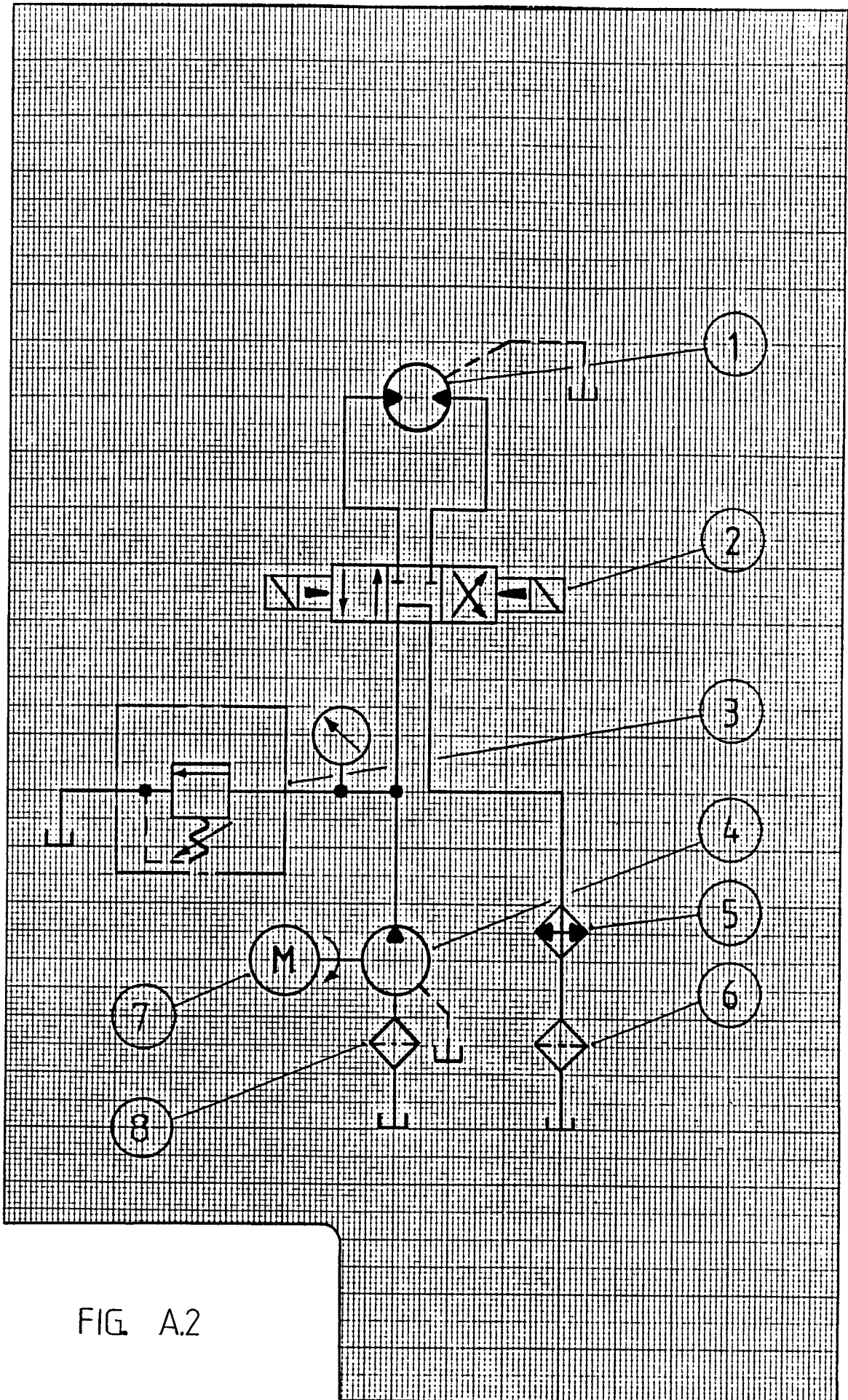


FIG A.2



HYDRAULIC CIRCUIT FOR THE ROTATION MOTOR

PART NO.	DESCRIPTION	CATALOG DESCRIPTION
1	REVERSABLE ROTATION MOTOR	STAFFA 3 80
2	THREE POSITION SOLENOID OPERATED VALVE	WANDFLUH - VP4D 3
3	PRESSURE RELIEF VALVE	VICKERS - CT-06-F40
4	GEAR PUMP	ASAPPA - CP44D
5	HEAT EXCHANGER - WATER COOLED	
6	FILTER 10 MICRON	
7	ELECTRIC MOTOR - 3 PHASE 380 V	SIEMENS 29 KW
8	FILTER 125 MICRON	

## APPENDIX B

Description of control program "T\_T\_TEST".

```

1000 ! *****
      ! CST MACHINE CONTROL PROGRAM *****
1010 !
1020 ! PROGRAM NAME "T_T_TEST" - CAN HANDLE 10 CURVES
1030 !
1040 ! TO BE USED WITH PROGRAM "T_T_PLOT" 19/10/93
1050 !
1060 ! NEED TO RUN "FSMALL" TO DECREASE DATA FILE SIZE BY FACTOR OF 4.
1070 ! RUN "FSMALL" BEFORE RUNNING "T_T_PLOT"
1080 !
1090 ! PROGRAM MODIFIED BY G.REBEL / E.SALZMANN
1100 !
1110 ! *****
1120 !
1130 CLEAR
1140 PAGESIZE 24
1150 GOSUB Title
1160 GOSUB Prepare_rope
1170 GOSUB Zero_rotation
1180 GOSUB Amplifires
1190 GOSUB Dimensions
1200 GOSUB Initialize_instruments
1210 GOSUB General_info
1220 GOSUB Create_file
1230 GOSUB Set_plotter
1240 GOSUB Max_force
1250 GOSUB Zero_force
1260 GOSUB Calibration
1270 GOSUB Elong_diam_cal
1280 GOSUB Print_info
1290 GOSUB Print_cal
1300 GOSUB Speed
1310 !
1320 New_curve:
1330 GOSUB Next_curve
1340 GOSUB Set_rotation
1350 GOSUB Bedding
1360 GOSUB Control_parameters1
1370 GOSUB Initialize_array
1380 GOSUB Start_screen
1390 GOSUB First_point
1400 GOSUB Cycle_up
1410 GOSUB Top_hold
1420 GOSUB Cycle_down
1430 GOSUB Store_results
1440 GOSUB Plot_results
1450 GOSUB Print_results
1460 GOTO New_curve
1470 !
1480 Test_end:
1490 GOSUB Store_info
1500 END
1510 !
1520 ! *****

```

The previous page shows the first section of the torque-tension test machine control program "T\_T\_TEST". The listing details the order of the subroutines which make up the program. Below is a description of the operations executed by each of the subroutines.

**Title :** Displays the start screen and requests the user to follow instructions carefully. The program is written in such a way as to guide the user step by step so that the tests can be completed safely and correctly.

**Prepare\_rop**e : Prompts the user to ensure that the rope rotation is at 0° and that the friction brake is on.

**Zero\_rotati**on : Specifies that the rotation is 0°.

**Amplifiers :** Prompts the user to set the calibration level of the strain gauge amplifiers at 3000, to make the rope slack and to check that the bridges are balanced. Also, the user is prompted to physically adjust the diameter LVDT's so that the voltage readings on the diameter DVM's lie between -4.5 V to -4 V. This is done with a preload on the rope specimen.

**Dimensions :** Arrays and string variables used by the program are dimensioned.

**Initialize\_in**struments : Allocates addresses to all the computer peripheral devices. This includes all the DVM's and the plotter. The user is prompted to check that the devices addresses agree with those set physically by the DIP switches on each unit.

**General\_info :** The user is prompted for general information regarding the test. This includes the rope diameters, lay lengths and specimen gauge length. The rope braking force as determined by a destructive test is also asked for. The entered data is then displayed on the screen for verification.

**Create\_file** : The user is asked whether the results must be stored. If so then the relevant file name is entered. An empty file is created on a disk which has sufficient space for all ten sets of test data.

**Set\_plotter** : If the user so requests, an empty graph frame is plotted by the HP pen plotter connected to the computer. This frame is later used for the plotting of the torque versus tension curves.

**Max\_force** : If 30% of the rope braking force, entered under the general information section, is greater than 500 kN then the user is prompted to enter the required maximum test force. This value must be less than 500 kN. In such a case the user is also prompted to enter a new value for the maximum bedding in cycle force. This is usually taken as 10 % of the rope braking force.

**Zero\_force** : The user is prompted to slacken the rope so that the zero torque and force reference voltages can be read. The computer reads these voltages by direct interfacing with the HP 3478A DVM's.

**Calibration** : Prompts the user to switch the torque tension load-cell calibration switches on. The computer then instructs the user to adjust the attenuation and gain button on the strain gauge amplifiers so that the readings on the torque and force DVM's are at certain values. These values were calculated by the computer so that the calibration of the load-cell will be within  $\pm 1\%$  of the exact predetermined calibration values. The computer then displays the actual and exact calibrations for the user's approval.

**Elong\_diam\_cal** : The user is instructed to set the tension in the rope to a certain value. The computer automatically specifies a voltage range for the force DVM which will correspond to this specific force. Once this is done, the zero diameter and elongation voltages are read and the user is prompted to insert calibration plates of known size at

the five LVDT's. The calibration values are calculated and displayed on the screen for approval.

**Print\_info / Print\_cal** : The general test information and calibration data are printed out. Examples of these printouts are contained in APPENDIX C.

**Speed** : The user is given a choice of the test speed. Values between 2 and 8 can be selected. The bedding in cycles are automatically run at a speed three higher than that selected for the actual test.

**Next\_curve** : Tells the user the curve number and prompts whether that curve must be run. After ten curves the user is informed that no more curves can be run.

**Set\_rotation** : The current rotation and twist of the rope is displayed on screen and the user is given an opportunity to physically alter the rotation and the enter the new value.

**Bedding** : The bedding in cycles are then run. The user has the option not to run them. Bedding cycle two follows automatically after cycle one.

**Control\_parameters1 / Initialize\_array / Start\_screen** : These procedures are called in preparation for the actual test.

**First\_point** : Reads and records the starting values of all the test parameters.

**Cycle\_up / Top\_hold / Cycle\_down** : Control the tension generated by the hydraulic cylinder. Continuous readings of test parameters are taken and recorded. The force and torque values are monitored to ensure that they do not exceed 500 kN or 3000 Nm. The test parameter measurements are displayed on screen so that the user can monitor the actual testing.

**Store\_results** : All the data collected during the test is written to the file which was created earlier in the program.

**Plot\_results** : The torque versus tension curve is plotted on the graph frame already created.

**Print results** : The user is given the option to print out all the test parameter measurements.

**Store\_info** : Stores the general test information, required by the plotting program "T\_T\_PLOT", in a file, Inform. This includes the maximum and minimum forces attained during the testing.

#### **PROGRAM MODIFICATIONS**

The original control program "Test C&T" was not able to run independently. It relied on data created by another testing program "Test ASm" which is a 50 cycle test control program usually run before "Test C&T". The necessary changes were made to "Test C&T" so that it could run independently and it was renamed "T\_T\_TEST".

The overall program was made more user friendly and more informative. For this nearly every subroutine had to be altered and in some cases more subroutines added.

The trial and error method of calibrating the load-cell was replaced by an exact instruction from the computer as to the setting required for an exact calibration.

Also the load setting for the diameter and elongation calibration was made more exact by the computer specifying the required DVM reading.

It would be tedious to specify all the changes made to the program. The main point to be made is that "T\_T\_TEST" it is

a definite improvement on the program "Test C&T".



## APPENDIX C

General test information, calibration data and  
CSIR rope test certificate.

GENERAL TEST INFORMATION

File name : BCKLL

---

Test date : 29 SEP 1993  
W/O number : 124931 (002)  
Construction : 6\*32(14/12/6+3T)/F  
Product code : N/A  
Lay direction : RH

Tensile grade : 1800 [MPa]  
Breaking force : 1730 [kN]

Nominal diameter : 48 [mm]  
Actual diameter at 1+2 : 47.3 [mm]  
Actual diameter at 3+4 : 47.6 [mm]  
Mean diameter : 47.45 [mm]

Nominal lay length : 361 [mm]  
Actual lay length : 427 [mm]  
Gauge length : 4050 [mm]

Maximum test force : 500 [kN]  
Maximum bedding in force : 173 [kN]  
Minimum test force : 8.665 [kN]  
Number of bedding cycles : 2

TEST CALIBRATION DATA

File name : BCKUL

---

Test Date : 29 SEP 1993  
W/O Number : 124931 (002)

Zero Force = .0255782 [Volt]  
Zero Torque = -.0121474 [Volt]  
Zero Elong = -.01414526 [Volt]  
Zero Diam1 = -4.65918 [Volt]  
Zero Diam2 = -4.52157 [Volt]  
Zero Diam3 = -4.64963 [Volt]  
Zero Diam4 = -4.57547 [Volt]

Force Cal = 411.765554519 [kN/Volt]  
Torque Cal = 2088.35998474 [Nm/Volt]  
Elong Cal = 13.6502853142 [mm/Volt]  
Diam1 Cal = .220390046304 [mm/Volt]  
Diam2 Cal = .222730542217 [mm/Volt]  
Diam3 Cal = .165401072791 [mm/Volt]  
Diam4 Cal = .170990298845 [mm/Volt]

GENERAL TEST INFORMATION

File name : MIDUL

---

Test date : 4 OCT 1993  
W/O number : 124931 (002)  
Construction : 6\*32(14/12/6+3T)/F  
Product code : N/A  
Lay direction : RH

Tensile grade : 1800 [MPa]  
Breaking force : 1730 [kN]

Nominal diameter : 48 [mm]  
Actual diameter at 1+2 : 48.44 [mm]  
Actual diameter at 3+4 : 48.54 [mm]  
Mean diameter : 48.49 [mm]

Nominal lay length : 361 [mm]  
Actual lay length : 525 [mm]  
Gauge length : 4050 [mm]

Maximum test force : 500 [kN]  
Maximum bedding in force : 173 [kN]  
Minimum test force : 8.664 [kN]  
Number of bedding cycles : 2

TEST CALIBRATION DATA

File name : MIDUL

---

Test Date : 4 OCT 1993  
W/O Number : 124931 (002)

Zero Force = .02973 [Volt]  
Zero Torque = .02261 [Volt]  
Zero Elong = -4.03485 [Volt]  
Zero Diam1 = -4.56756 [Volt]  
Zero Diam2 = -4.45231 [Volt]  
Zero Diam3 = -4.62414 [Volt]  
Zero Diam4 = -4.48482 [Volt]

Force Cal = 411.129917054 [kN/Volt]  
Torque Cal = 2082.0048017 [Nm/Volt]  
Elong Cal = 13.1778348817 [mm/Volt]  
Diam1 Cal = .221885449418 [mm/Volt]  
Diam2 Cal = .220448833826 [mm/Volt]  
Diam3 Cal = .165006971545 [mm/Volt]  
Diam4 Cal = .171179969205 [mm/Volt]

GENERAL TEST INFORMATION

File name : FNTUL

---

Test date : 1 OCT 1993  
W/O number : 124931 (002)  
Construction : 6\*32(14/12/6+3T)/F  
Product code : N/A  
Lay direction : RH

Tensile grade : 1800 [MPa]  
Breaking force : 1730 [kN]

Nominal diameter : 48 [mm]  
Actual diameter at 1+2 : 47.4 [mm]  
Actual diameter at 3+4 : 47 [mm]  
Mean diameter : 47.2 [mm]

Nominal lay length : 361 [mm]  
Actual lay length : 385 [mm]  
Gauge length : 4050 [mm]

Maximum test force : 500 [kN]  
Maximum bedding in force : 173 [kN]  
Minimum test force : 8.86 [kN]  
Number of bedding cycles : 2

TEST CALIBRATION DATA

File name : FNTUL

---

Test Date : 1 OCT 1993  
W/O Number : 124931 (002)

Zero Force = .03624 [Volt]  
Zero Torque = -.01693 [Volt]  
Zero Elong = -4.44115 [Volt]  
Zero Diam1 = -4.33848 [Volt]  
Zero Diam2 = -3.97304 [Volt]  
Zero Diam3 = -4.30465 [Volt]  
Zero Diam4 = -4.47469 [Volt]

Force Cal = 410.683363127 [kN/Volt]  
Torque Cal = 2081.12490646 [Nm/Volt]  
Elong Cal = 13.8838110136 [mm/Volt]  
Diam1 Cal = .22213953695 [mm/Volt]  
Diam2 Cal = .220129281927 [mm/Volt]  
Diam3 Cal = .164648487827 [mm/Volt]  
Diam4 Cal = .171462178015 [mm/Volt]

# UNDERLAY ROPE



Materials  
Science and  
Technology

CSIR

## Mine Hoisting Technology

Private Bag X28  
Auckland Park  
2006 South Africa

3-21312 SA  
 Navorsmin  
Auckland Park

National (011) 726-7100  
International + 27 11  
Fax: (011) 726-6418

Delivery Address:  
Cor. Menton Road and Frost Avenue  
Cottesloe 2092 Johannesburg

Application received: 89.06.21  
Rope received: 89.06.20

Certificate No: 166756  
Date of Test: 89.06.23

### CERTIFICATE OF TEST CONDUCTED ON WINDING ROPE

Particulars supplied by Applicant:

Name of mine (if applicable)	HAGGIE RAND LIMITED	Date of manufacture	89.06.15
Specimen supplied by	Haggie Rand Limited	Type of shaft	
Name of manufacturer		Length of wind (m)	
Name of shaft		Date rope put on	
Name of compartment		Length of rope (m)	2 600
Winding plant cert. no		Mass per length (kg m)	9,81
Coil no. of rope	124931/002 W/O 124931 (002)	Type of lay	RHL
Nom. diameter of rope (mm)	48,0	Nom. length of lay (mm)	361
Construction of rope	Compound Triangular Strand 6x32(14/12/6+3T)/F		
Number of strands	6		
Lubricant			
Type of heart of rope	Fibre		
Number of wires in strand	32(14/12/6+3T)		
Diameter of wires (mm)	3,10 2,24 1,92 1,44		
Type of strand core	Plaited		
Tensile grade of steel	1 800	MPa Wire finish	Ungalvanized
Breaking force of new rope		kN	
Breaking force of previous test		kN Length of specimen supplied (m)	3,50
Minimum allowable breaking force		kN Date cut	

### RESULTS OF TEST AND EXAMINATION

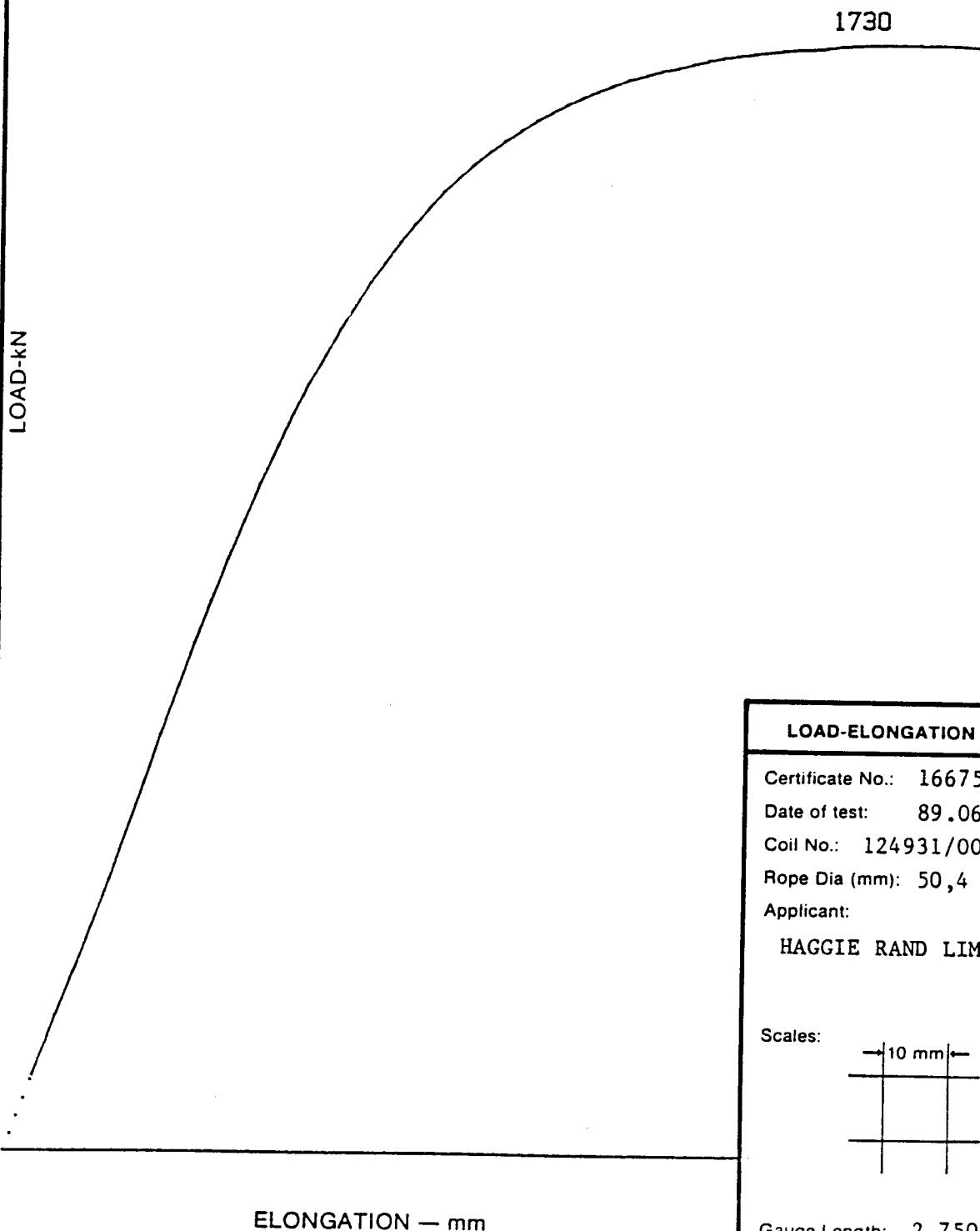
Breaking force of rope	1 730	kN Gauge length of test specimen (m)	2,75
Least dimension of outer wire (mm)		Length of lay (mm)	408
Corrosion	None	Diameter of rope (mm)	50,4 : 49,3
Condition of lubrication	Good		
Appearance of wires at fracture	Ductile		
Number of strands broken	Three		
Position of fracture	Centre		
Remarks	The fibre core fluffed over the full test length		

Cottesloe, the 89.06.23

Testing Officer:

Programme Manager: Mine Hoisting Technology

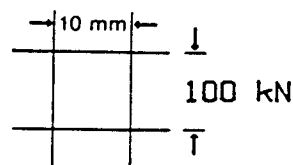
STRAIN ENERGY TO FAILURE= 195.6 kJ  
 PLASTIC FRACTION OF ENERGY= 140.7 kJ  
 PLASTIC FRACTION OF ELONG. = 86.9 mm  
 SLOPE= 27.2 kN/mm



**LOAD-ELONGATION DIAGRAM**

Certificate No.: 166756  
 Date of test: 89.06.23  
 Coil No.: 124931/002 WO 124931(002)  
 Rope Dia (mm): 50,4 : 49,3  
 Applicant:  
**HAGGIE RAND LIMITED**

Scales:



Gauge Length: 2 750 mm

**Division of Materials Science and Technology**  
 CSIR  
**MINE HOISTING TECHNOLOGY**  
 PRIVATE BAG X28 AUCKLAND PARK 2008

APPROVED:

**PROGRAMME MANAGER**  
**MINE HOISTING TECHNOLOGY**

## APPENDIX D

Description of data manipulation program "T\_T\_PLOT".

```

1000 ! ***** C&T MACHINE PLOTTING PROGRAM *****
1010 !
1020 ! PROGRAM NAME "T_T_PLOT" - CAN HANDLE 10 CURVES
1030 !
1040 ! 16 OCTOBER 1993
1050 !
1060 ! TO BE USED WITH PROGRAM "T_T_TEST"
1070 !
1080 ! *****
1090 !
1100 CLEAR
1110 GOSUB Title
1120 GOSUB Dimensions
1130 GOSUB Bring_data
1140 GOSUB Information
1150 GOSUB Form_matrix
1160 GOSUB C_factor_cal
1170 GOSUB T_factor_cal
1180 GOTO Select_option
1190 END
1200 !
1210 ! -----
1220 Title:
1230 DISP @ DISP
1240 DISP " Program to plot torque tension elongation and diameter curves"
1250 DISP " obtained during a torque tension test with various end rotations."
1260 DISP @ DISP
1270 DISP " This program runs with 'T_T_TEST' and is set up to process 10 curve
s."
1280 DISP @ DISP
1290 DISP " Modified by G.REBEL and E.SALZMANN."
1300 DISP " 16 October 1993"
1310 DISP @ DISP
1320 DISP " Please press <CONT>"
1330 PAUSE
1340 RETURN
1350 !
1360 ! -----

```



The previous page shows the first section of the torque-tension test data manipulation program "T\_T\_PLOT". The listing details the order of the subroutines which make up the program. Below is a description of the operations executed by each of the subroutines.

**Title :** Displays starting screen of program.

**Dimensions :** Arrays and string variables used by the program are dimensioned.

**Bring\_data :** Loads the data which was created by the program "T\_T\_TEST" into memory. Also reads the relevant general test information from the file "Inform".

**Information :** Asks the user to confirm whether the information read from "Inform" is correct. If not then the user is given an opportunity to change this information.

**Form\_matrix :** Generates one matrix with all the raw test results for the ten curves.

**C\_factor\_cal / T\_factor\_cal :** The Torque factor and Torsional stiffness is calculated for all ten tests and stored in the relevant matrices.

**Select\_option :** Once all the calculations have been done the user is able to view any of the curves found in Figures 5.1 to 5.15. The curves can be displayed on screen or can be plotted by the HP pen plotter. The user also has an option to zoom in on any portion of the curves.

#### **PROGRAM MODIFICATIONS**

The original program "Plot C&T" was only able to process seven curves per test. The program was modified so that the ten curves run by "T\_T\_TEST" could be processed. Also, the

end rotation associated with each curve was automatically included next to each line. This was done to make subsequent interpretation of the results more precise.

## APPENDIX E

File conversion program "FSMALL".

```

1000 ! *****
1010 !
1020 ! PROGRAM NAME "FSMALL"
1030 !
1040 ! PROGRAM TO MAKE "T_T_TEST" DATA FILES 4 TIMES SMALLER
1050 !
1060 ! "FSMALL" READS THE DATA FILES OF "T_T_TEST" AND REWRITES THEM IN A
1070 ! FORMAT ACCEPTABLE TO "T_T_PLOT"
1080 !
1090 ! RUN THIS PROGRAM AFTER "T_T_TEST" AND BEFORE "T_T_PLOT"
1100 !
1110 ! WRITTEN BY G.REBEL / E.SALZMANN          14/10/1993
1120 !
1130 ! *****
1140 CLEAR
1150 OPTION BASE 1
1160 SHORT C1(460,7),C2(460,7),C3(460,7),C4(460,7),C5(460,7),C6(460,7),C7(460,7)
1170 SHORT C8(460,7),C9(460,7),C10(460,7)
1180 SHORT D1(115,7),D2(115,7),D3(115,7),D4(115,7),D5(115,7),D6(115,7),D7(115,7)
1190 SHORT D8(115,7),D9(115,7),D10(115,7)
1200 DISP "PUT TEST DATA DISC IN DRIVE AND PRESS CONT"
1210 DISP @ DISP
1220 PAUSE
1230 CAT
1240 DISP @ DISP
1250 DISP "INPUT THE FILE NAME"
1260 INPUT FILE$
1270 ASSIGN# 1 TO FILE$
1280 READ# 1,1 ; C1(),Angle(1)
1290 READ# 1,2 ; C2(),Angle(2)
1300 READ# 1,3 ; C3(),Angle(3)
1310 READ# 1,4 ; C4(),Angle(4)
1320 READ# 1,5 ; C5(),Angle(5)
1330 READ# 1,6 ; C6(),Angle(6)
1340 READ# 1,7 ; C7(),Angle(7)
1350 READ# 1,8 ; C8(),Angle(8)
1360 READ# 1,9 ; C9(),Angle(9)
1370 READ# 1,10 ; C10(),Angle(10)
1380 ASSIGN# 1 TO *
1390 CLEAR
1400 DISP "CONVERTING ...."
1410 I=1
1420 J=0
1430 FOR K=1 TO 7
1440   D1(I,K)=C1(I+J,K)
1450   D2(I,K)=C2(I+J,K)
1460   D3(I,K)=C3(I+J,K)
1470   D4(I,K)=C4(I+J,K)
1480   D5(I,K)=C5(I+J,K)
1490   D6(I,K)=C6(I+J,K)
1500   D7(I,K)=C7(I+J,K)
1510   D8(I,K)=C8(I+J,K)
1520   D9(I,K)=C9(I+J,K)
1530   D10(I,K)=C10(I+J,K)
1540 NEXT K

```

```

1550 J=2
1560 FOR I=2 TO 115
1570   FOR K=1 TO 7
1580     D1(I,K)=C1(I+J,K)
1590     D2(I,K)=C2(I+J,K)
1600     D3(I,K)=C3(I+J,K)
1610     D4(I,K)=C4(I+J,K)
1620     D5(I,K)=C5(I+J,K)
1630     D6(I,K)=C6(I+J,K)
1640     D7(I,K)=C7(I+J,K)
1650     D8(I,K)=C8(I+J,K)
1660     D9(I,K)=C9(I+J,K)
1670     D10(I,K)=C10(I+J,K)
1680   NEXT K
1690   J=J+3
1700 NEXT I
1710 CLEAR
1720 DISP "REWRITING FILE : ";FILE#
1730 PURGE FILE#
1740 PACK
1750 CREATE FILE#,10,116*7*8
1760 ASSIGN# 1 TO FILE#
1770 PRINT# 1,1 ; D1(),Angle(1)
1780 PRINT# 1,2 ; D2(),Angle(2)
1790 PRINT# 1,3 ; D3(),Angle(3)
1800 PRINT# 1,4 ; D4(),Angle(4)
1810 PRINT# 1,5 ; D5(),Angle(5)
1820 PRINT# 1,6 ; D6(),Angle(6)
1830 PRINT# 1,7 ; D7(),Angle(7)
1840 PRINT# 1,8 ; D8(),Angle(8)
1850 PRINT# 1,9 ; D9(),Angle(9)
1860 PRINT# 1,10 ; D10(),Angle(10)
1870 ASSIGN# 1 TO *
1880 CLEAR
1890 END
1900 !
1910 ! *****

```

## APPENDIX F

MATLAB program to determine rotation as  
a function of rope length.

```

% MATLAB PROGRAM TO DETERMINE TWIST AND ROTATION IN TERMS OF ROPE LENGTH
%
% WRITTEN BY G.REBEL      -      20/10/93
%
%
clc
format long
load xrot
load ylay
load Length
load Lay
%
p=polyfit(ylay,xrot,4)
disp('Press ENTER')
pause
x1=280:5:680;
f=polyval(p,x1);
plot(ylay,xrot,'--',x1,f,'-')
xlabel('Lay length (mm)')
ylabel('Rope twist (deg/m)')
meta t_f_l1
pause
%
clc
p1=polyfit(Length,Lay,3)
disp('Press ENTER')
pause
L1=0:21.96:2196;
f1=polyval(p1,L1);
plot(Length,Lay,'--',L1,f1,'-')
xlabel('Rope length (m)')
ylabel('Lay length mm')
meta l1_f_1
pause
%
clc
i = 0:21.96:2196;
%
fitp1=polyval(p1,i);
newrot=polyval(p,fitp1);
%
n=polyfit(i,newrot,4);
nfit=polyval(n,i);
%
plot(i,newrot,'--',i,nfit,'-')
xlabel('Distance from skip (m)')
ylabel('Rope twist (deg/m)')
pause
meta APXT
clc
%
disp('polynomial for length vs rotation')

```

```

n
%
pause
%
% INTEGRATE TWIST wrt LENGTH TO GET ROTATION
%
pRot=[n(:,1)/5,n(:,2)/4,n(:,3)/3,n(:,4)/2,n(:,5),0];
Rota=polyval(pRot,i);
%
plot(i,Rota/360,'-')
xlabel('Distance from skip (m)')
ylabel('Rope rotation (No. of turns)')
pause
meta APXR
%
% END OF PROGRAM

```

---

		Length =
		1.0e+003 *
		0
		0.2745
		0.5490
		1.0980
		1.6470
		1.9215
		2.1960
xrot =	ylay =	
-267	660.0000	
-237	610.0000	
-207	580.0000	
-178	555.0000	
-148	517.5000	
-119	490.0000	
-89	480.0000	
-59	465.0000	
-30	442.5000	
0	405.7000	
30	381.5000	
59	362.0000	
89	350.0000	
119	337.5000	
148	315.0000	
178	310.0000	
207	305.0000	Lay =
237	295.0000	335
267	290.0000	345
		370
		408
		448
		478
		503



## APPENDIX G

MATLAB programs for the Direct Data Fit method.

```

% MATLAB PROGRAM TO DETERMINE TORQUE i.t.o FORCE AND ROTATION
%
% WRITTEN BY G.REBEL          -          24/10/93
%
%
clc
F=[0;25;50;75;100;150;200;300;400;500];
%
T_1080=[-390;-305;-232;-146;-61;122;298;671;1037;1419];
T_960=[-354;-268;-190;-95;0;183;366;756;1134;1524];
T_840=[-307;-220;-146;-49;49;244;439;841;1244;1634];
T_720=[-268;-176;-98;0;98;305;512;927;1341;1756];
T_600=[-220;-134;-49;49;159;378;590;1024;1451;1902];
T_480=[-171;-85;0;110;220;451;683;1122;1561;2000];
T_360=[-122;-37;73;171;305;537;756;1220;1683;2146];
T_240=[-73;24;122;232;366;610;854;1329;1805;2280];
T_120=[-48;73;173;305;427;695;951;1451;1939;2439];
%
T0=[0;134;256;384;518;780;1043;1563;2074;2598];
%
T120=[98;207;337;463;610;866;1146;1683;2232;2780];
T240=[207;312;427;561;695;963;1244;1810;2366;2927];
T360=[293;390;524;634;780;1061;1341;1927;2488;3037];
T480=[378;463;580;707;854;1146;1439;2049;2634;3244];
T600=[439;524;622;756;915;1207;1515;2134;2732;3390];
T720=[512;598;707;829;1000;1293;1610;2244;2866;3537];
T840=[585;659;780;902;1073;1383;1707;2354;2976;3683];
T960=[683;768;878;1000;1171;1476;1805;2488;3146;3854];
T1080=[793;854;963;1098;1244;1573;1902;2610;3341;4073];
%
TORQUE=[T_1080,T_960,T_840,T_720,T_600,T_480,T_360,T_240,T_120,T0,T120,
,T480,T600,T720,T840,T960,T1080];
%
plot(F,TORQUE)
xlabel('Tensile load (kN)')
ylabel('Rope torque (Nm)')
title('RAW DATA')
pause
print
%
F1=0:20:500;
F1=F1';
%
P_1080=polyfit(F,T_1080,3);
fit_1080=polyval(P_1080,F1);
P_960=polyfit(F,T_960,3);
fit_960=polyval(P_960,F1);
P_840=polyfit(F,T_840,3);
fit_840=polyval(P_840,F1);
P_720=polyfit(F,T_720,3);
fit_720=polyval(P_720,F1);
P_600=polyfit(F,T_600,3);
fit_600=polyval(P_600,F1);
P_480=polyfit(F,T_480,3);
fit_480=polyval(P_480,F1);
P_360=polyfit(F,T_360,3);
fit_360=polyval(P_360,F1);
P_240=polyfit(F,T_240,3);

```

```

fit_240=polyval(P_240,F1);
P_120=polyfit(F,T_120,3);
fit_120=polyval(P_120,F1);
%
P0=polyfit(F,T0,3);
fit0=polyval(P0,F1);
%
P1080=polyfit(F,T1080,3);
fit1080=polyval(P1080,F1);
P960=polyfit(F,T960,3);
fit960=polyval(P960,F1);
P840=polyfit(F,T840,3);
fit840=polyval(P840,F1);
P720=polyfit(F,T720,3);
fit720=polyval(P720,F1);
P600=polyfit(F,T600,3);
fit600=polyval(P600,F1);
P480=polyfit(F,T480,3);
fit480=polyval(P480,F1);
P360=polyfit(F,T360,3);
fit360=polyval(P360,F1);
P240=polyfit(F,T240,3);
fit240=polyval(P240,F1);
P120=polyfit(F,T120,3);
fit120=polyval(P120,F1);
%
TORQUE_fit=[fit_1080,fit_960,fit_840,fit_720,fit_600,fit_480,fit_360
_120,fit0,fit120,fit240,fit360,fit480,fit600,fit720,fit840,fit960
%
plot(F1,TORQUE_fit)
xlabel('Tensile load (kN)')
ylabel('Rope torque (Nm)')
title('3rd ORDER POLYNOMIAL FIT')
pause
%
plot(F,TORQUE,F1,TORQUE_fit)
xlabel('Tensile load (kN)')
ylabel('Rope torque (Nm)')
title('RAW DATA and FIT')
pause
%
ROT=[-1080;-960;-840;-720;-600;-480;-360;-240;-120;0;120;240;360;480;600;
960;1080];
ROT=ROT/4.050;
%
P=[P_1080;P_960;P_840;P_720;P_600;P_480;P_360;P_240;P_120;P0;P120;P240;
P600;P720;P840;P960;P1080];
%
P1=P(:,1);
P2=P(:,2);
P3=P(:,3);
P4=P(:,4);
%
plot(ROT,P)
xlabel('Rope rotation (deg/m)')
ylabel('Torque vs Force polyn. consts.')
pause
%

```

```

ROT1=-1080:30:1080;
ROT1=ROT1';
ROT1=ROT1/4.050;
%
pp1=polyfit(ROT,P1,4);
P1fit=polyval(pp1,ROT);
pp2=polyfit(ROT,P2,4);
P2fit=polyval(pp2,ROT);
pp3=polyfit(ROT,P3,4);
P3fit=polyval(pp3,ROT);
pp4=polyfit(ROT,P4,4);
P4fit=polyval(pp4,ROT);
%
plot(ROT,P1,ROT,P1fit)
xlabel('Rope rotation (deg/m)')
ylabel('Torque vs Force polyn. const.')
title('Polyn. constant 1 and FIT')
pause
%
plot(ROT,P2,ROT,P2fit)
xlabel('Rope rotation (deg/m)')
ylabel('Torque vs Force polyn. const.')
title('Polyn. constant 2 and FIT')
pause
%
plot(ROT,P3,ROT,P3fit)
xlabel('Rope rotation (deg/m)')
ylabel('Torque vs Force polyn. const.')
title('Polyn. constant 3 and FIT')
pause
%
plot(ROT,P4,ROT,P4fit)
xlabel('Rope rotation (deg/m)')
ylabel('Torque vs Force polyn. const.')
title('Polyn. constant 4 and FIT')
pause
:lc
%
pp=[pp1;pp2;pp3;pp4];
%
:lc
format long
disp('T = p1(R).F^3 + p2(R).F^2 + p3(R).F + p4(R)')
disp('')
disp('With F in (kN) and R in (deg/m)')
disp('')
disp('Where the constants for the 4th order polynomials p1,p2,p3,p4 are :')
disp('')
pp
pause
%
POLY=[P1fit,P2fit,P3fit,P4fit];
POLY1=POLY(1,:);
POLY2=POLY(2,:);
POLY3=POLY(3,:);
POLY4=POLY(4,:);
POLY5=POLY(5,:);
POLY6=POLY(6,:);

```

```

POLY7=POLY(7,:);
POLY8=POLY(8,:);
POLY9=POLY(9,:);
POLY10=POLY(10,:);
POLY11=POLY(11,:);
POLY12=POLY(12,:);
POLY13=POLY(13,:);
POLY14=POLY(14,:);
POLY15=POLY(15,:);
POLY16=POLY(16,:);
POLY17=POLY(17,:);
POLY18=POLY(18,:);
POLY19=POLY(19,:);
%
T1=polyval(POLY1,F1);
T2=polyval(POLY2,F1);
T3=polyval(POLY3,F1);
T4=polyval(POLY4,F1);
T5=polyval(POLY5,F1);
T6=polyval(POLY6,F1);
T7=polyval(POLY7,F1);
T8=polyval(POLY8,F1);
T9=polyval(POLY9,F1);
T10=polyval(POLY10,F1);
T11=polyval(POLY11,F1);
T12=polyval(POLY12,F1);
T13=polyval(POLY13,F1);
T14=polyval(POLY14,F1);
T15=polyval(POLY15,F1);
T16=polyval(POLY16,F1);
T17=polyval(POLY17,F1);
T18=polyval(POLY18,F1);
T19=polyval(POLY19,F1);
%
TORQUE_EST=[T1,T2,T3,T4,T5,T6,T7,T8,T9,T10,T11,T12,T13,T14,T15,T16,T17,
%
T18,T19];
plot(F,TORQUE,F1,TORQUE_EST)
xlabel('Tensile load (kN)')
ylabel('Rope torque (Nm)')
title('RAW DATA and FINAL COMPLETE FIT')
pause
%
```

```

% MATLAB PROGRAM TO DETERMINE ROTATION i.t.o TORQUE AND FORCE
%
% WRITTEN BY G.REBEL - 24/10/93
%
%
clc
format short
F=[0;25;50;75;100;150;200;300;400;500];
%
T_1080=[-390;-305;-232;-146;-61;122;298;671;1037;1419];
T_960=[-354;-268;-190;-95;0;183;366;756;1134;1524];
T_840=[-307;-220;-146;-49;49;244;439;841;1244;1634];
T_720=[-268;-176;-98;0;98;305;512;927;1341;1756];
T_600=[-220;-134;-49;49;159;378;590;1024;1451;1902];
T_480=[-171;-85;0;110;220;451;683;1122;1561;2000];
T_360=[-122;-37;73;171;305;537;756;1220;1683;2146];
T_240=[-73;24;122;232;366;610;854;1329;1805;2280];
T_120=[-48;73;173;305;427;695;951;1451;1939;2439];
%
T0=[0;134;256;384;518;780;1043;1563;2074;2598];
%
T120=[98;207;337;463;610;866;1146;1683;2232;2780];
T240=[207;312;427;561;695;963;1244;1810;2366;2927];
T360=[293;390;524;634;780;1061;1341;1927;2488;3037];
T480=[378;463;580;707;854;1146;1439;2049;2634;3244];
T600=[439;524;622;756;915;1207;1515;2134;2732;3390];
T720=[512;598;707;829;1000;1293;1610;2244;2866;3537];
T840=[585;659;780;902;1073;1383;1707;2354;2976;3683];
T960=[683;768;878;1000;1171;1476;1805;2488;3146;3854];
T1080=[793;854;963;1098;1244;1573;1902;2610;3341;4073];
%
TORQUE=[T_1080,T_960,T_840,T_720,T_600,T_480,T_360,T_240,T_120,T0,T120,
,T480,T600,T720,T840,T960,T1080];
T240,T360
%
ROT=[-1080;-960;-840;-720;-600;-480;-360;-240;-120;0;120;240;360;480;
;960;1080];
ROT=ROT/4.050;
600;720;840
%
TF0=TORQUE(1,:)' ;
TF25=TORQUE(2,:)' ;
TF50=TORQUE(3,:)' ;
TF75=TORQUE(4,:)' ;
TF100=TORQUE(5,:)' ;
TF150=TORQUE(6,:)' ;
TF200=TORQUE(7,:)' ;
TF300=TORQUE(8,:)' ;
TF400=TORQUE(9,:)' ;
TF500=TORQUE(10,:)' ;
%
TF=[TF0,TF25,TF50,TF75,TF100,TF150,TF200,TF300,TF400,TF500];
pause
%
plot(TF,ROT)
xlabel('Torque (Nm)')
ylabel('Rope rotation (deg/m)')
title('RAW DATA ROT vs TORQUE')
pause
print

```

```

%
P0=polyfit(TF0,ROT,3);
P25=polyfit(TF25,ROT,3);
P50=polyfit(TF50,ROT,3);
P75=polyfit(TF75,ROT,3);
P100=polyfit(TF100,ROT,3);
P150=polyfit(TF150,ROT,3);
P200=polyfit(TF200,ROT,3);
P300=polyfit(TF300,ROT,3);
P400=polyfit(TF400,ROT,3);
P500=polyfit(TF500,ROT,3);
%
P=[P0;P25;P50;P75;P100;P150;P200;P300;P400;P500];
%
P1=P(:,1);
P2=P(:,2);
P3=P(:,3);
P4=P(:,4);
%
pp1=polyfit(F,P1,5);
P1fit=polyval(pp1,F);
%
pp2=polyfit(F,P2,5);
P2fit=polyval(pp2,F);
%
pp3=polyfit(F,P3,5);
P3fit=polyval(pp3,F);
%
pp4=polyfit(F,P4,5);
P4fit=polyval(pp4,F);
%
clc
%
pp=[pp1;pp2;pp3;pp4];
%
clc
format long
disp('R = p1(F).T^3 + p2(F).T^2 + p3(F).T + p4(F)')
disp('')
disp('With F in (kN) and T in (Nm)')
disp('')
disp('Where the constants for the 5th order polynomials p1,p2,p3,p4 are :')
disp('')
pp
pause
%
POLY=[P1fit,P2fit,P3fit,P4fit];
POLY1=POLY(1,:);
POLY2=POLY(2,:);
POLY3=POLY(3,:);
POLY4=POLY(4,:);
POLY5=POLY(5,:);
POLY6=POLY(6,:);
POLY7=POLY(7,:);
POLY8=POLY(8,:);
POLY9=POLY(9,:);
POLY10=POLY(10,:);
%

```

```
T1=polyval(POLY1,TF0);
T2=polyval(POLY2,TF25);
T3=polyval(POLY3,TF50);
T4=polyval(POLY4,TF75);
T5=polyval(POLY5,TF100);
T6=polyval(POLY6,TF150);
T7=polyval(POLY7,TF200);
T8=polyval(POLY8,TF300);
T9=polyval(POLY9,TF400);
T10=polyval(POLY10,TF500);
%
ROT_EST=[T1,T2,T3,T4,T5,T6,T7,T8,T9,T10];
%
plot(TF,ROT,TF,ROT_EST)
xlabel('Rope torque (Nm)')
ylabel('Rope rotation (deg/m)')
title('RAW DATA and FINAL COMPLETE FIT')
pause
%
```



```

% MATLAB PROGRAM TO DETERMINE ROTATION i.t.o TORQUE AND ROPE LENGTH z
%
% WRITTEN BY G.REBEL - 25/10/93
%
%
clc
format short
F=[0;25;50;75;100;150;200;300;400;500];
%
T_1080=[-390;-305;-232;-146;-61;122;298;671;1037;1419];
T_960=[-354;-268;-190;-95;0;183;366;756;1134;1524];
T_840=[-307;-220;-146;-49;49;244;439;841;1244;1634];
T_720=[-268;-176;-98;0;98;305;512;927;1341;1756];
T_600=[-220;-134;-49;49;159;378;590;1024;1451;1902];
T_480=[-171;-85;0;110;220;451;683;1122;1561;2000];
T_360=[-122;-37;73;171;305;537;756;1220;1683;2146];
T_240=[-73;24;122;232;366;610;854;1329;1805;2280];
T_120=[-48;73;173;305;427;695;951;1451;1939;2439];
%
T0=[0;134;256;384;518;780;1043;1563;2074;2598];
%
T120=[98;207;337;463;610;866;1146;1683;2232;2780];
T240=[207;312;427;561;695;963;1244;1810;2366;2927];
T360=[293;390;524;634;780;1061;1341;1927;2488;3037];
T480=[378;463;580;707;854;1146;1439;2049;2634;3244];
T600=[439;524;622;756;915;1207;1515;2134;2732;3390];
T720=[512;598;707;829;1000;1293;1610;2244;2866;3537];
T840=[585;659;780;902;1073;1383;1707;2354;2976;3683];
T960=[683;768;878;1000;1171;1476;1805;2488;3146;3854];
T1080=[793;854;963;1098;1244;1573;1902;2610;3341;4073];
%
TORQUE=[T_1080,T_960,T_840,T_720,T_600,T_480,T_360,T_240,T_120,T0,T120,
,T480,T600,T720,T840,T960,T1080];
%
ROT=[-1080;-960;-840;-720;-600;-480;-360;-240;-120;0;120;240;360;480;
;960;1080];
ROT=ROT/4.050;
%
TF0=TORQUE(1,:);
TF25=TORQUE(2,:);
TF50=TORQUE(3,:);
TF75=TORQUE(4,:);
TF100=TORQUE(5,:);
TF150=TORQUE(6,:);
TF200=TORQUE(7,:);
TF300=TORQUE(8,:);
TF400=TORQUE(9,:);
TF500=TORQUE(10,:);
%
TF=[TF0,TF25,TF50,TF75,TF100,TF150,TF200,TF300,TF400,TF500];
%
plot(TF,ROT)
xlabel('Torque (Nm)')
ylabel('Rope rotation (deg/m)')
title('RAW DATA. ROT vs TORQUE')
pause
%
P0=polyfit(TF0,ROT,3);

```

```

P25=polyfit(TF25,ROT,3);
P50=polyfit(TF50,ROT,3);
P75=polyfit(TF75,ROT,3);
P100=polyfit(TF100,ROT,3);
P150=polyfit(TF150,ROT,3);
P200=polyfit(TF200,ROT,3);
P300=polyfit(TF300,ROT,3);
P400=polyfit(TF400,ROT,3);
P500=polyfit(TF500,ROT,3);
%
P=[P0;P25;P50;P75;P100;P150;P200;P300;P400;P500];
%
P1=P(:,1);
P2=P(:,2);
P3=P(:,3);
P4=P(:,4);
%
pp1=polyfit(F,P1,5);
P1fit=polyval(pp1,F);
%
pp2=polyfit(F,P2,5);
P2fit=polyval(pp2,F);
%
pp3=polyfit(F,P3,5);
P3fit=polyval(pp3,F);
%
pp4=polyfit(F,P4,5);
P4fit=polyval(pp4,F);
%
clc
%
pp=[pp1;pp2;pp3;pp4];
%
FF1=[0.096,211];
FF2=conv(FF1,FF1);
FF3=conv(FF2,FF1);
FF4=conv(FF3,FF1);
FF5=conv(FF4,FF1);
%
FE1=[0.096,96];
FE2=conv(FE1,FE1);
FE3=conv(FE2,FE1);
FE4=conv(FE3,FE1);
FE5=conv(FE4,FE1);
%
pC6E=pp(:,1)*FE5;
pC5E=pp(:,2)*FE4;
pC4E=pp(:,3)*FE3;
pC3E=pp(:,4)*FE2;
pC2E=pp(:,5)*FE1;
pC1E=pp(:,6);
%
pC6F=pp(:,1)*FF5;
pC5F=pp(:,2)*FF4;
pC4F=pp(:,3)*FF3;
pC3F=pp(:,4)*FF2;
pC2F=pp(:,5)*FF1;
pC1F=pp(:,6);

```

```

%
B=[0;0;0;0];
%
pC5E=[B,pC5E];
pC4E=[B,B,pC4E];
pC3E=[B,B,B,pC3E];
pC2E=[B,B,B,B,pC2E];
pC1E=[B,B,B,B,B,pC1E];
%
pC5F=[B,pC5F];
pC4F=[B,B,pC4F];
pC3F=[B,B,B,pC3F];
pC2F=[B,B,B,B,pC2F];
pC1F=[B,B,B,B,B,pC1F];
%
pCE=[pC6E+pC5E+pC4E+pC3E+pC2E+pC1E];
pCF=[pC6F+pC5F+pC4F+pC3F+pC2F+pC1F];
%
z=0:19:2204;
z=z';
%
P1E=polyval(pCE(1,:),z);
P2E=polyval(pCE(2,:),z);
P3E=polyval(pCE(3,:),z);
P4E=polyval(pCE(4,:),z);
%
P1F=polyval(pCF(1,:),z);
P2F=polyval(pCF(2,:),z);
P3F=polyval(pCF(3,:),z);
P4F=polyval(pCF(4,:),z);
%
TrqE=1025
TrqF=1619
%
ROT_E=[(P1E*TrqE^3)+(P2E*TrqE^2)+(P3E*TrqE)+(P4E)];
ROT_F=[(P1F*TrqF^3)+(P2F*TrqF^2)+(P3F*TrqF)+(P4F)];
%
plot(z,ROT_E,'-',z,ROT_F,'--')
xlabel('Rope length (m)')
ylabel('Rope twist (deg/m)')
title('ROPE TWIST FOR A CONSTANT TORQUE')
pause
%
clc
format short e
disp('R = p1(z).T^3 + p2(z).T^2 + p3(z).T + p4(z)')
disp('')
disp('With z in (m), T in (Nm) and R in (deg/m)')
disp('')
disp('Where the constants for the 5th order polynomials p1,p2,p3,p4 are :')
disp('')
Empty_skip=pCE
Full_skip=pCF
pause
%
IpCE=[(pCE(:,1)/6),(pCE(:,2)/5),(pCE(:,3)/4),(pCE(:,4)/3),(pCE(:,5)/2),
),B];
IpCF=[(pCF(:,1)/6),(pCF(:,2)/5),(pCF(:,3)/4),(pCF(:,4)/3),(pCF(:,5)/2),
(pCF(:,6)
(pCF(:,6)

```

```

),B];
%
clc
disp('PHI = p1(z).T^3 + p2(z).T^2 + p3(z).T + p4(z)')
disp('')
disp('With z in (m), T in (Nm) and PHI in (deg)')
disp('')
disp('Where the constants for the 6th order polynomials p1,p2,p3,p4 are :')
disp('')
Empty_skip=IpCE
pause
clc
Full_skip=IpCF
pause
%
clc
TrqE=input('Enter the rope torque with an empty skip (Nm) : ');
disp('')
TrqF=input('Enter the rope torque with a full skip (Nm) : ');
%
R1E=polyval(IpCE(1,:),z);
R2E=polyval(IpCE(2,:),z);
R3E=polyval(IpCE(3,:),z);
R4E=polyval(IpCE(4,:),z);
%
R1F=polyval(IpCF(1,:),z);
R2F=polyval(IpCF(2,:),z);
R3F=polyval(IpCF(3,:),z);
R4F=polyval(IpCF(4,:),z);
%
PHI_E=[(R1E*TrqE^3)+(R2E*TrqE^2)+(R3E*TrqE)+(R4E)];
PHI_F=[(R1F*TrqF^3)+(R2F*TrqF^2)+(R3F*TrqF)+(R4F)];
%
plot(z,(PHI_E/360),z,(PHI_F/360),z,(PHI_E/360)-(PHI_F/360))
xlabel('Rope length (m)')
ylabel('Rope rotation      ')
title('ROPE ROTATION FOR A CONSTANT TORQUE')
pause
%

```

## APPENDIX H

MATLAB programs for the C and T factor method.

```

% MATLAB PROGRAM TO DETERMINE bc AS A FUNCTION OF ROPE FORCE
%
% WRITTEN BY G.REBEL          -          28/10/93
%
load r0;
load r59;
load r119;
load r178;
load r237;
f=[50;75;100;125;150;175;200;250;300;350;400;450];
%
d1=-(r59-r0)/59;
d2=-(r119-r59)/59;
d3=-(r178-r119)/59;
d4=-(r237-r178)/59;
%
D=(d1+d2+d3+d4)/4;
%
plot(f,d1,'--',f,d2,'--',f,d3,'--',f,d4,'--',f,D,'-')
xlabel('Tensile load (kN)')
ylabel('bc')
pause
%
clc
odr=input('Enter the order of the fit : ');
%
p=polyfit(f,D,odr);
Dfit=polyval(p,f);
%
plot(f,D,'--',f,Dfit,'-')
xlabel('Tensile load (kN)')
ylabel('bc')
pause
%
clc
format short e
disp('The coefficients in the polynomial bc = f(F) are :')
disp('')
p

```

---

The coefficients in the polynomial  $bc = f(F)$  are :

p =

1.0917e-015 -2.8198e-012 2.3745e-009 -8.8840e-007

»

1.5454e-004 -4.5811e-003

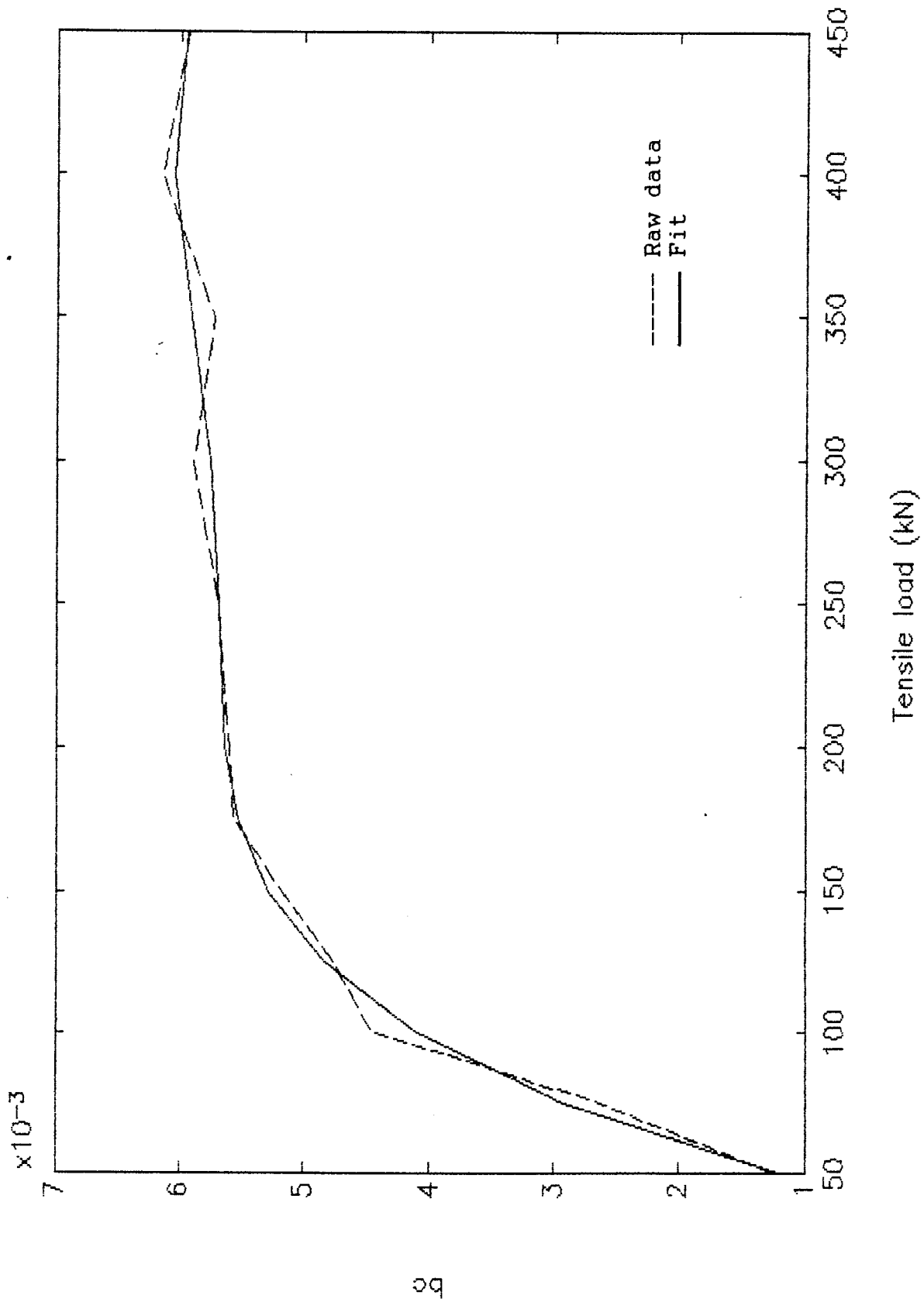


FIG. H.1 -  $b_c$  versus rope force

```

% MATLAB PROGRAM TO DETERMINE ROTATION (No OF TURNS) BY THE C & T
% FACTOR METHOD.
%
% ALSO TO PLOT ACTUAL C AND T FACTOR CURVES AND TORQUE-TENSION
% ROTATION CURVES AS USED BY THE PROGRAM TO DETERMINE ROTATION.
%
% WRITTEN BY G.REBEL          -      29/10/93
%
%
% R is  $d\phi/dz$ 
%
%
clc
bt=5.90e-3;
ct=1.71e-3;
at=2.05;
ac=5.25;
% bc= a function of F as defined below;
%
Pf=211;
Pe=96;
q=0.096;
%
clc
Me=input('Enter the estimated torque in the rope (skip empty) : ');
disp('')
Mf=input('Enter the estimated torque in the rope (skip full) : ');
%
PHIe(111,:)= -360;
PHIe(111,:)=1080;
PHIf(111,:)= -360;
PHIf(111,:)=1080;
%
while (PHIe(111,:)/360)<0 ; (PHIe(111,:)/360)>2 ; (PHIf(111,:)/360)<0 ;
(PHIf(111,:)/360)>2
%
%
z=0;
A=ct;
Fe=Pe;
Ff=Pf;
bce=1.0197e-15*Fe^5-2.8198e-12*Fe^4+2.3745e-9*Fe^3-8.884e-7*Fe^2+1.5454e-4*
Fe-4.45811e-3;
bcf=1.0197e-15*Ff^5-2.8198e-12*Ff^4+2.3745e-9*Ff^3-8.884e-7*Ff^2+1.5454e-4*
Ff-4.45811e-3;
Be=(bce*(Pe+q*z)+at+bt*(Pe+q*z));
Bf=(bcf*(Pf+q*z)+at+bt*(Pf+q*z));
Ce=(ac*(Pe+q*z)-Me);
Cf=(ac*(Pf+q*z)-Mf);
pln_e=[A,Be,Ce];
pln_f=[A,Bf,Cf];
re=roots(pln_e);
rf=roots(pln_f);
Re=re(2,:);
Rf=rf(2,:);
R=[z,Re,Rf];
%
CFe=ac+bce*Re;

```



```

CFf=ac+bcf*Rf;
TFe=at+bt*(Pe+q*z)+ct*Re;
TFf=at+bt*(Pf+q*z)+ct*Rf;
Cfact=[CFe,CFf];
Tfact=[TFe,TFf];
%
%
for z=20:20:2200,
    A=ct;
    Fe=Pe+q*z;
    Ff=Pf+q*z;
    %
    if Fe<300,
bce=1.0197e-15*Fe^5-2.8198e-12*Fe^4+2.3745e-9*Fe^3-8.884e-7*Fe^2+1.5454e-4*
Fe-4.45811e-3;
    else
    bce=bce;
    end
    %
    if Ff<300,
bcf=1.0197e-15*Ff^5-2.8198e-12*Ff^4+2.3745e-9*Ff^3-8.884e-7*Ff^2+1.5454e-4*
Ff-4.45811e-3;
    else
    bcf=bcf;
    end
    %
    Be=(bce*(Pe+q*z)+at+bt*(Pe+q*z));
    Bf=(bcf*(Pf+q*z)+at+bt*(Pf+q*z));
    Ce=(ac*(Pe+q*z)-Me);
    Cf=(ac*(Pf+q*z)-Mf);
    pln_e=[A,Be,Ce];
    pln_f=[A,Bf,Cf];
    re=roots(pln_e);
    rf=roots(pln_f);
    Re=re(2,:);
    Rf=rf(2,:);
    R=[R;z,Re,Rf];
    %
    CFe=ac+bce*Re;
    CFf=ac+bcf*Rf;
    TFe=at+bt*(Pe+q*z)+ct*Re;
    TFf=at+bt*(Pf+q*z)+ct*Rf;
    Cfact=[Cfact;CFe,CFf];
    Tfact=[Tfact;TFe,TFf];
    %
end
%
pie=polyfit(R(:,1),R(:,2),3);
Re_fit=polyval(pie,R(:,1));
%
p1f=polyfit(R(:,1),R(:,3),3);
Rf_fit=polyval(p1f,R(:,1));
%
% INTEGRATE TWIST POLYNOMIALS
%
p2e=[pie(:,1)/4,pie(:,2)/3,pie(:,3)/2,pie(:,4),0];
PHIe=polyval(p2e,R(:,1));
%
```

```

p2f=[p1f(:,1)/4,p1f(:,2)/3,p1f(:,3)/2,p1f(:,4),0];
PHIf=polyval(p2f,R(:,1));
%
% ADJUSTING THE TORQUE ESTIMATE
%
if (PHIe(111,:)/360)<0,
    Me=Me+1;
end
if (PHIe(111,:)/360)<-6,
    Me=Me+5;
end
if (PHIe(111,:)/360)<-12,
    Me=Me+10;
end
%
if (PHIe(111,:)/360)>2,
    Me=Me-1;
end
if (PHIe(111,:)/360)>8,
    Me=Me-5;
end
if (PHIe(111,:)/360)>14,
    Me=Me-10;
end
%
if (PHIf(111,:)/360)<0,
    Mf=Mf+1;
end
if (PHIf(111,:)/360)<-6,
    Mf=Mf+5;
end
if (PHIf(111,:)/360)<-12,
    Mf=Mf+10;
end
%
if (PHIf(111,:)/360)>2,
    Mf=Mf-1;
end
if (PHIf(111,:)/360)>8,
    Mf=Mf-5;
end
if (PHIf(111,:)/360)>14,
    Mf=Mf-10;
end
%
clc
disp('          ITERATING.....')
disp('')
disp('No of turns at 2200m from skip for empty and full skips')
disp('')
disp('Both values should be 0 since  $\phi = 0$  at  $z = \text{total length}$ ')
disp('')
PHIe(111,:)/360
PHIf(111,:)/360
%
end
% of while loop
%
```

```

%
plot(R(:,1),R(:,2),R(:,1),R(:,3),R(:,1),Re_fit,R(:,1),Rf_fit)
xlabel('Distance from skip (m)')
ylabel('Rope twist (deg/m)')
pause
meta TWIST1
%
clc
disp('Empty and full torques which satisfy boundry conditions :')
disp('')
Me
Mf
pause
%
plot(R(:,1),PHIe/360,'-',R(:,1),PHIf/360,'--',R(:,1),PHIe/360-PHIf/360)
xlabel('Distance from skip (m)')
ylabel('Rope rotation (No. of turns)')
pause
meta R1
%
% DETERMINE ACTUAL C AND T CURVES
%
x=1;
y=1;
for Rot = -237:59.25:237,
    for Frc = 50:20:470,
        %
        if Frc<300,
bc=1.0197e-15*Frc^5-2.8198e-12*Frc^4+2.3745e-9*Frc^3-8.884e-7*Frc^2+1.5454e
-4*Frc-4.45811e-3;
        else
            bc=bc;
        end
        %
        C=ac+bc*Rot;
        T=at+bt*Frc+ct*Rot;
        CF(x,y)=C;
        TF(x,y)=T;
        x=x+1;
    end
    y=y+1;
    x=1;
end
%
% DETERMINE TORQUE-TENSION ROTATION CURVES ( M = C.F + T.R )
%
M1=[CF(1,:) *50; CF(2,:) *70; CF(3,:) *90; CF(4,:) *110; CF(5,:) *130; CF(6,:) *150; CF
(7,:) *170; CF(8,:) *190; CF(9,:) *210; CF(10,:) *230; CF(11,:) *250; CF(12,:) *270; CF
(13,:) *290; CF(14,:) *310; CF(15,:) *330; CF(16,:) *350];
M1=[M1; CF(17,:) *370; CF(18,:) *390; CF(19,:) *410; CF(20,:) *430; CF(21,:) *450; CF(
22,:) *470];
M2=[TF(:,1) *(-237), TF(:,2) *(-177.75), TF(:,3) *(-118.5), TF(:,4) *(-59.25), TF(
:,5) *0, TF(:,6) *59.25, TF(:,7) *118.5, TF(:,8) *177.75, TF(:,9) *273];
M=M1+M2;
for i=1:111,
    ME(i,1)=Me;
    MF(i,1)=Mf;
end

```

```

%
% PLOT THE BASIC C AND T FACTOR CURVES AND THE ACTUAL VALUES USED IN CALC.
%
z1=0:20:2200;
z1=z1';
f1=Pe+q*z1;
f2=Pf+q*z1;
f3=50:20:470;
f3=f3';
%
plot(f3,CF,':',f1,Cfact(:,1),'-',f2,Cfact(:,2),'--')
xlabel('Rope tensile load (kN)')
ylabel('Torque factor (Nm/kN)')
title('ACTUAL C FACTORS AS USED IN ROTATION CALCULATION')
pause
meta C1
%
plot(f3,TF,':',f1,Tfact(:,1),'-',f2,Tfact(:,2),'--')
xlabel('Rope tensile load (kN)')
ylabel('Torsional stiffnness (Nm/(deg/m))')
title('ACTUAL T FACTORS AS USED IN ROTATION CALCULATION')
pause
meta T1
%
plot(f3,M,':',f1,ME,'-',f2,MF,'--')
xlabel('Rope tensile load (kN)')
ylabel('Rope torque (Nm)')
title('ACTUAL TORQUE-TENSION ROTATION CURVES')
pause
meta M1
%
%
% END OF PROGRAM

```

## APPENDIX I

Rotation computer model "T\_T\_CURVE".

```

1000 ! ***** ROTATION CURVE PLOTTING PROGRAM *****
1010 !
1020 ! PROGRAM NAME "T_T_CURVE"
1030 !
1040 ! WRITTEN BY G.REBEL / E.SALZMANN          22/10/1993
1050 !
1060 ! THIS PROGRAM ALLOWS THE ROTATION OF A TRIANGULAR STRAND ROPE TO BE
1070 ! PREDICTED FOR DIFFERENT LOADS AND ROPE LENGTHS.
1080 !
1090 ! THE MASS/m OF THE ROPE CAN ALSO BE VARIED
1100 !
1110 ! *****
1120 !
1130 CLEAR
1140 GOSUB DIMENSIONS
1150 GOSUB CONSTANTS
1160 GOSUB INFORMATION
1170 GOSUB EST_ROTATION
1180 GOSUB ROPE_FORCE
1190 GOSUB C_FACTOR_FNT
1200 GOSUB T_FACTOR_FNT
1210 GOSUB C_FACTOR
1220 GOSUB T_FACTOR
1230 FOR J=1 TO 3
1240   CLEAR @ DISP "ITERATION No. "; J
1250   GOSUB ACTUAL_ROTATION_FNT
1260   GOSUB ACTUAL_ROTATION
1270   GOSUB NEW_C_FACTOR
1280   GOSUB NEW_T_FACTOR
1290   GOSUB NEW_C_FACTOR_FNT
1300   GOSUB NEW_T_FACTOR_FNT
1310 NEXT J
1320 GOSUB PLOT_CURVE
1330 GOSUB MOMENT
1340 CLEAR @ BEEP @ BEEP @ BEEP
1350 END
1360 !
1370 ! -----
1380 DIMENSIONS:
1390 !
1400 OPTION BASE 0
1410 DIM ROT(100),PHI_F(100),PHI_E(100),PHI_GUESS(100)
1420 DIM d_PHI_F(100),d_PHI_E(100),M_E(100),M_F(100)
1430 DIM FE(100),FF(100),CF_FNT_F(100),TF_FNT_F(100),CF_F(100),TF_F(100)
1440 DIM CF_FNT_E(100),TF_FNT_E(100),CF_E(100),TF_E(100)
1450 RETURN
1460 !
1470 ! -----
1480 !
1490 CONSTANTS:
1500 !
1510 ! TORSIONAL STIFFNESS
1520 !
1530 At=-2.2
1540 Bt=-.0000059
1550 Ct=-.0026
1560 !
1570 At_FNT=-2.39
1580 Bt_FNT=-.00000575
1590 Ct_FNT=-.00142
1600 !

```

```

1610 ! TORQUE FACTOR
1620 !
1630 Ac=-.005375
1640 Bc=-.00000563
1650 !
1660 RETURN
1670 !
1680 ! -----
1690 !
1700 ROPE_FORCE:
1710 !
1720 FOR I=0 TO 100
1730   FE(I)=Pe+I/100*h*q
1740   FF(I)=Pf+I/100*h*q
1750 NEXT I
1760 RETURN
1770 !
1780 ! -----
1790 !
1800 INFORMATION:
1810 !
1820 CLEAR
1830 DISP "ENTER THE LENGTH OF THE ROPE (FROM SHEAVE TO SKIP) [m] : "
1840 INPUT ROPE_LENGTH
1850 DISP
1860 DISP "ENTER THE MASS PER UNIT LENGTH OF THE ROPE [kg/m] : "
1870 INPUT MASS_PER_M
1880 CLEAR
1890 DISP "ENTER THE MASS OF THE SKIP (EMPTY) [kg] : "
1900 INPUT M_SKIP_EMPT
1910 DISP
1920 DISP "ENTER THE MASS OF THE SKIP (FULL) [kg] : "
1930 INPUT M_SKIP_FULL
1940 DISP
1950 DISP "ENTER THE POINT OF INTEREST [m FROM SKIP] : "
1960 INPUT DIST_SKIP
1970 CLEAR
1980 DISP "THERE ARE TWO FORMULAE WHICH PREDICT THE ROTATION. ONE FOR THE"
1990 DISP "FRONT END AND ONE FOR THE MIDDLE/BACK END."
2000 DISP
2010 DISP "ENTER THE PERCENTAGE OF ROPE LENGTH FROM THE SKIP FOR WHICH THE"
2020 DISP "FRONT END FORMULA MUST BE USED. THE PROGRAM WILL AUTOMATICALLY"
2030 DISP "USE THE MIDDLE/BACK FORMULA FOR THE REMAINDER OF THE ROPE LENGTH"
2040 DISP
2050 INPUT F_COUNT
2060 F_COUNT=IP (F_COUNT)
2070 MB_COUNT=F_COUNT+1
2080 IF F_COUNT=0 THEN MB_COUNT=0
2090 IF F_COUNT=100 THEN MB_COUNT=100
2100 CLEAR
2110 DISP "FRONT FORMULA ";F_COUNT;" % OF ROPE LENGTH FROM SKIP."
2120 DISP
2130 DISP "MIDDLE/BACK FORMULA, LAST ";100-F_COUNT;" % OF ROPE LENGTH."
2140 DISP @ DISP @ DISP "PRESS <CONT>"
2150 PAUSE
2160 CLEAR
2170 DISP "CALCULATING....."
2180 !
2190 h=ROPE_LENGTH
2200 q=MASS_PER_M*9.81
2210 Pe=M_SKIP_EMPT*9.81

```

```

2220 Pf=M_SKIP_FULL*9.81
2230 z=DIST_SKIP
2240 RETURN
2250 !
2260 ! -----
2270 !
2280 EST_ROTATION:
2290 !
2300 FOR I=0 TO 100
2310   L=h*I/100
2320   ROT(I)=-(.0000000000001*L^4)-.000000006685*L^3+.000034630703*L^2-.14216281
9571*L+122.099042819
2330   PHI_GUESS(I)=-(.0000000000001*L^5/5)-.000000006685*L^4/4+.000034630703*L^3
/3-.142162819571*L^2/2+122.099042819*L
2340 NEXT I
2350 PHI_GUESS(100)=0 !   SLIGHT ERROR WITH INTEGRAL OF ROT(I)
2360 RETURN
2370 !
2380 ! -----
2390 !
2400 C_FACTOR_FNT:
2410 !
2420 FOR I=0 TO F_COUNT
2430   A1=4.25802E-20*ROT(I)^4-1.76137935E-17*ROT(I)^3+1.9412488598E-15*ROT(I)^2
-3.86433553793E-14*ROT(I)-2.41590186985E-12
2440   B1=- (4.58637E-17*ROT(I)^4)+1.83494335E-14*ROT(I)^3-1.8739875485E-12*ROT(I
)^2+2.68134812397E-11*ROT(I)+3.2751696683E-9
2450   C1=1.76567E-14*ROT(I)^4-6.6994776E-12*ROT(I)^3+5.938003672E-10*ROT(I)^2-1
.8385937384E-9*ROT(I)-1.687030666E-6
2460   D1=- (2.98875E-12*ROT(I)^4)+1.04109426E-9*ROT(I)^3-6.769316798E-8*ROT(I)^2
-1.76290293221E-6*ROT(I)+4.128681508E-4
2470   E1=2.2488E-10*ROT(I)^4-6.934501E-8*ROT(I)^3+1.81933832E-6*ROT(I)^2+.00031
6292766*ROT(I)-4.80886646893E-2
2480   G1=- (5.39572E-9*ROT(I)^4)+1.31218815E-6*ROT(I)^3+9.61399819E-5*ROT(I)^2-2
.00995971254E-2*ROT(I)-3.1678344154
2490   CF_FNT_F(I)=(A1*(FF(I)/1000)^5+B1*(FF(I)/1000)^4+C1*(FF(I)/1000)^3+D1*(FF
(I)/1000)^2+E1*(FF(I)/1000)+G1)/1000
2500   CF_FNT_E(I)=(A1*(FE(I)/1000)^5+B1*(FE(I)/1000)^4+C1*(FE(I)/1000)^3+D1*(FE
(I)/1000)^2+E1*(FE(I)/1000)+G1)/1000
2510 NEXT I
2520 RETURN
2530 !
2540 ! -----
2550 !
2560 T_FACTOR_FNT:
2570 !
2580 FOR I=0 TO F_COUNT
2590   TF_FNT_F(I)=At_FNT+Bt_FNT*FF(I)+Ct_FNT*ROT(I)
2600   TF_FNT_E(I)=At_FNT+Bt_FNT*FE(I)+Ct_FNT*ROT(I)
2610 NEXT I
2620 RETURN
2630 !
2640 ! -----
2650 !
2660 C_FACTOR:
2670 !
2680 FOR I=MB_COUNT TO 100
2690   CF_F(I)=Ac+Bc*ROT(I)
2700   CF_E(I)=Ac+Bc*ROT(I)

```



```

2710 NEXT I
2720 RETURN
2730 !
2740 ! -----
2750 !
2760 T_FACTOR:
2770 !
2780 FOR I=MB_COUNT TO 100
2790   TF_F(I)=At+Bt*FF(I)+Ct*ROT(I)
2800   TF_E(I)=At+Bt*FE(I)+Ct*ROT(I)
2810 NEXT I
2820 RETURN
2830 !
2840 ! -----
2850 !
2860 ACTUAL_ROTATION_FNT:
2870 !
2880 FOR I=0 TO F_COUNT
2890   PHI_F(I)=CF_FNT_F(I)*q/2/TF_FNT_F(I)*(I/100*h*h-(I/100*h)^2) ! FOR T FNT
2900   PHI_E(I)=CF_FNT_E(I)*q/2/TF_FNT_E(I)*(I/100*h*h-(I/100*h)^2) ! FOT T FNT
2910   d_PHI_F(I)=CF_FNT_F(I)*q/TF_FNT_F(I)*(h/2-I/100*h) ! FOR C FNT
2920   d_PHI_E(I)=CF_FNT_E(I)*q/TF_FNT_E(I)*(h/2-I/100*h) ! FOR C FNT
2930 NEXT I
2940 RETURN
2950 !
2960 ! -----
2970 !
2980 ACTUAL_ROTATION:
2990 !
3000 FOR I=MB_COUNT TO 100
3010   PHI_F(I)=CF_F(I)*q/2/TF_F(I)*(I/100*h*h-(I/100*h)^2)
3020   PHI_E(I)=CF_E(I)*q/2/TF_E(I)*(I/100*h*h-(I/100*h)^2)
3030 NEXT I
3040 RETURN
3050 !
3060 ! -----
3070 !
3080 NEW_C_FACTOR:
3090 !
3100 IF MB_COUNT=0 THEN MB_COUNT=1
3110 FOR I=MB_COUNT TO 100
3120   CF_F(I)=Bc*PHI_F(I)/(I/100*h)+Ac
3130   CF_E(I)=Bc*PHI_E(I)/(I/100*h)+Ac
3140 NEXT I
3150 RETURN
3160 !
3170 ! -----
3180 !
3190 NEW_T_FACTOR:
3200 !
3210 IF MB_COUNT=0 THEN MB_COUNT=1

```

X

X

X

X

```

3220 FOR I=MB_COUNT TO 100
3230   TF_F(I)=PHI_F(I)*Ct/(I/100*h)+At+Bt*Pf+.5*Bt*q*(I/100*h)
3240   TF_E(I)=PHI_E(I)*Ct/(I/100*h)+At+Bt*Pe+.5*Bt*q*(I/100*h)
3250 NEXT I
3260 RETURN
3270 !
3280 ! -----
3290 !
3300 NEW_C_FACTOR_FNT:
3310 !
3320 FOR I=0 TO F_COUNT
3330   !
3340   A1_F=4.25802E-20*d_PHI_F(I)^4-1.76137935E-17*d_PHI_F(I)^3+1.9412488598E-1
5*d_PHI_F(I)^2-3.86433553793E-14*d_PHI_F(I)-2.41590186985E-12
3350   B1_F=-(4.58637E-17*d_PHI_F(I)^4)+1.83494335E-14*d_PHI_F(I)^3-1.8739875485
E-12*d_PHI_F(I)^2+2.68134812397E-11*d_PHI_F(I)+3.2751696683E-9
3360   C1_F=1.76567E-14*d_PHI_F(I)^4-6.6994776E-12*d_PHI_F(I)^3+5.938003672E-10*
d_PHI_F(I)^2-1.8385937384E-9*d_PHI_F(I)-1.687030666E-6
3370   D1_F=-(2.98875E-12*d_PHI_F(I)^4)+1.04109426E-9*d_PHI_F(I)^3-6.769316798E-
8*d_PHI_F(I)^2-1.76290293221E-6*d_PHI_F(I)+4.128681508E-4
3380   E1_F=2.2488E-10*d_PHI_F(I)^4-6.934501E-8*d_PHI_F(I)^3+1.81933832E-6*d_PHI
_F(I)^2+.000316292766*d_PHI_F(I)-4.80886646893E-2
3390   G1_F=-(5.39572E-9*d_PHI_F(I)^4)+1.31218815E-6*d_PHI_F(I)^3+9.61399819E-5*
d_PHI_F(I)^2-2.00995971254E-2*d_PHI_F(I)-3.1678344154
3400   !
3410   A1_E=4.25802E-20*d_PHI_E(I)^4-1.76137935E-17*d_PHI_E(I)^3+1.9412488598E-1
5*d_PHI_E(I)^2-3.86433553793E-14*d_PHI_E(I)-2.41590186985E-12
3420   B1_E=-(4.58637E-17*d_PHI_E(I)^4)+1.83494335E-14*d_PHI_E(I)^3-1.8739875485
E-12*d_PHI_E(I)^2+2.68134812397E-11*d_PHI_E(I)+3.2751696683E-9
3430   C1_E=1.76567E-14*d_PHI_E(I)^4-6.6994776E-12*d_PHI_E(I)^3+5.938003672E-10*
d_PHI_E(I)^2-1.8385937384E-9*d_PHI_E(I)-1.687030666E-6
3440   D1_E=-(2.98875E-12*d_PHI_E(I)^4)+1.04109426E-9*d_PHI_E(I)^3-6.769316798E-
8*d_PHI_E(I)^2-1.76290293221E-6*d_PHI_E(I)+4.128681508E-4
3450   E1_E=2.2488E-10*d_PHI_E(I)^4-6.934501E-8*d_PHI_E(I)^3+1.81933832E-6*d_PHI
_E(I)^2+.000316292766*d_PHI_E(I)-4.80886646893E-2
3460   G1_E=-(5.39572E-9*d_PHI_E(I)^4)+1.31218815E-6*d_PHI_E(I)^3+9.61399819E-5*
d_PHI_E(I)^2-2.00995971254E-2*d_PHI_E(I)-3.1678344154
3470   !
3480   CF_FNT_F(I)=(A1_F*(FF(I)/1000)^5+B1_F*(FF(I)/1000)^4+C1_F*(FF(I)/1000)^3+
D1_F*(FF(I)/1000)^2+E1_F*(FF(I)/1000)+G1_F)/1000
3490   CF_FNT_E(I)=(A1_E*(FE(I)/1000)^5+B1_E*(FE(I)/1000)^4+C1_E*(FE(I)/1000)^3+
D1_E*(FE(I)/1000)^2+E1_E*(FE(I)/1000)+G1_E)/1000
3500   !
3510 NEXT I
3520 RETURN
3530 !
3540 ! -----
3550 !
3560 NEW_T_FACTOR_FNT:
3570 !
3580 FOR I=1 TO F_COUNT
3590   TF_FNT_F(I)=PHI_F(I)*Ct_FNT/(I/100*h)+At_FNT+Bt_FNT*Pf+.5*Bt_FNT*q*(I/100
*h)
3600   TF_FNT_E(I)=PHI_E(I)*Ct_FNT/(I/100*h)+At_FNT+Bt_FNT*Pe+.5*Bt_FNT*q*(I/100
*h)
3610 NEXT I
3620 RETURN

```

X

X

```

3630 !
3640 ! -----
3650 !
3660 PLOT_CURVE;
3670 !
3680 FOR I=0 TO 100
3690 ! DISP I;I/100*h,PHI_E(I)/360,PHI_F(I)/360,(PHI_E(I)-PHI_F(I))/360
3700 NEXT I
3710 CLEAR
3720 DISP "PUT PAPER IN PLOTTER AND PRESS <CONT>"
3730 PAUSE
3740 CLEAR
3750 DISP "PLOTTING ROTATION VS ROPE LENGTH FOR FULL AND EMPTY SKIP AND"
3760 DISP "THE DIFFERENCE BETWEEN THE TWO."
3770 PLOTTER IS 705
3780 PEN 1
3790 LIMIT 30,272,0,191
3800 LOCATE 15,110,15,90
3810 SCALE 0,2200,0,300
3820 CSIZE 2.5
3830 FXD 0,0
3840 GRID 200,30
3850 LAXES -200,30
3860 CSIZE 3
3870 MOVE 1100,-25
3880 DEG @ LDIR 0
3890 LORG 6
3900 LABEL "Distance from skip (m)"
3910 MOVE 0,-50
3920 LABEL "REBEL / SALZMANN"
3930 LORG 4
3940 LDIR 90
3950 MOVE -200,150
3960 LABEL "Number of rotations"
3970 !
3980 LINE TYPE 4
3990 MOVE 0,0
4000 FOR I=0 TO 100
4010 DRAW I/100*h,PHI_F(I)/360
4020 NEXT I
4030 !
4040 LINE TYPE 1
4050 MOVE 0,0
4060 FOR I=0 TO 100
4070 DRAW I/100*h,PHI_E(I)/360
4080 NEXT I
4090 !
4100 LINE TYPE 8
4110 MOVE 0,0
4120 FOR I=0 TO 100
4130 DRAW I/100*h,(PHI_E(I)-PHI_F(I))/360
4140 NEXT I
4150 !
4160 CI=INT (z/h*100)
4170 CSIZE 2

```

```

4180 LDIR 0
4190 IF z<= .5*h THEN GOTO 4220
4200 IF z>.5*h THEN GOTO 4370
4210 !
4220 MOVE z,PHI_E(CI)/360
4230 LORG 5 @ LABEL "X"
4240 MOVE z,PHI_E(CI)/360+5
4250 LORG 8 @ LABEL INT (PHI_E(CI)/360)
4260 MOVE z,(PHI_E(CI)-PHI_F(CI))/360
4270 LORG 5 @ LABEL "X"
4280 MOVE z,(PHI_E(CI)-PHI_F(CI))/360+5
4290 LORG 8 @ LABEL INT ((PHI_E(CI)-PHI_F(CI))/360)
4300 MOVE z,PHI_F(CI)/360
4310 LORG 5 @ LABEL "X"
4320 MOVE z,PHI_F(CI)/360-5
4330 LORG 2 @ LABEL INT (PHI_F(CI)/360)
4340 PEN 0
4350 RETURN
4360 !
4370 MOVE z,PHI_E(CI)/360
4380 LORG 5 @ LABEL "X"
4390 MOVE z,PHI_E(CI)/360+5
4400 LORG 2 @ LABEL INT (PHI_E(CI)/360)
4410 MOVE z,(PHI_E(CI)-PHI_F(CI))/360
4420 LORG 5 @ LABEL "X"
4430 MOVE z,(PHI_E(CI)-PHI_F(CI))/360+5
4440 LORG 2 @ LABEL INT ((PHI_E(CI)-PHI_F(CI))/360)
4450 MOVE z,PHI_F(CI)/360
4460 LORG 5 @ LABEL "X"
4470 MOVE z,PHI_F(CI)/360-5
4480 LORG 8 @ LABEL INT (PHI_F(CI)/360)
4490 PEN 0
4500 RETURN
4510 !
4520 ! *****
4530 !
4540 MOMENT:
4550 !
4560 FOR I=0 TO F_COUNT
4570   M_E(I)=CF_FNT_E(I)*Pe+.5*CF_FNT_E(I)*q*(I/100*h)
4580   M_F(I)=CF_FNT_F(I)*Pf+.5*CF_FNT_F(I)*q*(I/100*h)
4590   DISP I,M_E(I),M_F(I)
4600 NEXT I
4610 !
4620 FOR I=MB_COUNT TO 100
4630   M_E(I)=CF_E(I)*Pe+.5*CF_E(I)*q*(I/100*h)
4640   M_F(I)=CF_F(I)*Pf+.5*CF_F(I)*q*(I/100*h)
4650   DISP I,M_E(I),M_F(I)
4660 NEXT I
4670 RETURN
4680 !
4690 ! *****

```

X

The preceding printout shows the entire rotation curve plotting program "T\_T\_CURVE". The C and T factor method was used in developing this program however an error was made in the derivation of the equations. Section 6.3.1 discusses this.

All the subroutines marked with a cross have incorrect equations in them.

The program splits the rope up into two parts, a front section and the rest of the rope. The reason for this is that it was decided that the equations for the front end C and T factors are different to the middle and back end ones. Comparing Figures 5.10 and 5.11 to Figure 5.12, Figure 5.13 and 5.14 to Figure 5.15 this is apparent.

All calculations in the program are done at 1% intervals along the rope length. The structure of the program is as follows :

1. The necessary arrays are dimensioned and the constants defined. Note that the constants are not the same as the constants used in Section 6.3. The method used to determine the constants was different.
2. The operator is prompted for general information required by the program. A choice is also given to the user as to what percentage of the rope length the front end equations must be used for.
3. The rope twist and rotation is then determined using the principle and formulae of Section 6.1 and APPENDIX F.
4. The tension along the rope is determined for empty and full skip conditions.
6. Using the tension and rotation estimate values, an estimate of C and T factor values are calculated for

the front end and the rest of the rope.

7. With these values of C and T, rope rotation is calculated for the front section and for the rest of the rope.
8. Using this rotation value new C and T factors are calculated.
9. Steps 7 and 8 are repeated until a desired accuracy is achieved.
10. The rotation curves are then plotted for empty and full skip conditions as well as for the difference between the two.
11. The torque along the length of the rope is displayed on screen. This value is supposed to be constant for all 101 points.

The equations for the front end C factor were determined by using a double polynomial fit method on MATLAB. Firstly, five 5th order least square polynomials were fitted to the five curves in Figure 5.12. Then six 4th order polynomials were fitted to the coefficients of the first five polynomials. This resulted in an equation for C factor in terms of twist and force :

$$C = A_1(R) \cdot F^5 + A_2(R) \cdot F^4 + A_3(R) \cdot F^3 + A_4(R) \cdot F^2 + A_5(R) \cdot F + A_6(R)$$

Where  $A_1$ ,  $A_2$ ,  $A_3$ ,  $A_4$ ,  $A_5$  and  $A_6$  are 4th order polynomials in R.

When the program was run, it was found that the rotation values were getting larger with every iteration. This divergence is most probably as a result of the incorrect formulae. Also, when the rope torque was displayed on the screen it was found to vary by as much as 400 Nm between the

front and back end of the rope.

Four examples of output plots for this program are shown in Figures I.1 to I.4. The bracketed numbers indicate the percentage of rope length for which the front end equations were used and the percentage for which the rest of the rope equations were used. (Front % / Rest %). All four figures were plotted after one iteration cycle had been completed.

The discontinuities in Figure I.2 and I.3 are as a result of the use of the two different sets of equations for rope rotation. The size of the discontinuities were found to increase as the number of iterations increased. This is another indication of the model instability.

(100 / 0)

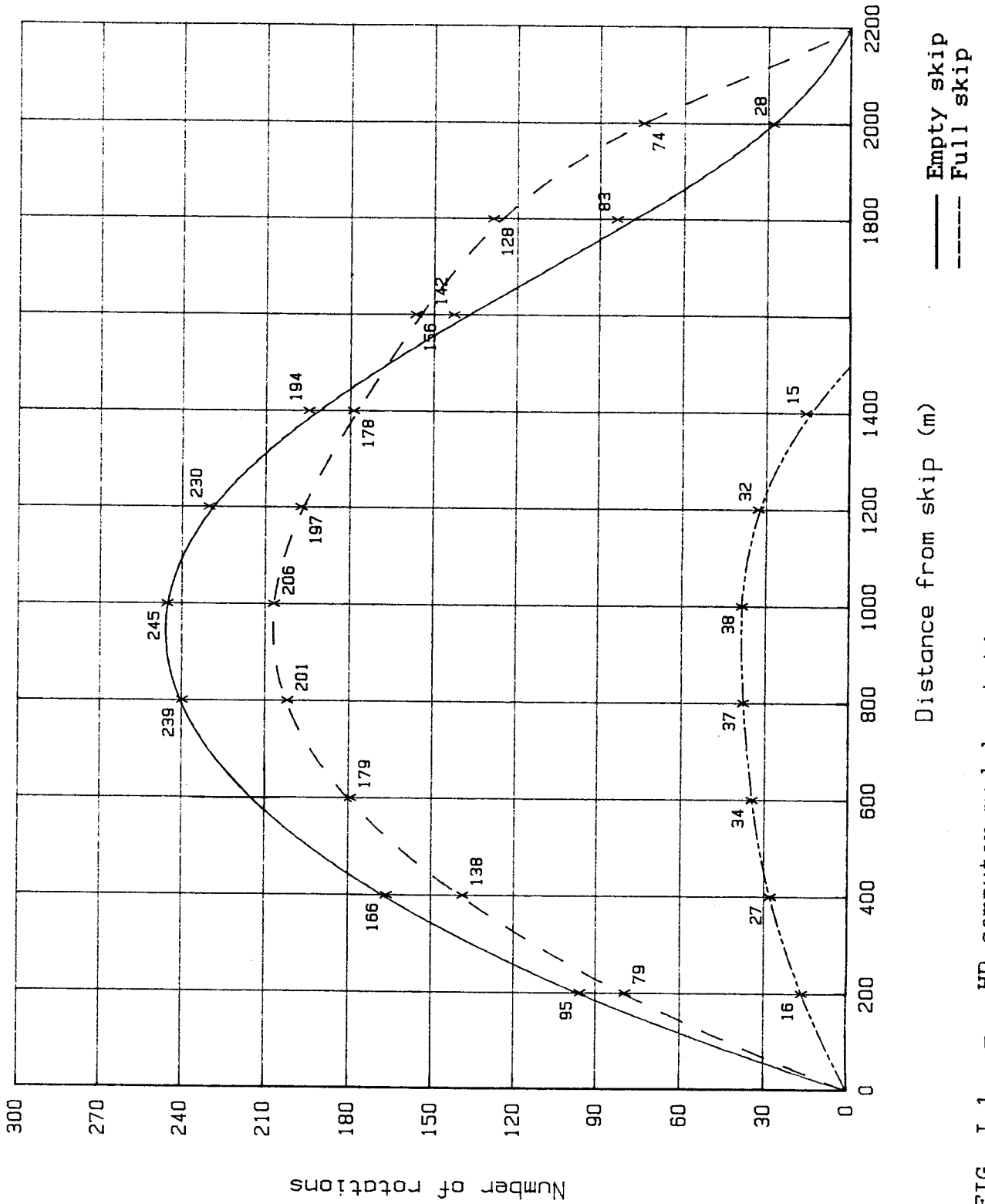


FIG. I.1 - HP computer model rotation curves (100/0).



(50/50)

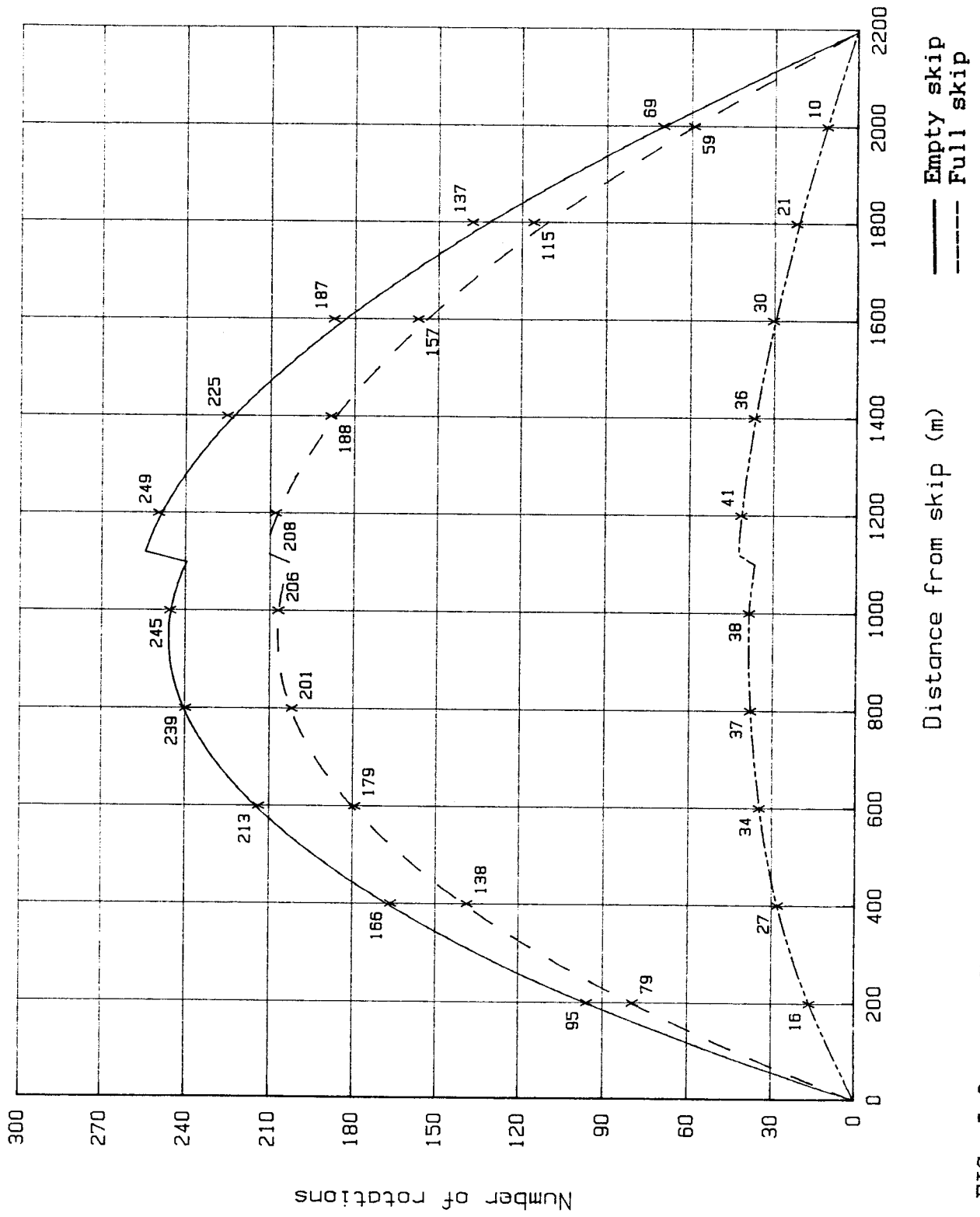


FIG. I.2 - HP computer model rotation curves (50/50).

(33/67)

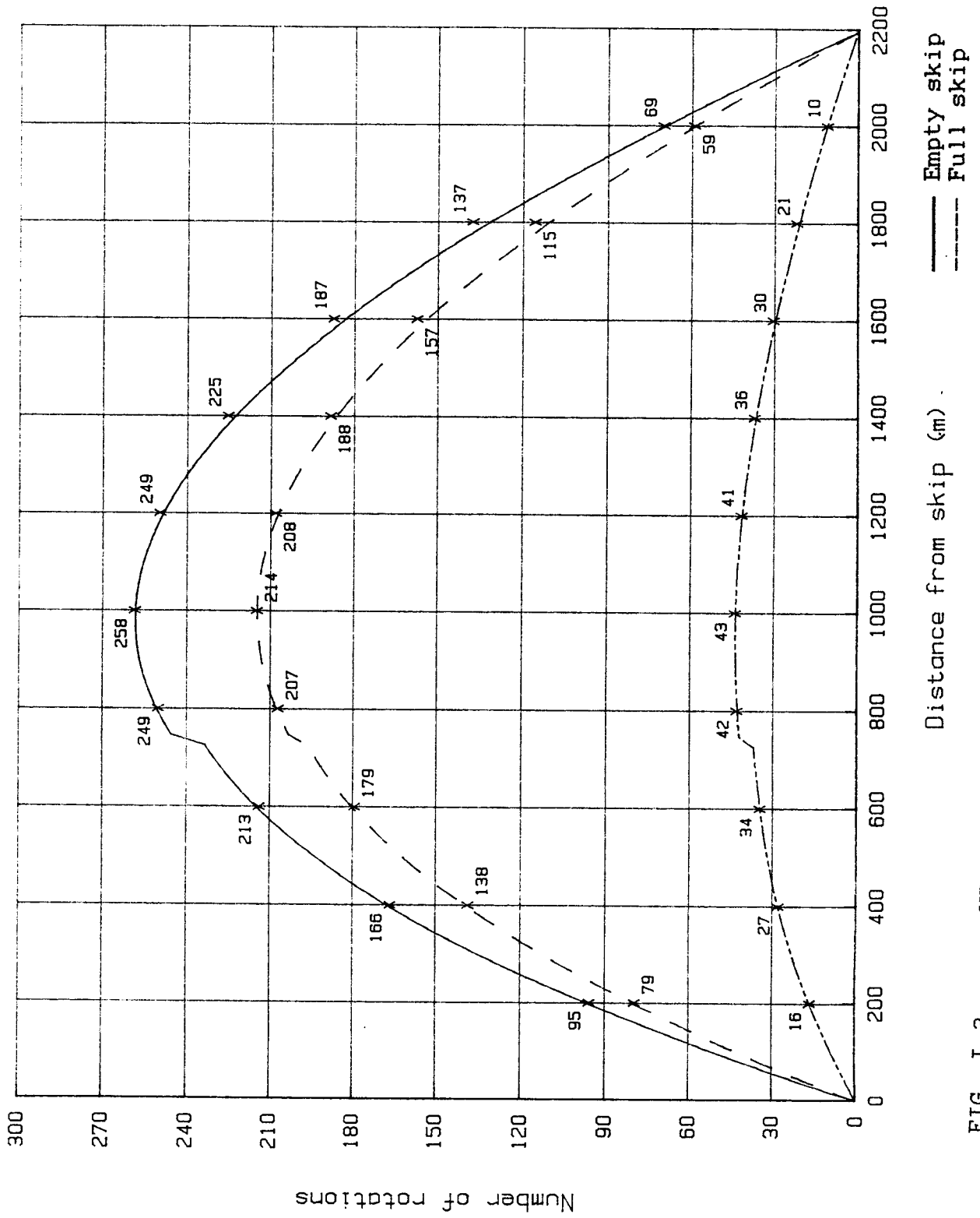


FIG. I.3 - HP computer model rotation curves (33/67).

(0/100)

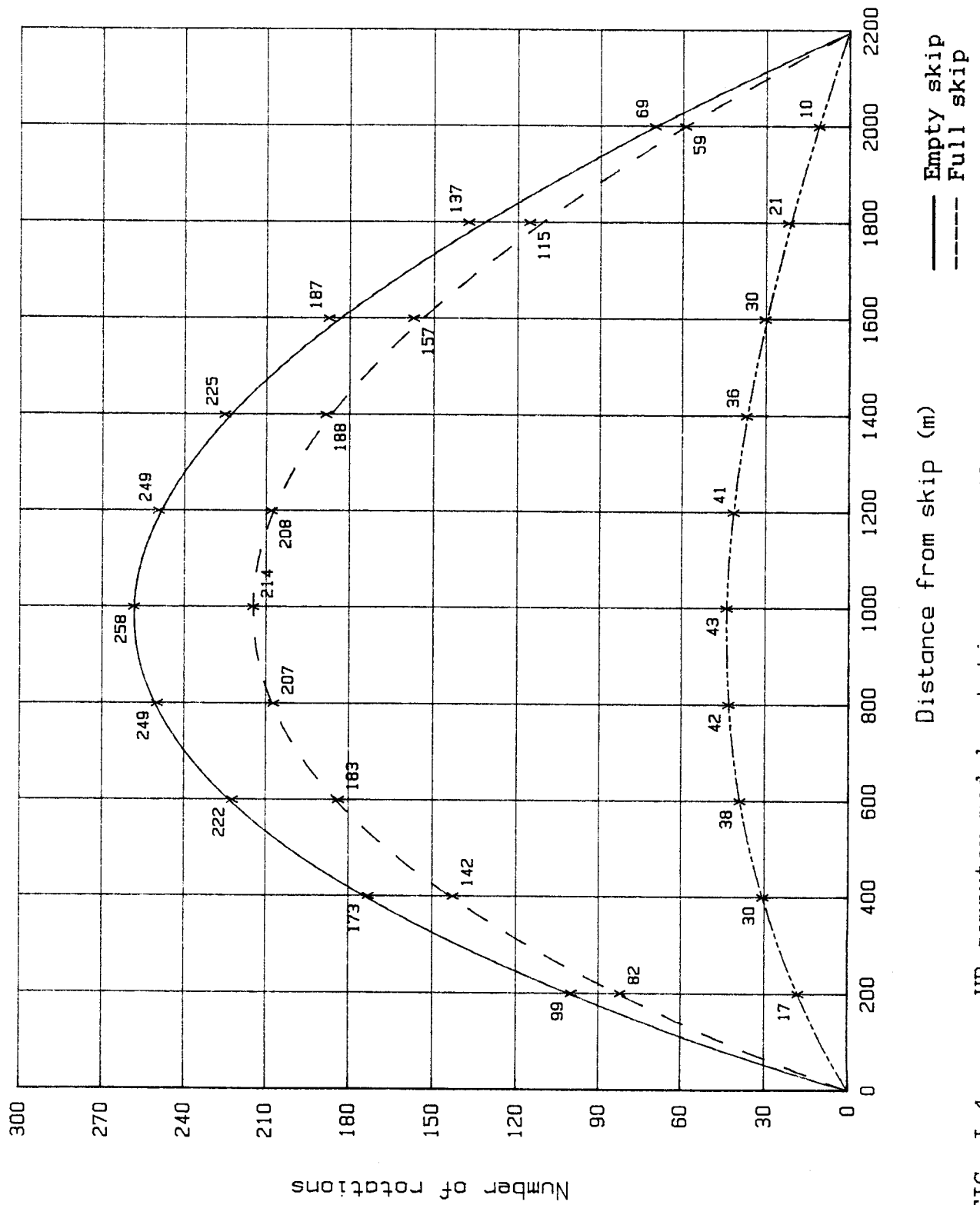


FIG. I.4 - HP computer model rotation curves (0/100).